Electronic Supplementary Material (ESI) for Organic & Biomolecular Chemistry.

Tuning the Exchange Dynamics of Boronic Acid Hydrazones and Oximes with pH and Redox Control

Gun Su Han and Dylan W. Domaille*

Department of Chemistry, Colorado School of Mines, 1500 Illinois St, Golden, CO 80401.

*Correspondence to ddomaille@mines.edu

Supplementary Materials

A. Equipment and Materials

Unless otherwise noted, all chemicals and solvents were used as received from commercial sources. Water (dd-H_2O) used in ultraviolet-visible (UV-Vis) spectrometry procedures was deionized using Barnstead E-pure Series 1090 water purification system (Thermo Fisher Scientific, USA). UV-Vis spectrometry experiments were carried out with Evolution 260 Bio UV-visible spectrometer, equipped with an 8-cell holder and a Peltier Control and Cooling Unit (PCCU1) (Thermo Fisher Scientific, USA). Standard 10mm rectangular quartz UV-Vis cuvettes were purchased from Thomas Scientific, USA (catalog number: 8490-D42). Nuclear magnetic resonance (NMR) spectroscopy experiments were carried out with JEOL ECA-500 NMR spectrometer (JEOL, USA). Chemical shifts are expressed as parts per million (ppm). Coupling constants are reported in hertz (Hz). HRMS was carried out with Waters Synapt G2 HDMS at the University of Colorado Boulder. Gas chromatography mass spectrometry (GC-MS) analysis was carried out with Agilent Technologies 7890B GC system paired with a 7693 Autosampler and 5977B MSD.

Monobasic sodium phosphate (>98%), hydrochloric acid (36.5 – 38.0%), and dimethyl sulfone (*Trace*CERT®) were purchased from Millipore Sigma (USA). Tribasic sodium phosphate (>98%), dimethyl sulfoxide (99.9%), and hydrogen peroxide (30%) were purchased from Fisher Scientific (USA). Sodium hydroxide (pellets) and 2-formylphenylboronic acid (>98%) were purchased from Oakwood Chemicals (USA). Acethydrazide (>98%), cyanoacetohydrazide (>97%), *tert*-butyl carbazate (>97%), and *O*-methylhydroxylamine hydrochloride (>97%) were purchased from TCI America (USA). Salicylaldehyde (99%), pivalic acid hydrazide (>98%), deuterium chloride (20% w/w), and sodium deuteroxide (40% w/w) were purchased from Acros Organics (USA). Dimethyl sulfoxide-d_6 and deuterium oxide were purchased from Cambridge Isotope Laboratories (USA). 2-Methylpropanohydrazide was purchased from Matrix Scientific (USA). 2-(Aminooxy)propane hydrochloride and O-tert-butylhydroxylamine hydrochloride were purchased from AA Blocks. *O*-Ethylhydroxylamine hydrochloride (>99%) was purchased from Chem-Impex International (USA). Dibasic sodium phosphate was purchased from MP Biomedicals (Japan).

B. General Procedure for UV-Vis Spectrometer Experiments

Stock solutions of 2-formylphenylboronic acid (2-FPBA), acethydrazide (AHz), *O*-methylhydroxylamine (MHA), and *O*-ethylhydroxylamine (EHA) were prepared in DMSO (50 mM). Using the stock solution, 2-FPBA solution (100 μM; 10 mL) was prepared in phosphate buffer (100 mM) at an appropriate pH (6.5, 7.4, 8.5, 9.5, or 12.0), and 3 mL of the prepared solution was transferred to a UV-vis cuvette. PCCU1 was set to an appropriate temperature (15, 35, 55, or 75 °C), and the UV-Vis spectrometer was blanked with the 100 μM 2-FPBA solution. Once the sample was equilibrated to the target temperature, 6 μL AHz or MHA stock solution was added. The sample was thoroughly mixed with the use of an autopipette. Formation of **1** was monitored at 295 nm; **2** was monitored at 260 nm for by measuring the absorbance of a sample as a function of time for up to 63 hours.

C. Effective Extinction Coefficient Calculation

Effective extinction coefficients were calculated at each pH and temperature based on both the product (**1a** or **2a**) and the reactant (2-FPBA) absorbance at 295 nm for **1a** and 260 nm for **2a** in the corresponding condition. The extinction coefficient (ε) of a product was obtained by adding 2-FPBA (50 mM, 1 μL each time) to 1 mM solution of the appropriate nucleophile (3 mL) and collecting a scan, up to 6 μL addition. For each condition, the extinction coefficient of 2-FPBA was obtained by adding 2-FPBA (50 mM, 1 μL each time) to PB and collecting a scan, up to 6 μL addition. According to the Beer-Lambert law, where $A = \varepsilon bC$, the slope of the trendline (A/C) was determined to be the extinction coefficient as the pathlength was fixed at 1 cm. The extinction coefficient of 2-FPBA was subtracted from the extinction coefficient of **1a** or **2a** to obtain effective extinction coefficients at 295 nm and 260 nm, respectively.

Table S1. Effective Extinction Coefficients of **1a** (M^{-1} cm^{-1}) at 295 nm

T (°C)	pH 6.5	pH 7.4	pH 8.5	pH 9.5	pH 12.0
15	16922	17646	18184	18259	18228
35	-	17541	-	-	-
55	-	17447	-	-	-
75	-	17354	-	-	-

Table S2. Effective Extinction Coefficients of **2a** (M^{-1} cm^{-1}) at 260 nm

T (°C)	pH 6.5	pH 7.4	pH 8.5	pH 9.5	pH 12.0
15	3879	8137	11463	11858	11897
35	-	7613	-	-	-
55	-	7178	-	-	-
75	-	6765	-	-	-

D. General Procedure for Monitoring Formations of 1, 2, 3, and 4a via NMR

D_2O was buffered with tribasic sodium phosphate (200 mM), and the pD was adjusted with DCl and NaOD to 7.5 with the use of pH strips. Buffered D_2O (500 µL) was combined with 2-FPBA (20 µL), or salicylaldehyde (20 µL), and AHz, or MHA (20 µL), and the sample was monitored up to 7 days. k_1 and k_{-1} for the formations were calculated with the second-order reversible kinetic model.

E. Second-Order Irreversible Kinetic Model

Data were fitted to a kinetic model that accounts for product formation under irreversible second-order conditions, derived by Perrin.[1]

F. Second-Order Reversible Kinetic Model

Data were fitted to a kinetic model that simultaneously accounts for product formation under second-order conditions and hydrolysis under first-order, initially derived by Dawson *et al.*:[2]

$$\boldsymbol{x(t) = \frac{a_+(x_0 - a_-) - a_-(x_0 - a_+)e^{-k_1(a_+ - a_-)t}}{(x_0 - a_-) - (x_0 - a_+)e^{-k_1(a_+ - a_-)t}}}$$

in which

$$\boldsymbol{a_+ = \frac{-k_{-1} + \sqrt{k^2_{-1} + 4k_1k_{-1}x_0}}{2k_1}}$$

$$\boldsymbol{a_- = \frac{-k_{-1} - \sqrt{k^2_{-1} + 4k_1k_{-1}x_0}}{2k_1}}$$

All kinetic data were collected in triplicate, and each data set was independently fitted to the model; data are reported as the mean ± SD of each independent fitting. K_{eq} was calculated based on $\frac{k_1}{k_{-1}} = K_{eq}$

G. Formations of hydrazone 1 and oxime 2

The formation kinetics of **1** and **2** were measured, following the general procedure (section D). Data were fitted into the second-order irreversible kinetic model (section E)

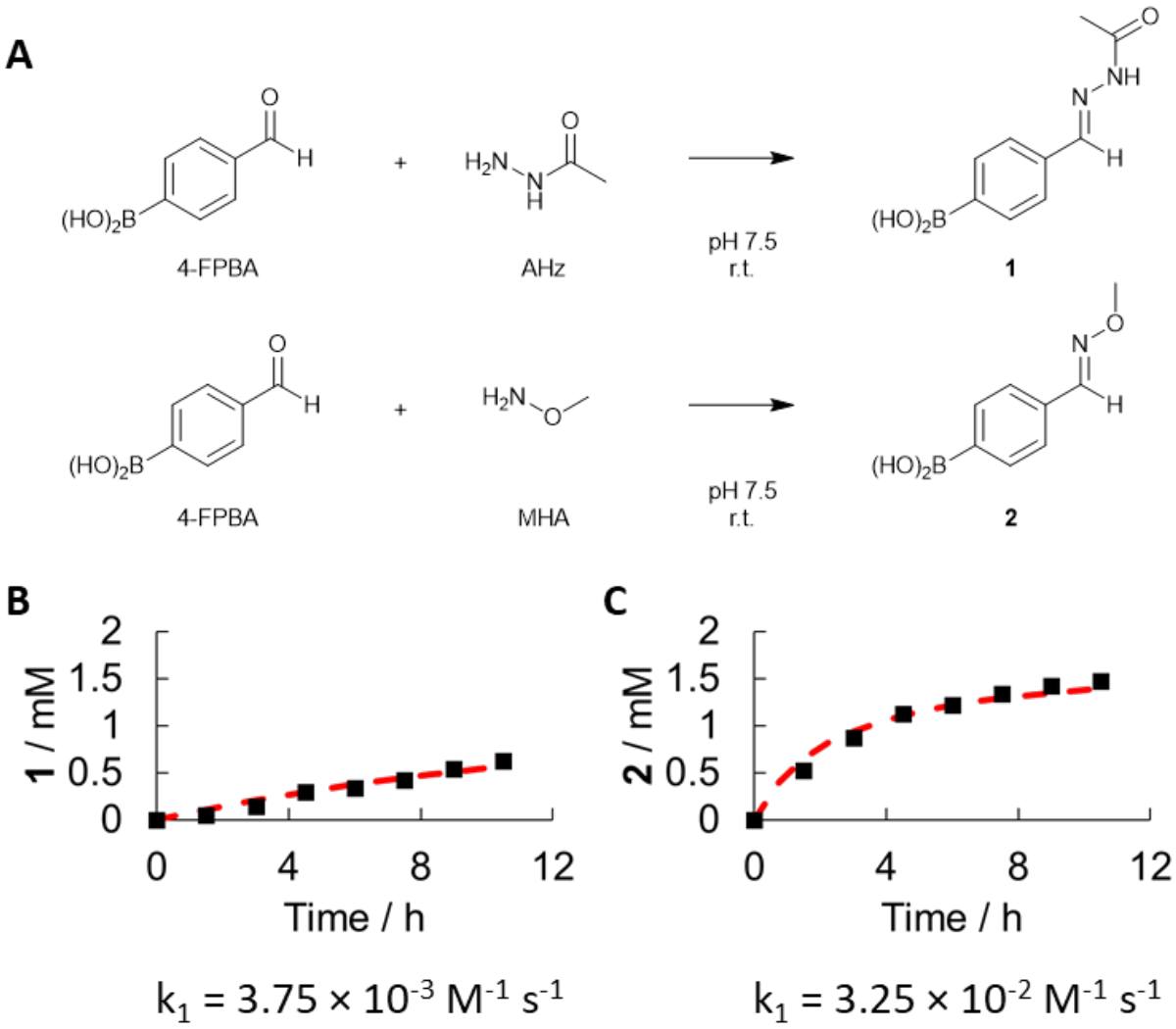

Fig. S1. (A) Reaction scheme. (B) Formation of **1**. (C) Formation of **2**.

H. Second-Order Irreversible Kinetic Model for formation of 1a

The obtained plot was fitted to a kinetic model only accounts for product formation under second-order conditions without concomitant hydrolysis.[1]

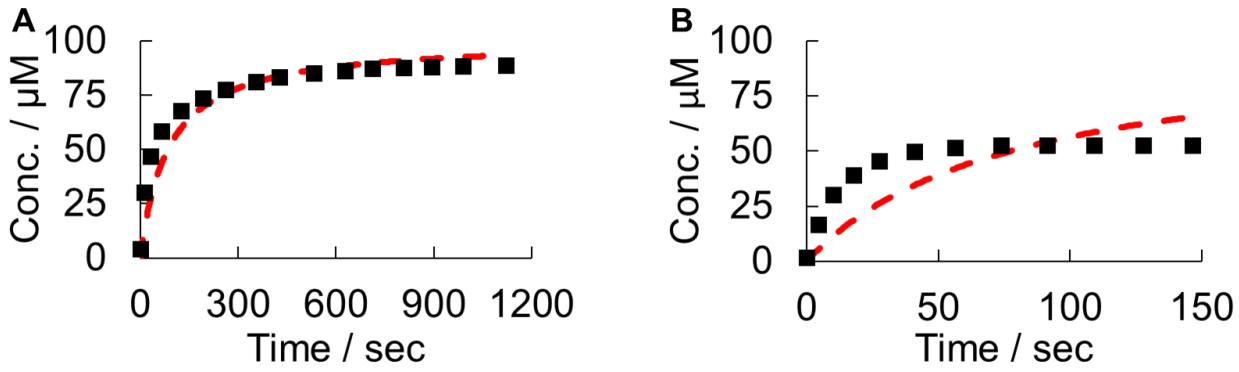

Fig. S2. Formation of **1a** fitted to the second-order irreversible kinetic model at (A) 15 °C and (B) 75 °C. An irreversible model does not account for hydrolysis, and the obtained data does not fit well at higher temperatures.

I. DAB Structure Confirmation of 1a

The DAB structure confirmation had previously been reported by Bane et al.[3] A similar structural confirmation was obtained by observing **1a** at pD 7.5, 6.5, and 5.5 (pD 7.5 200 mM PB) at 1.72 mM at room temperature.

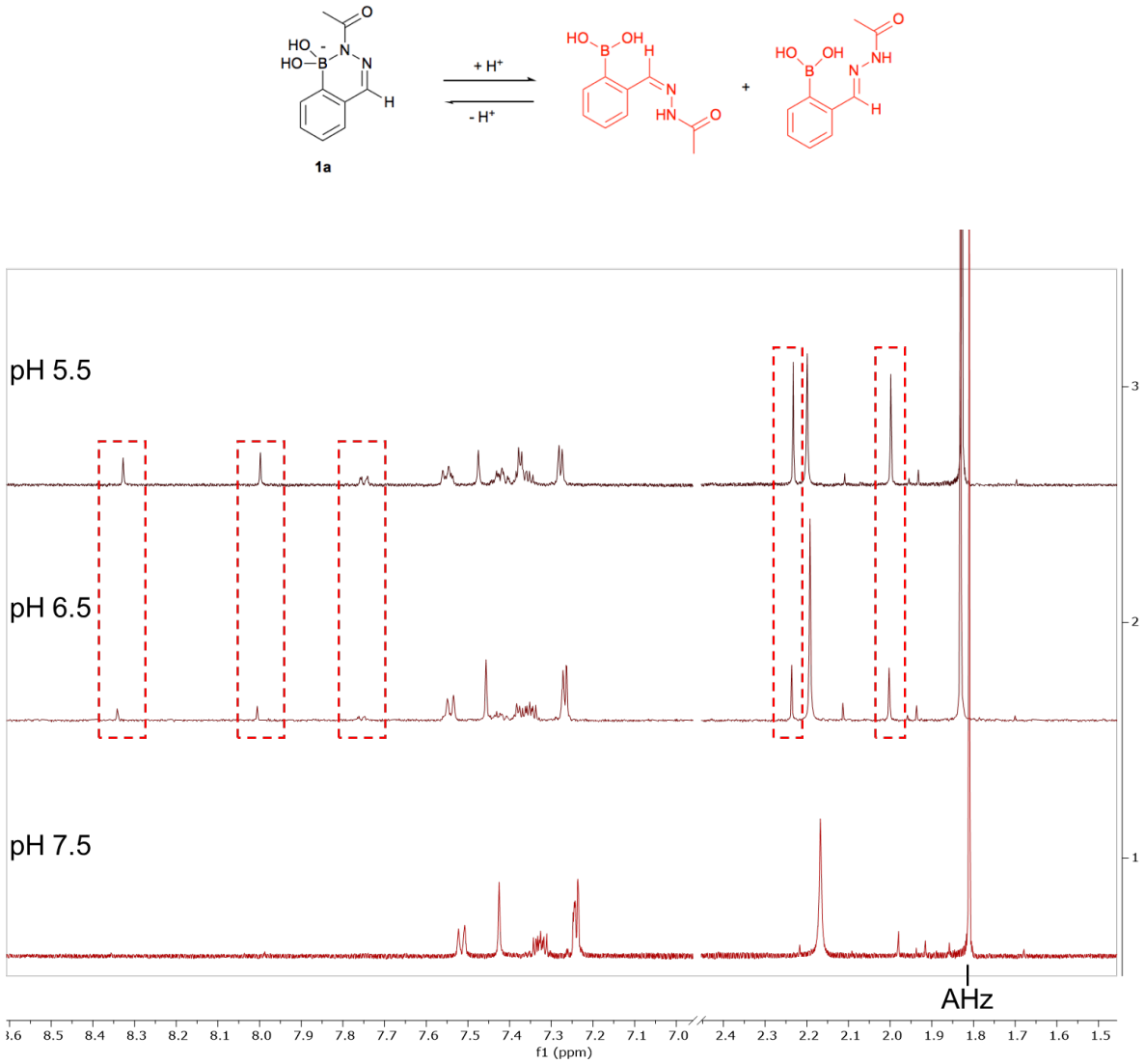

Fig. S3. 1a at pD 7.5, 6.5, and 5.5. Protons peaks of acyclic isomers (E/Z) can be observed at pD 6.5 and 5.5.

J. Eyring analysis

Eyring analysis was performed based on k_1 and k_{-1} at different temperatures by plotting ln(k/T) as an inverse function of temperature. $\Delta H^{\ddagger}$ was obtained from the slope of the trendline, and $\Delta S^{\ddagger}$ was obtained from the y-intercept of the trendline. $\Delta G^{\ddagger}$ was calculated at 298K.

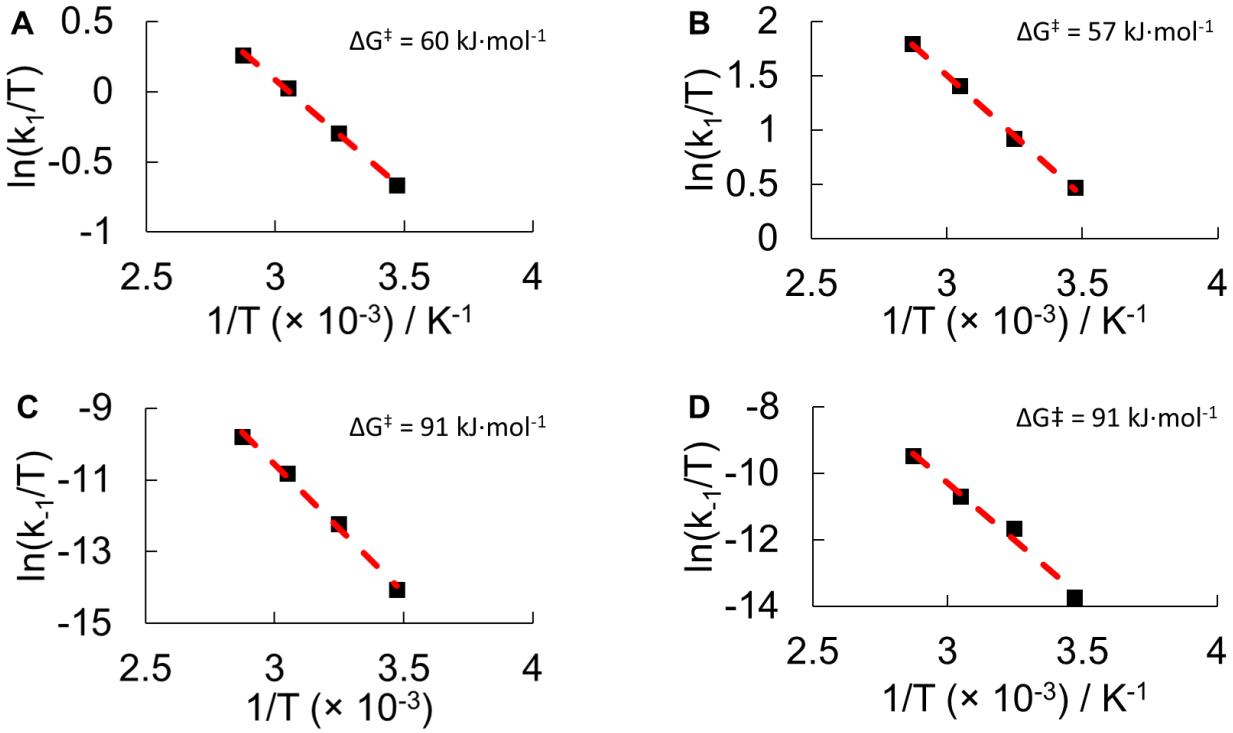

Fig. S4. Eyring Analyses. (A) Formation of **1a**. (B) Formation of **2a**. (C) Hydrolysis of **1a**. (D) Hydrolysis of **2a**.

K. General Procedures for Degenerate Exchange NMR Experiments

D_2O was buffered with tribasic sodium phosphate (200 mM), and the pD was adjusted with DCl and NaOD to 6.5, 7.5, 8.5, 9.5, or 12.0 with the use of pH strips. All experiments were conducted at room temperature. Unless otherwise noted, 2-FPBA, AHz, MHA, and EHA stock solutions were prepared in DMSO-d_6 at 50 mM. For the degenerate exchange of **1a** or **2a** with MHA or EHA, respectively, buffered D_2O (500 µL) was combined with 2-FPBA (20 µL) and AHz or MHA (60 µL), respectively. Once the initial formation was completed (less than a minute), 60 µL MHA or EHA, respectively, was added to the sample. The sample was then monitored with time-course NMR spectroscopy up to 20 hours. NaOD (5 µL, 40% w/w) was used to adjust the pD from 7.5 to 12.0, and DCl (9.5 µL, 20% w/w) was used to readjust the pD from 12.0 to 7.5. For all oxidation experiments, 3 equivalents of H_2O_2 (0.306 µL, 9.8 M) was used to fully oxidize the mixture. For the degenerate exchange of **3** or **4a**, buffered D_2O (500 µL) was combined with 20 µL **3** or **4a**, 40 µL AHz or MHA, and 60 µL MHA or EHA, respectively. The resulting mixture was monitored up to 16 hours. For the stoichiometric control, 24 equivalences of MHA was added to the sample (48 µL, 500 mM).

L. Hydrazone Exchanges with 1a

*L1. Hydrazone exchange between **1a** and PivHz at pD 7.5 at room temperature*

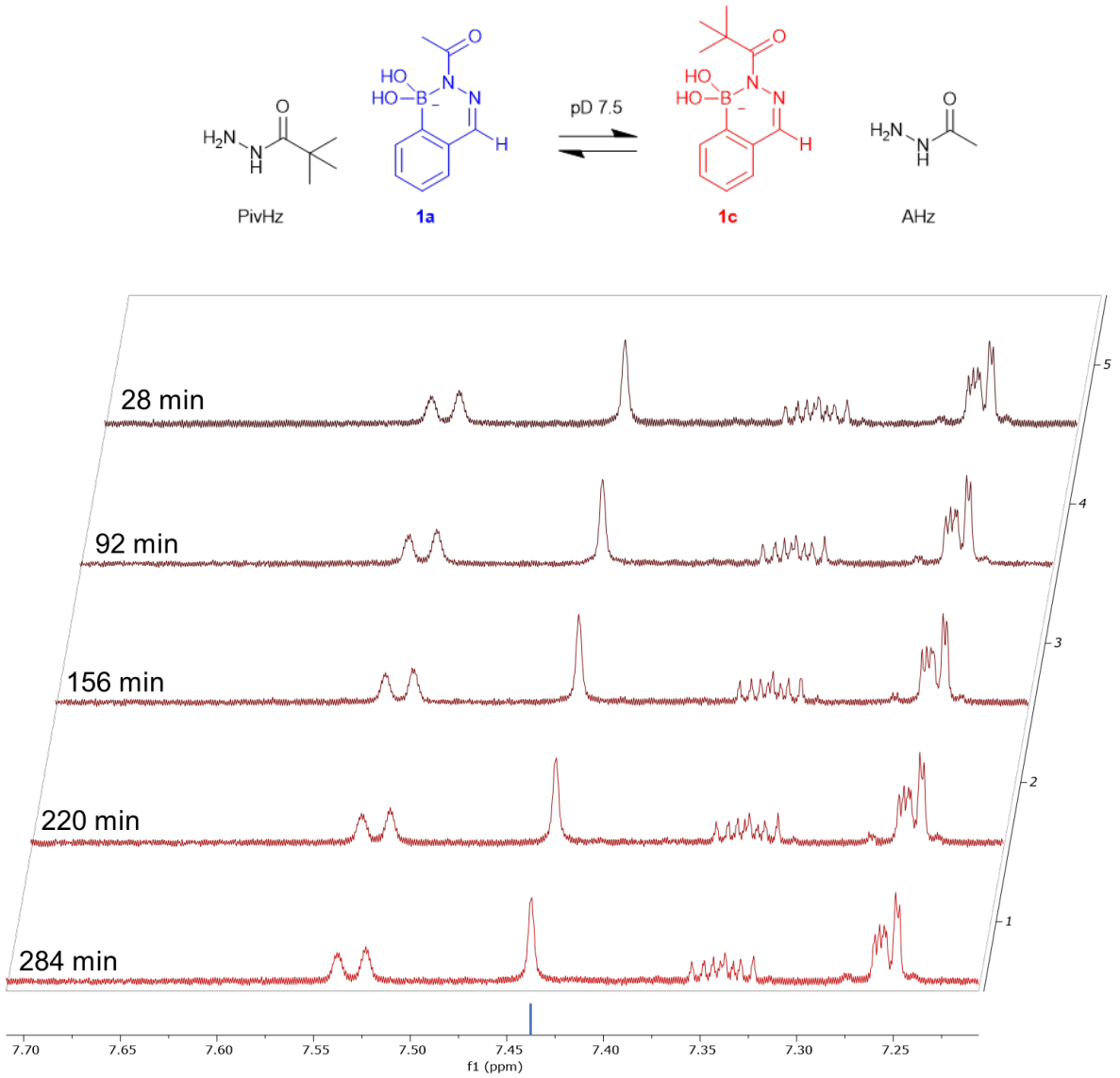

Fig. S5a. Aromatic region of the time-course ^{1}H NMR spectra of the degenerate exchange between **1a** and PivHz at pD 7.5 (200 mM PB). No exchange is observed.

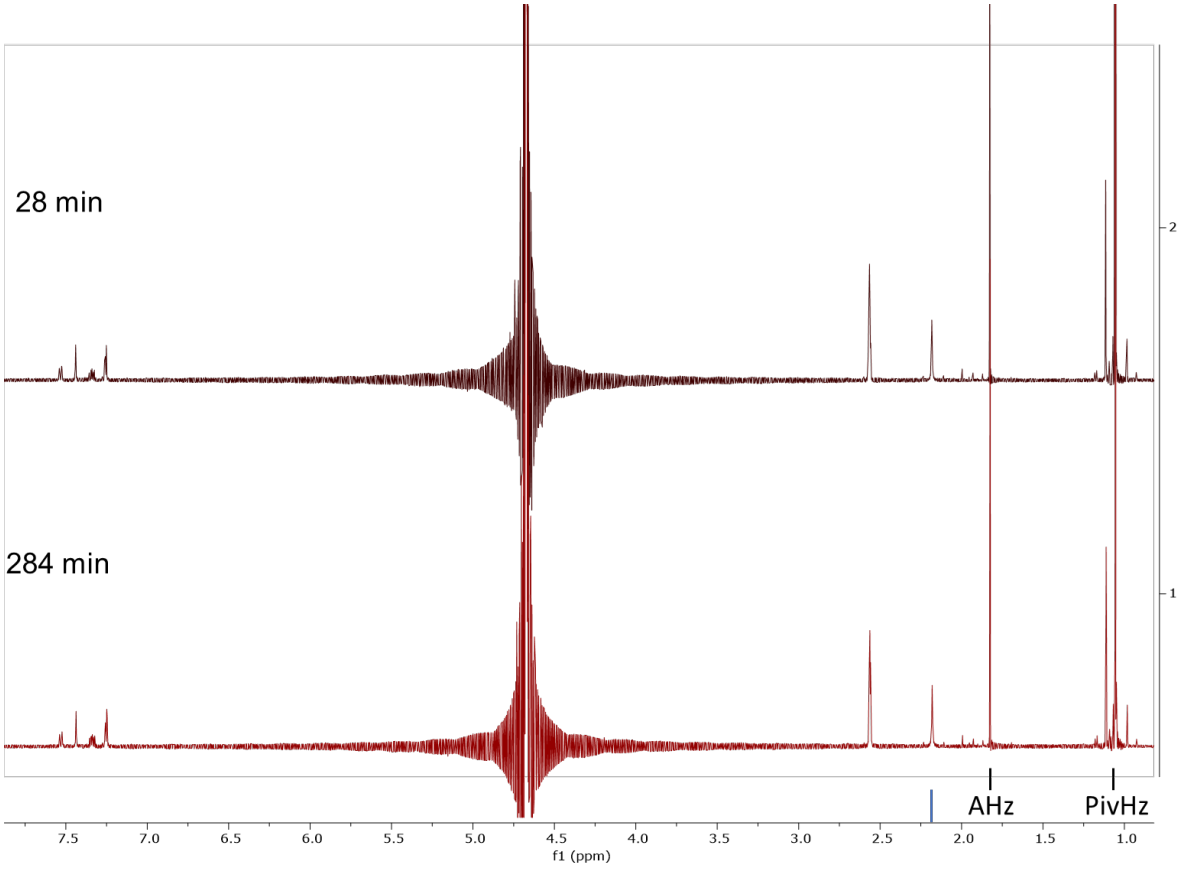

Fig. S5b. Time-course ^{1}H NMR spectra of the degenerate exchange between **1a** and PivHz at pD 7.5 (200 mM PB). No exchange is observed.

*L2. Hydrazone exchange between **1a** and iBHz at pD 7.5 at room temperature*

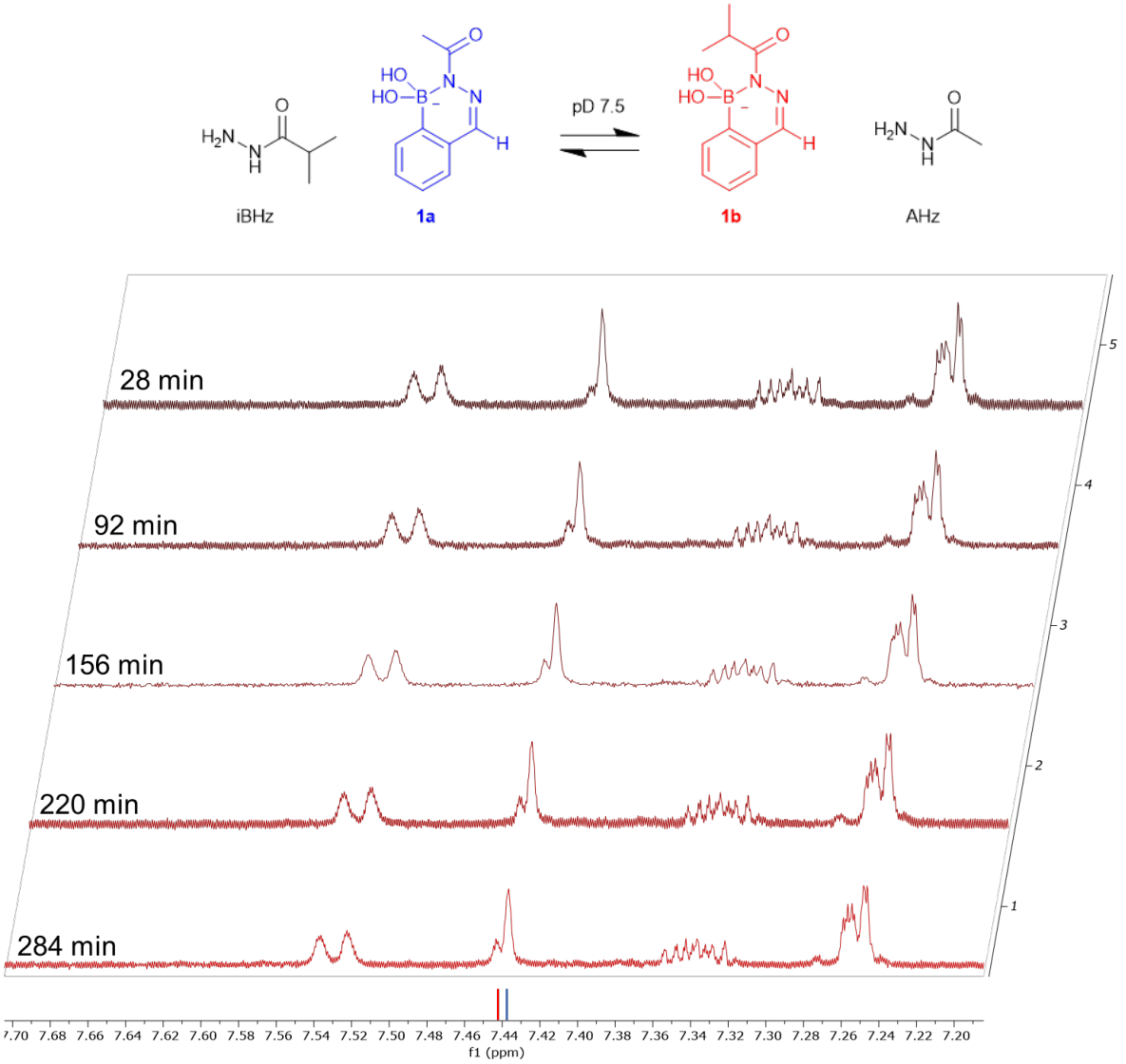

Fig. S6a. Aromatic region of the time-course ^{1}H NMR spectra of the degenerate exchange between **1a** and iBHz at pD 7.5 (200 mM PB). The ratios between **1a** and **1b** were measured by integrating imine-type CH proton peaks and were confirmed by terminal methyl proton integrations.

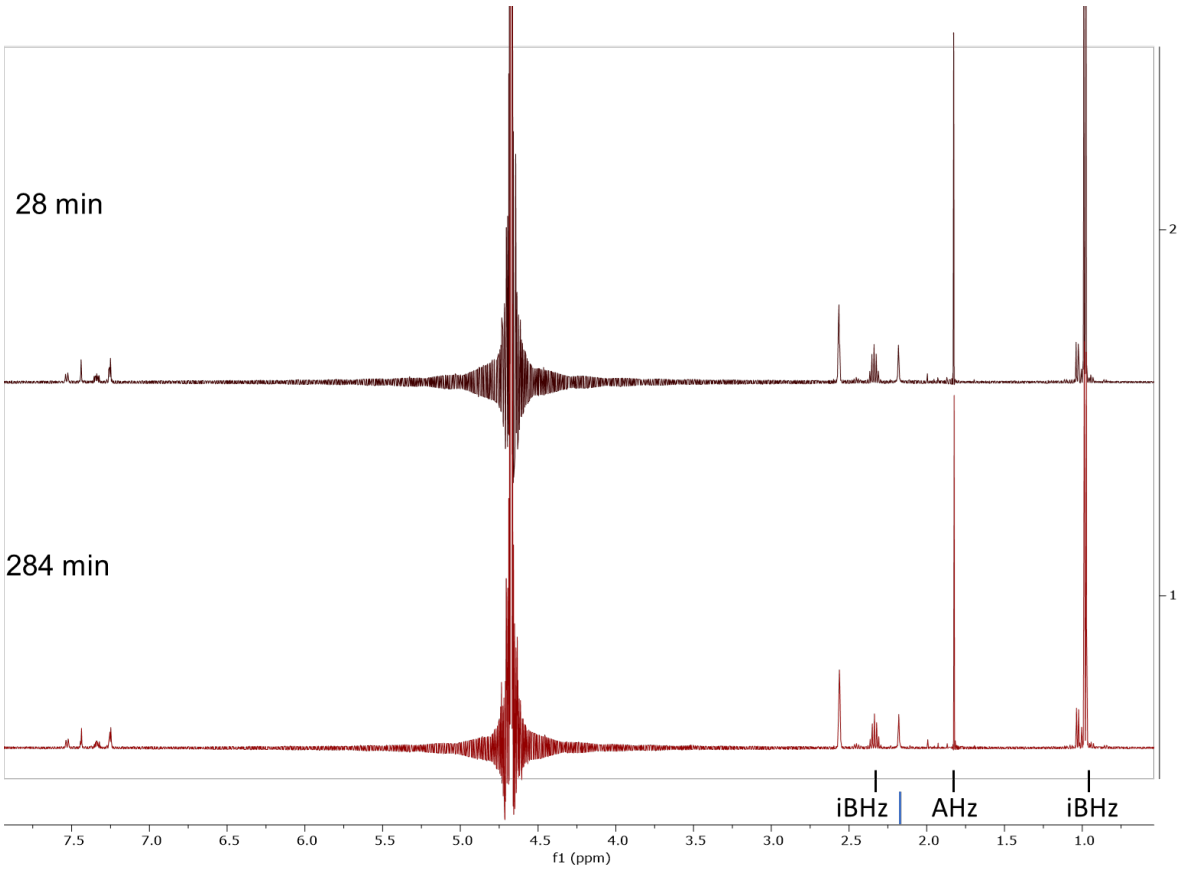

Fig. S6b. Time-course ^{1}H NMR spectra of the degenerate exchange between **1a** and iBHz at pD 7.5 (200 mM PB). The ratios between **1a** and **1b** were measured by integrating imine-type CH proton peaks and were confirmed by terminal methyl proton integrations.

*L3. Hydrazone exchange between **1a** and tBCz at pD 7.5 at room temperature*

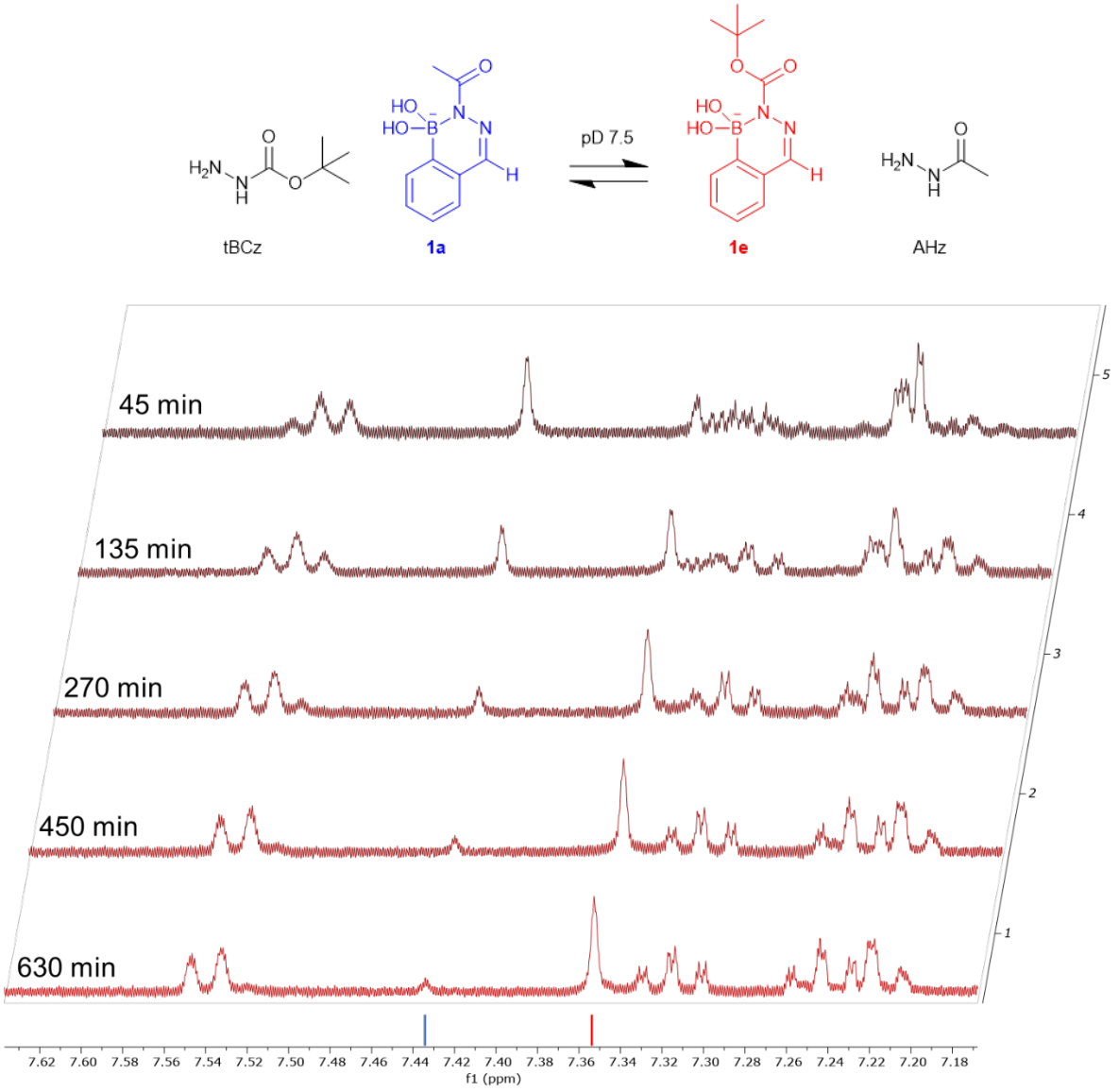

Fig. S7a. Aromatic region of the time-course ^{1}H NMR spectra of the degenerate exchange between **1a** and tBCz at pD 7.5 (200 mM PB). The ratios between **1a** and **1e** were measured by integrating imine-type CH proton peaks and were confirmed by terminal methyl proton integrations.

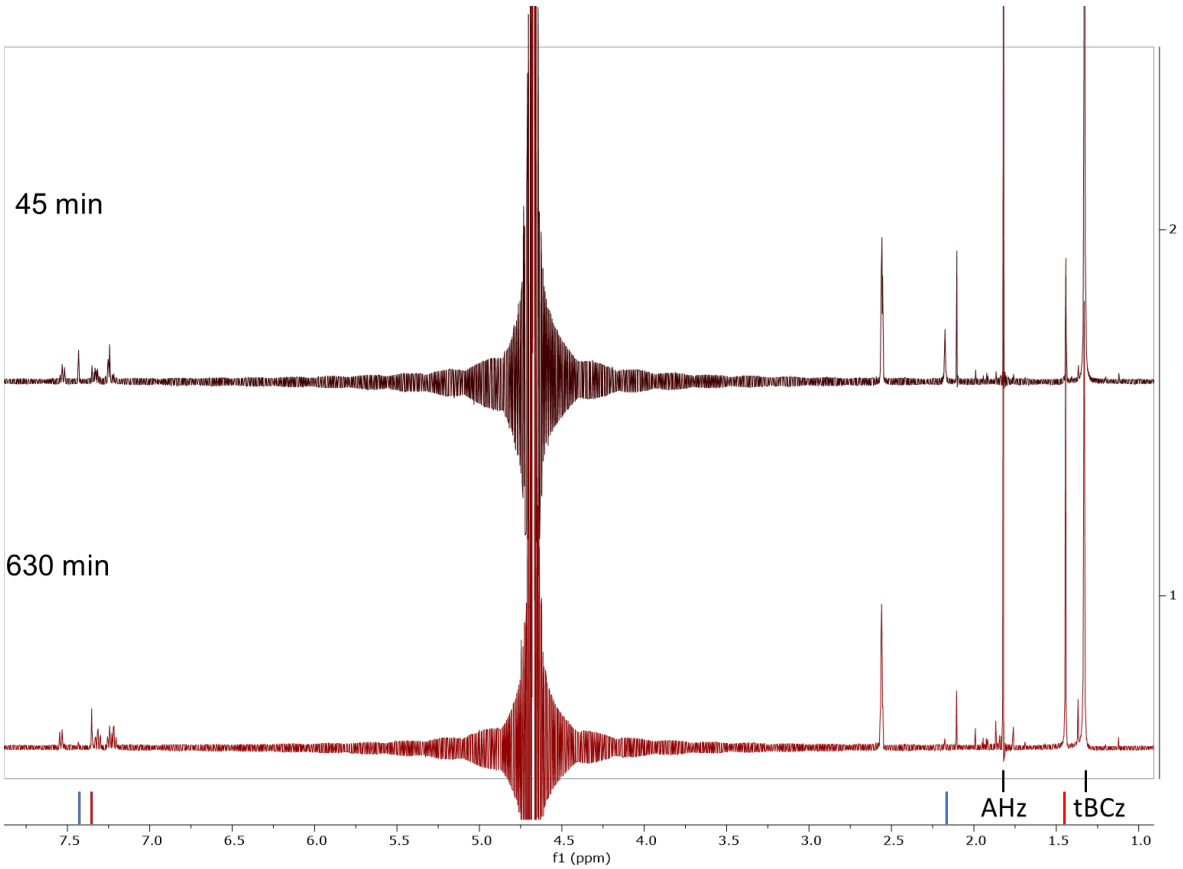

Fig. S7b. Time-course ^{1}H NMR spectra of the degenerate exchange between **1a** and tBCz at pD 7.5 (200 mM PB). The ratios between **1a** and **1e** were measured by integrating imine-type CH proton peaks and were confirmed by terminal methyl proton integrations.

*L4. Hydrazone exchange between **1a** and CAHz at pD 7.5 at room temperature*

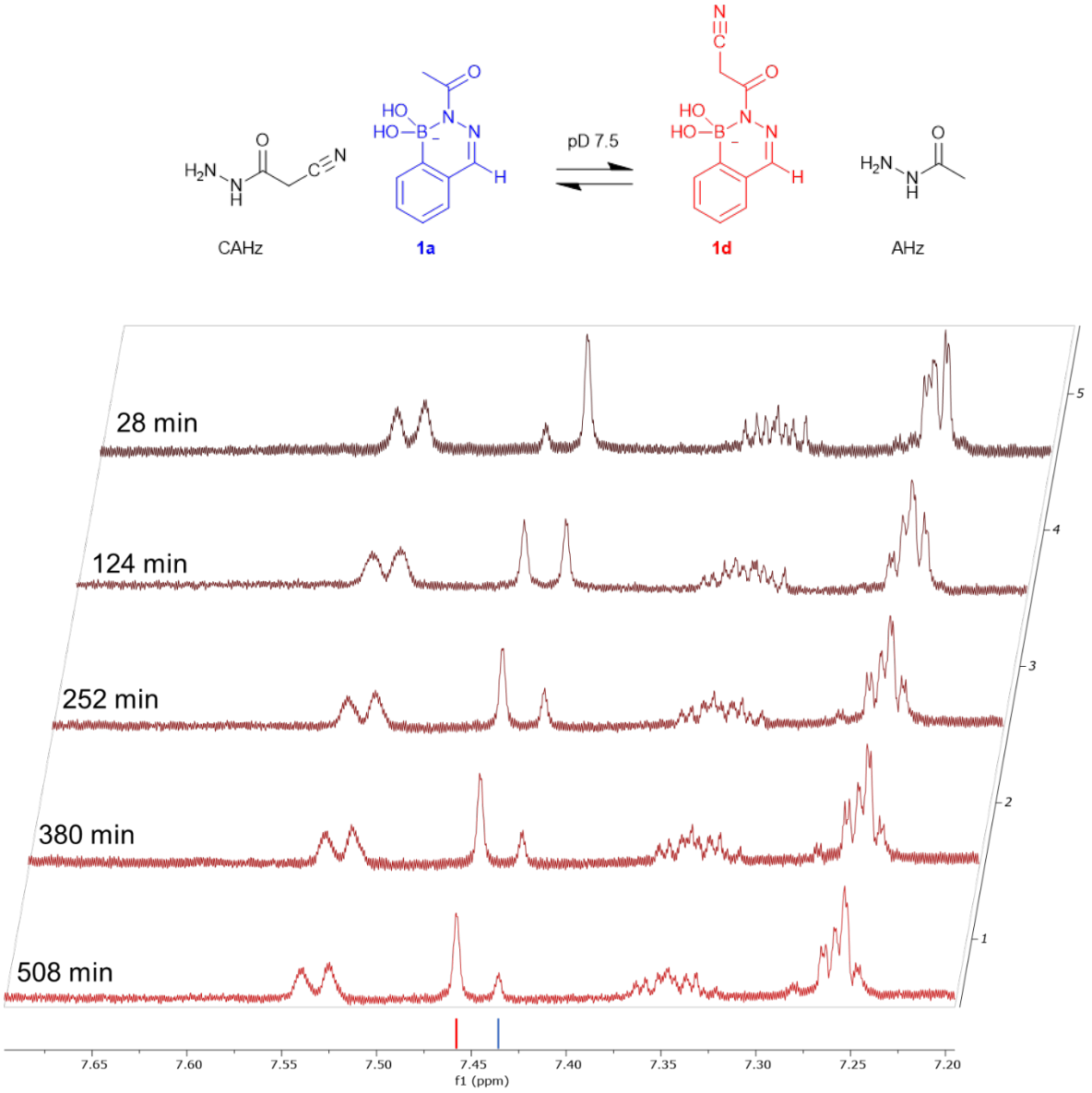

Fig. S8a. Aromatic region of the time-course ^{1}H NMR spectra of the degenerate exchange between **1a** and CAHz at pD 7.5 (200 mM PB). The ratios between **1a** and **1d** were measured by integrating imine-type CH proton peaks.

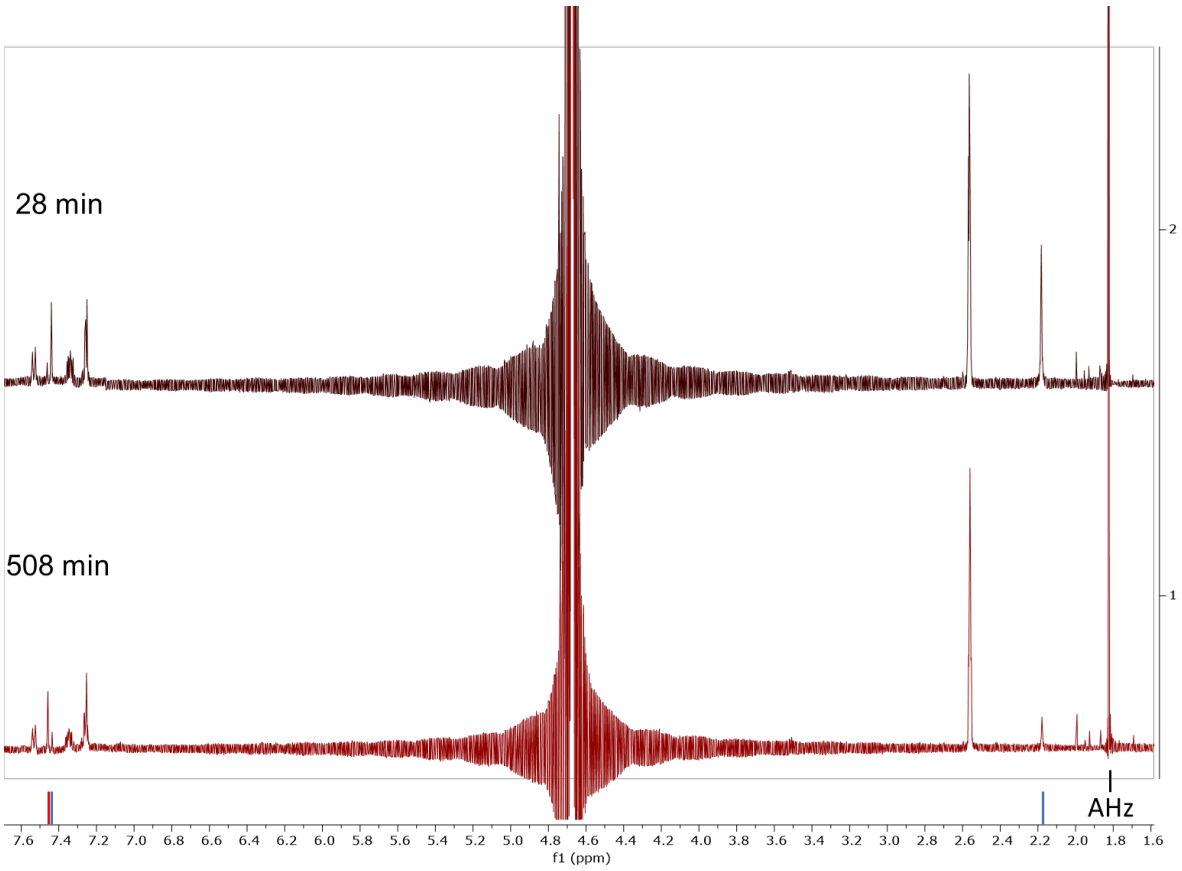

Fig. S8b. Time-course ^{1}H NMR spectra of the degenerate exchange between **1a** and CAHz at pD 7.5 (200 mM PB). The ratios between **1a** and **1d** were measured by integrating imine-type CH proton peaks.

*L5. Hydrazone exchange between **1a** and iBHz at pD 12.0 at room temperature*

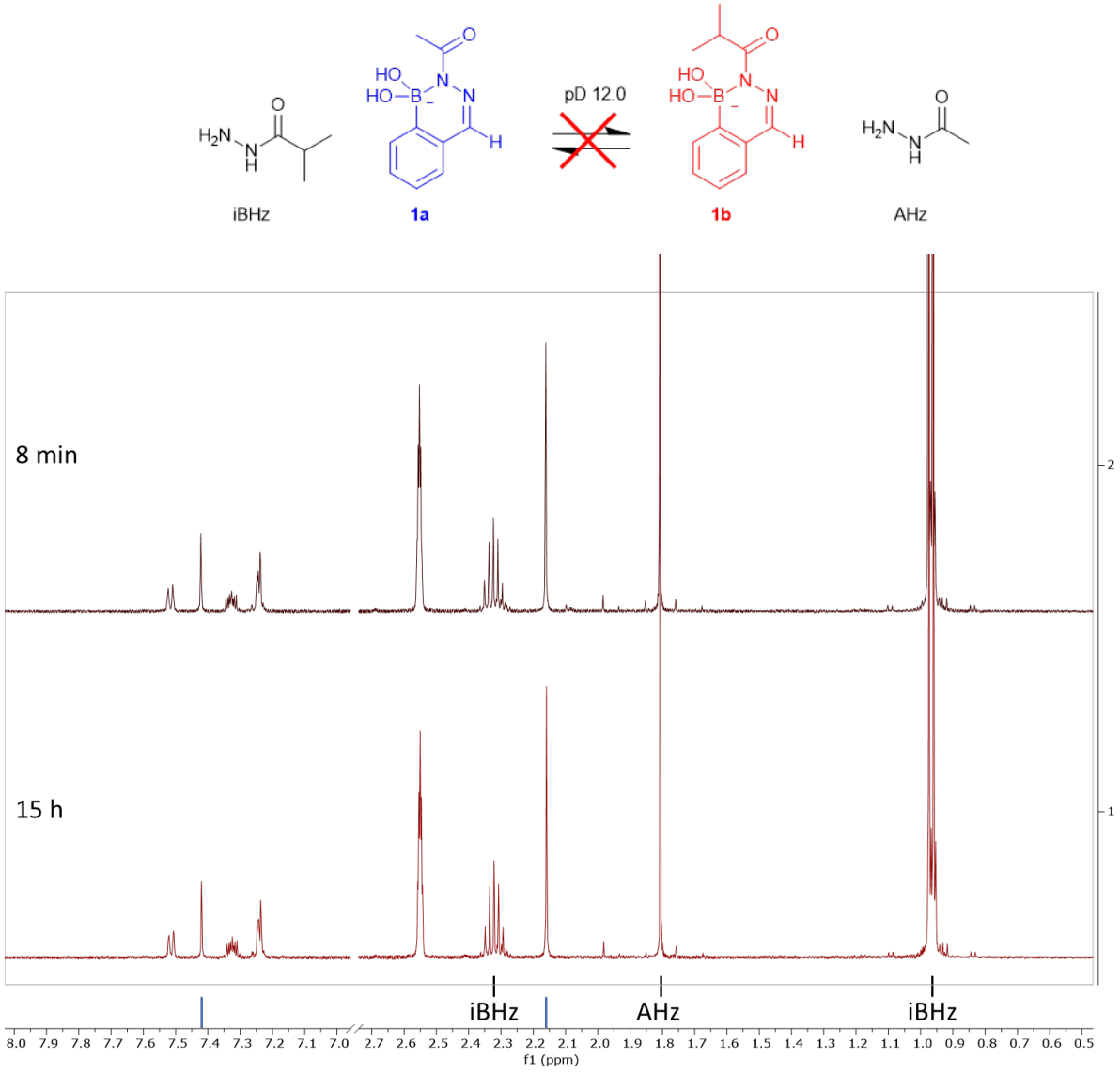

Fig. S9a. ^{1}H NMR spectrum of the degenerate exchange between **1a** and iBHz at pD 12.0. No exchange is observed over 15 hours.

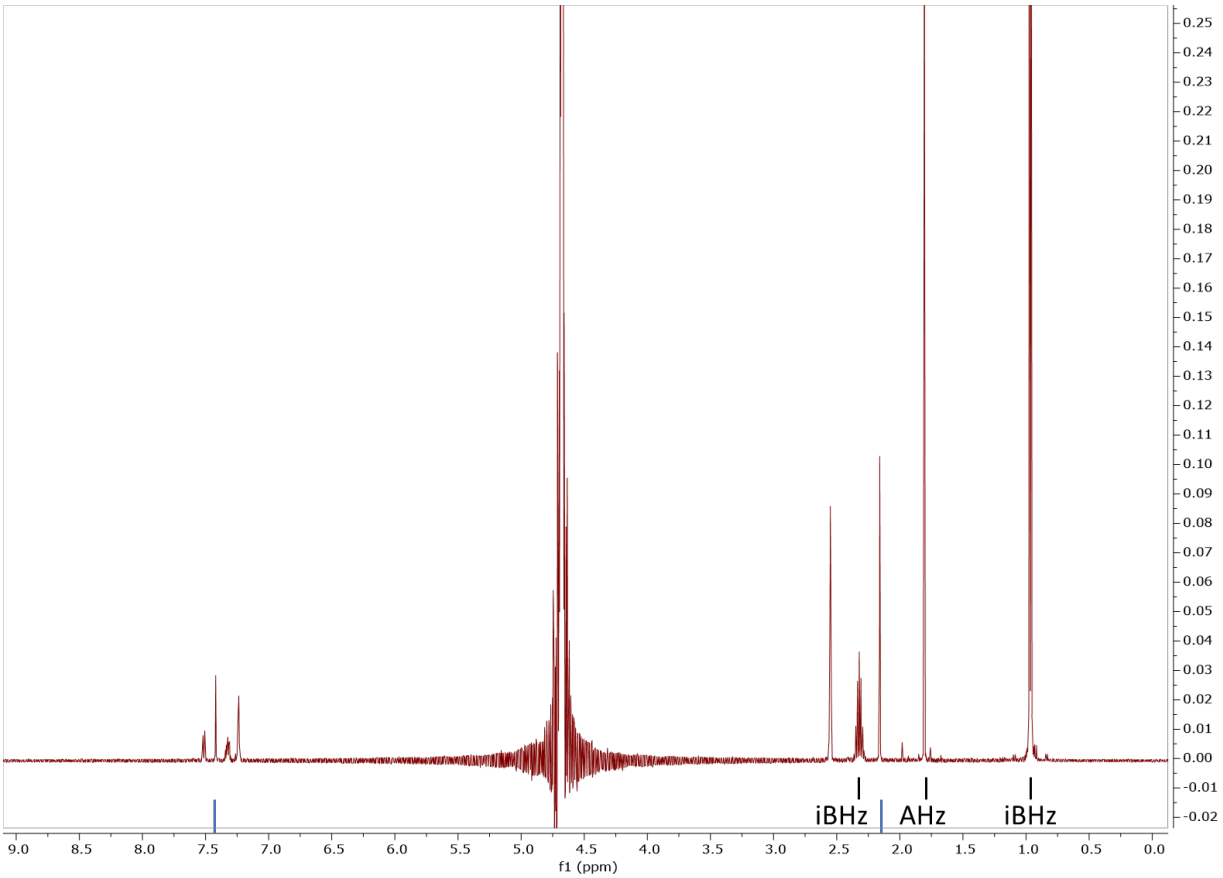

Fig. S9b. Full ^{1}H NMR spectrum of the exchange between **1a** and iBHz at pD 12.0. after 15 h.

*L6. Hydrazone exchange between **1a** and PivHz at pD 12.0 at room temperature*

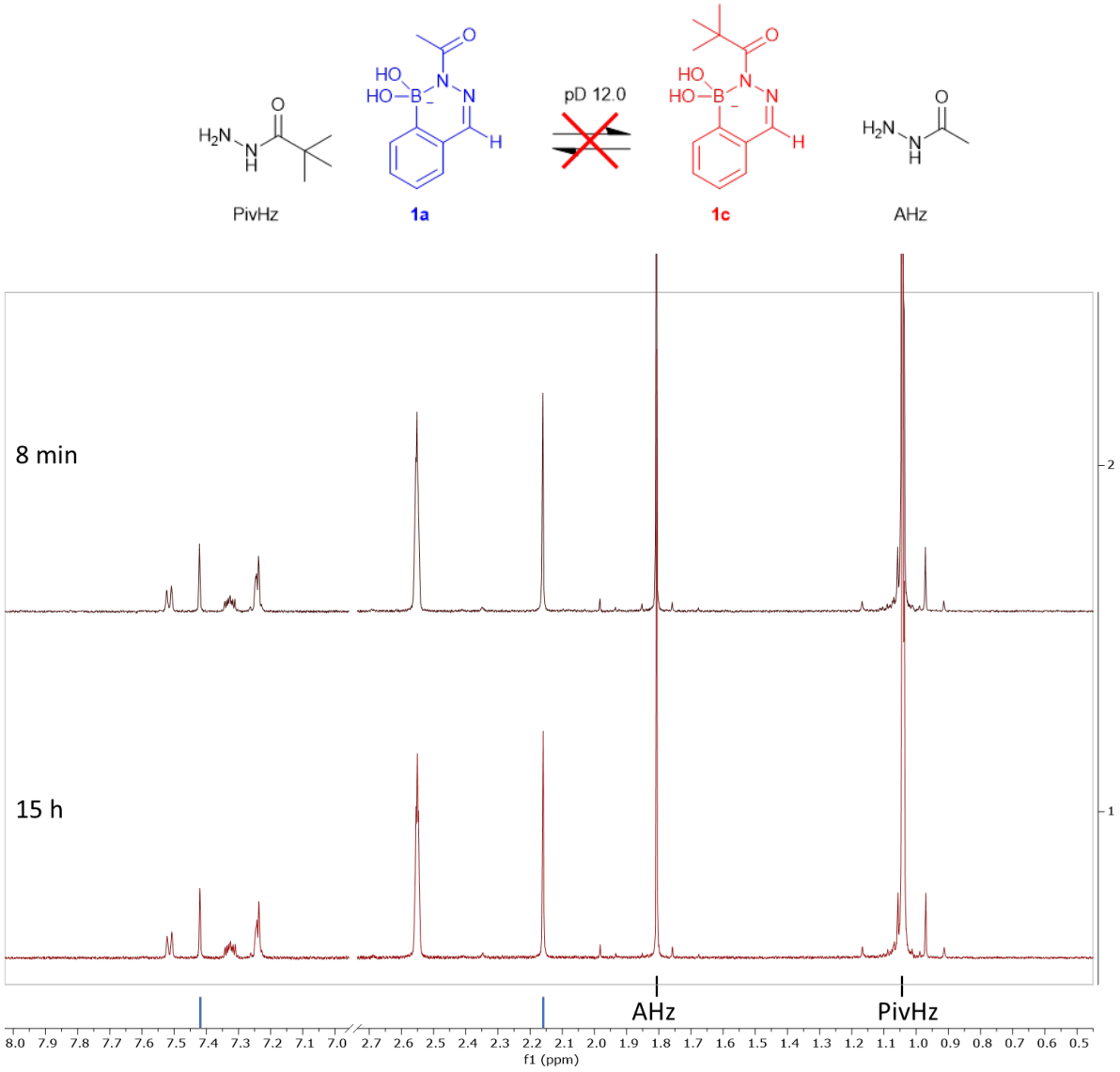

Fig. S10a. ^{1}H NMR spectrum of the degenerate exchange between **1a** and PivHz at pD 12.0. No exchange was observed over 15 hours.

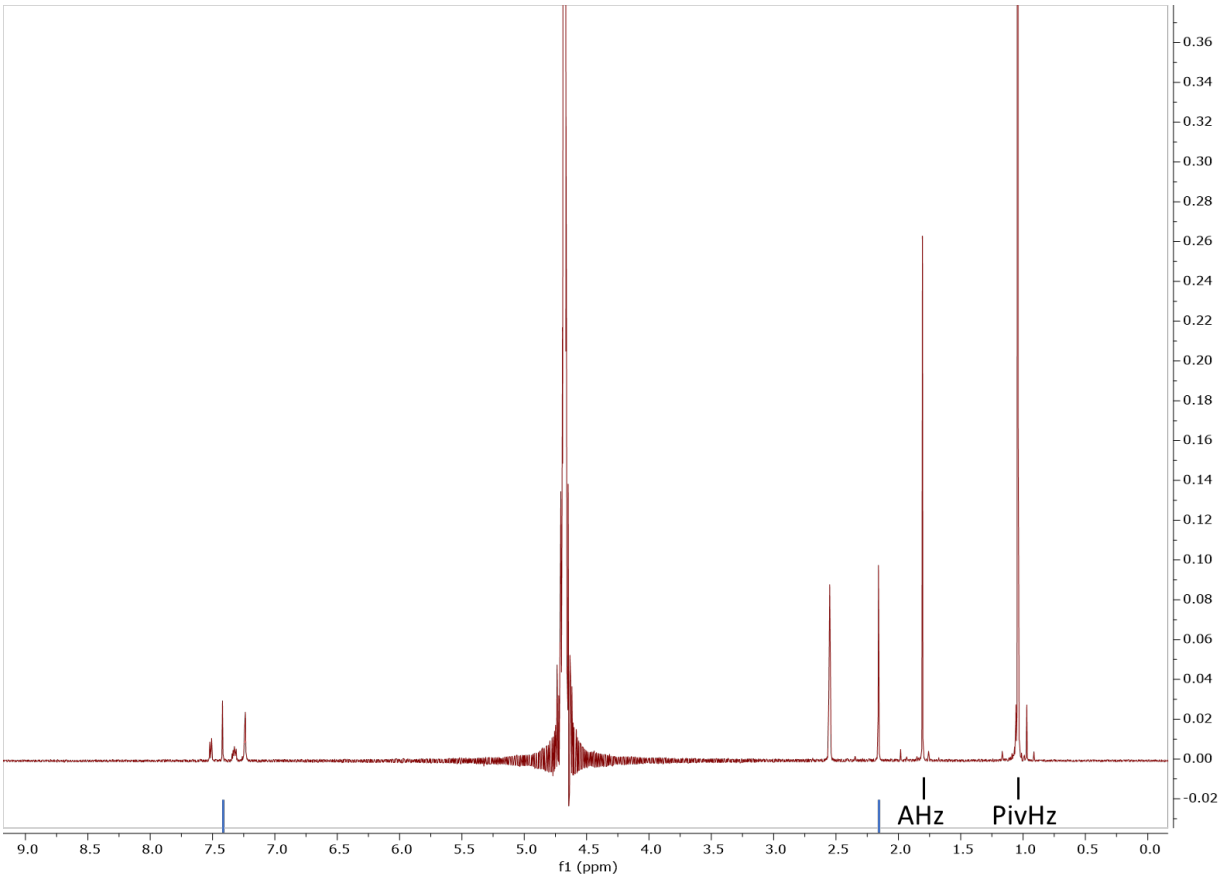

Fig. S10b. ^{1}H NMR spectrum of the degenerate exchange between **1a** and PivHz at pD 12.0 after 15 h.

*L7. Hydrazone exchange between **1a** and CAHz at pD 12.0 at room temperature*

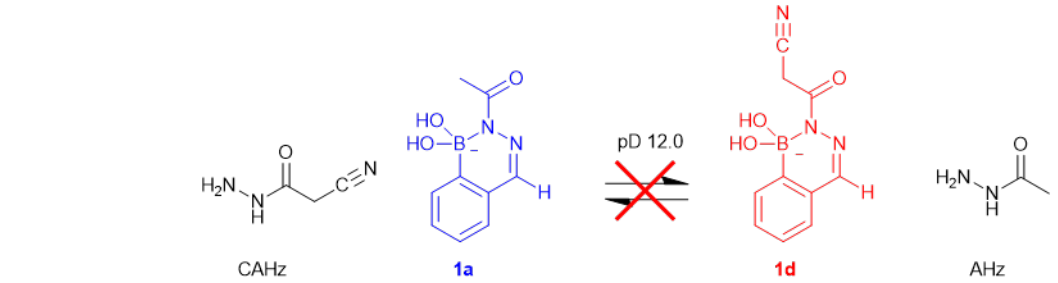

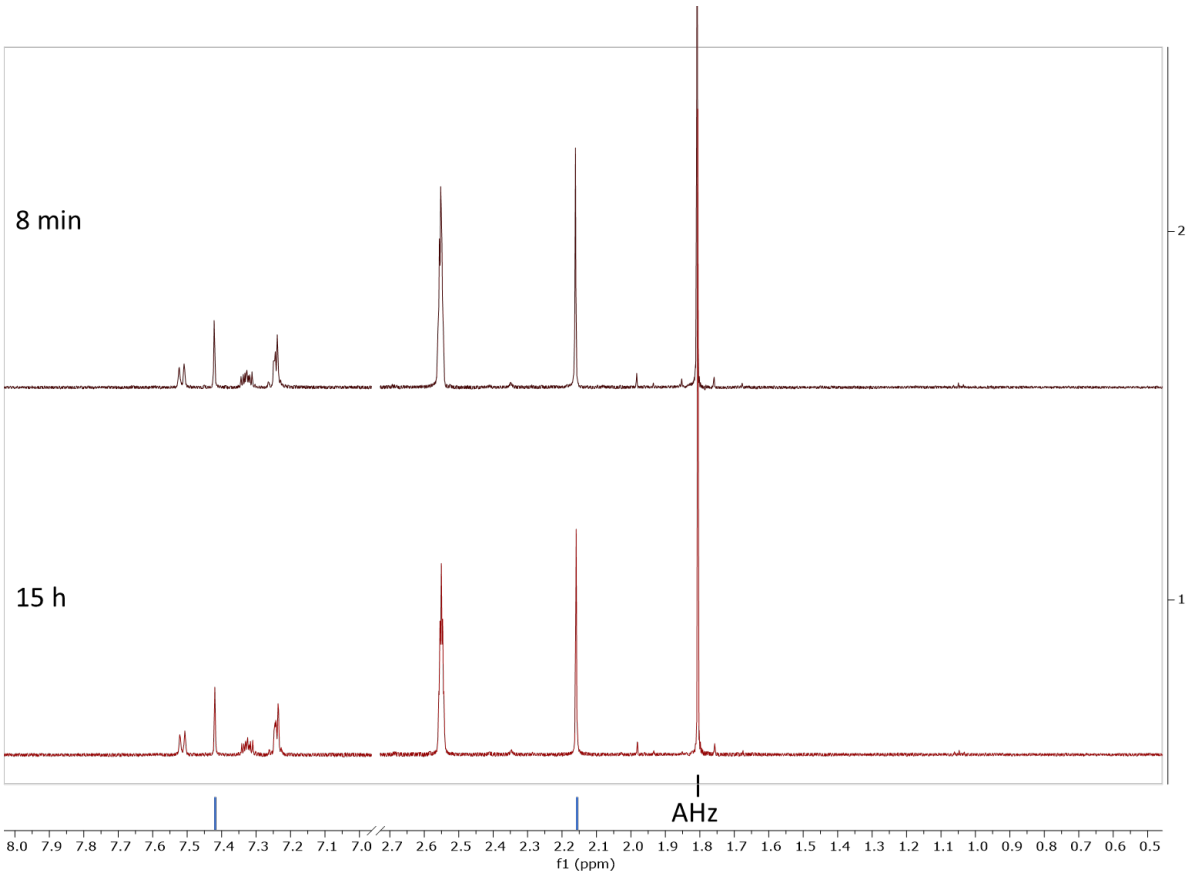

Fig. S11a. ^{1}H NMR spectrum of the degenerate exchange between **1a** and CAHz at pD 12.0. No exchange is observed over 15 hours.

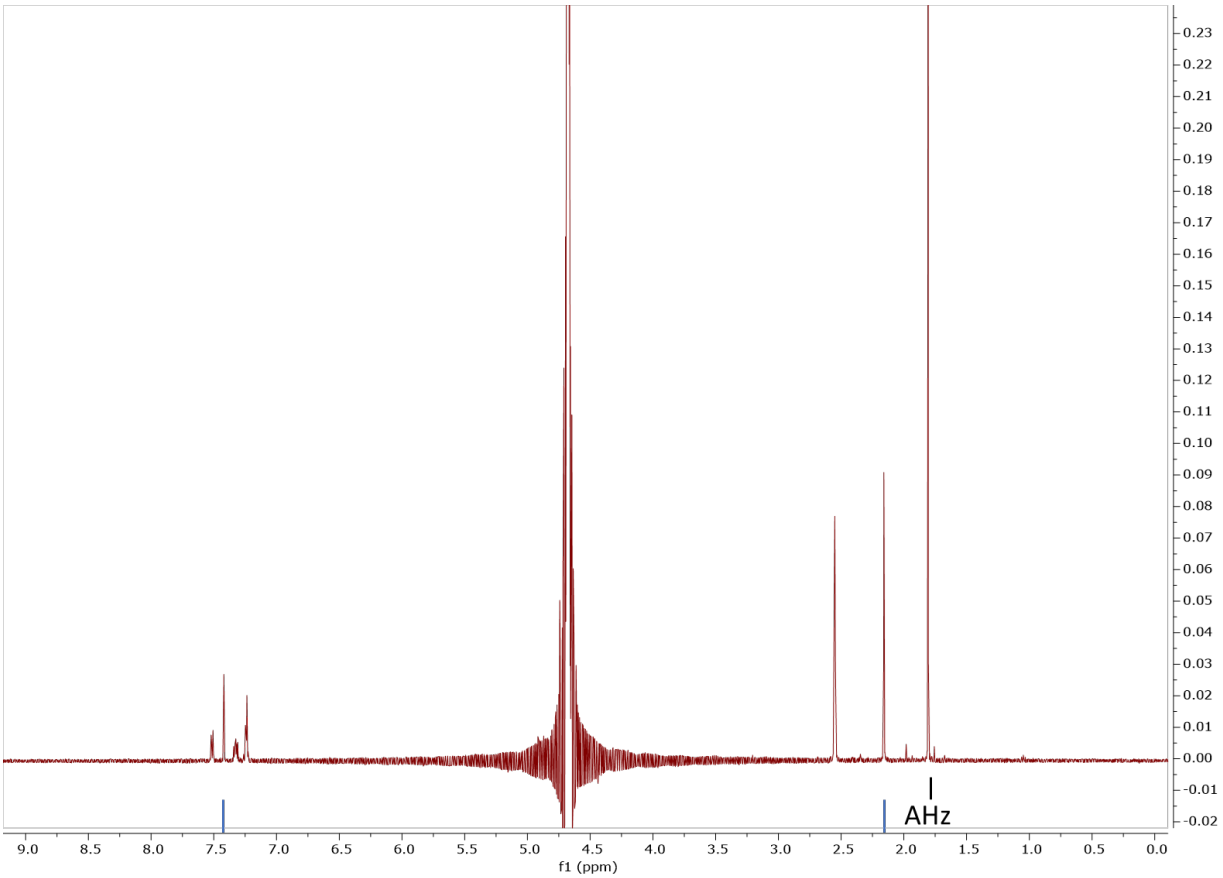

Fig. S11b. Full ^{1}H NMR spectrum of the degenerate exchange between **1a** and CAHz at pD 12.0 after 15 h. No exchange is observed over 15 hours.

*L8. Hydrazone exchange between **1a** and tBCz at pD 12.0 at room temperature*

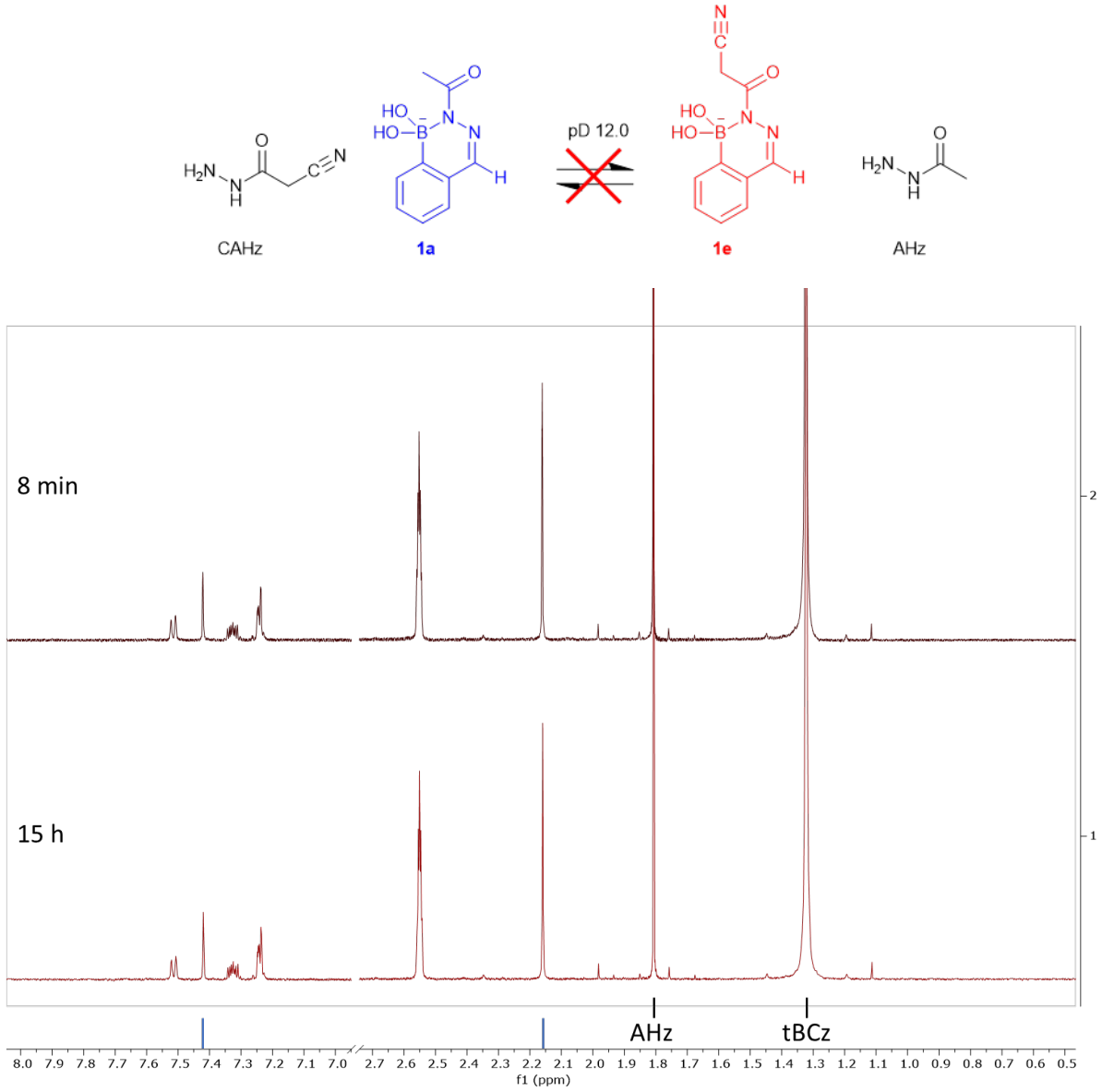

Fig. S12a. ^{1}H NMR spectrum of the degenerate exchange between **1a** and tBCz at pD 12.0. No exchange is observed over 15 hours.

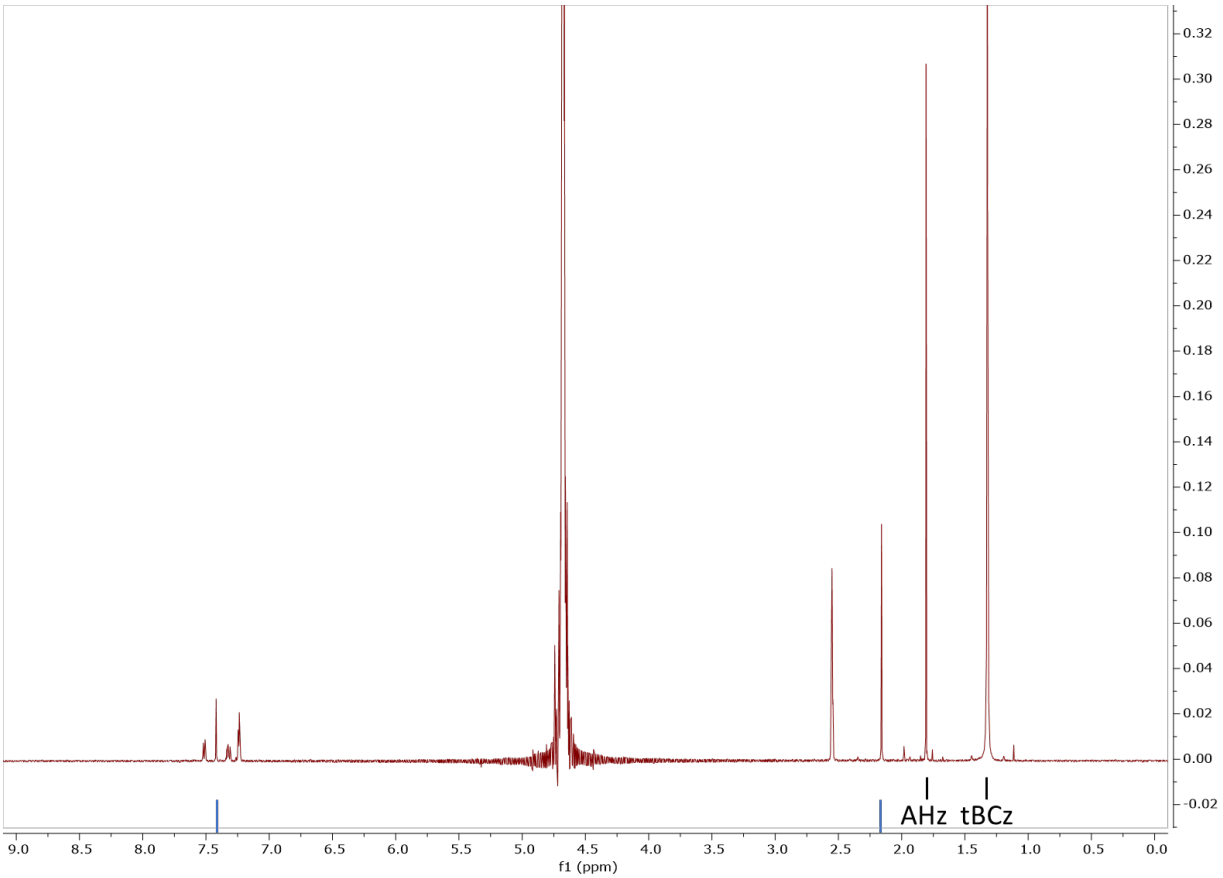

Fig. S12b. Full ^{1}H NMR spectrum of the degenerate exchange between **1a** and tBCz at pD 12.0 after 15 h.

M. Oxime Exchanges with 2a

*M1. Oxime exchange between **2a** and EHA at pD 7.5 at room temperature*

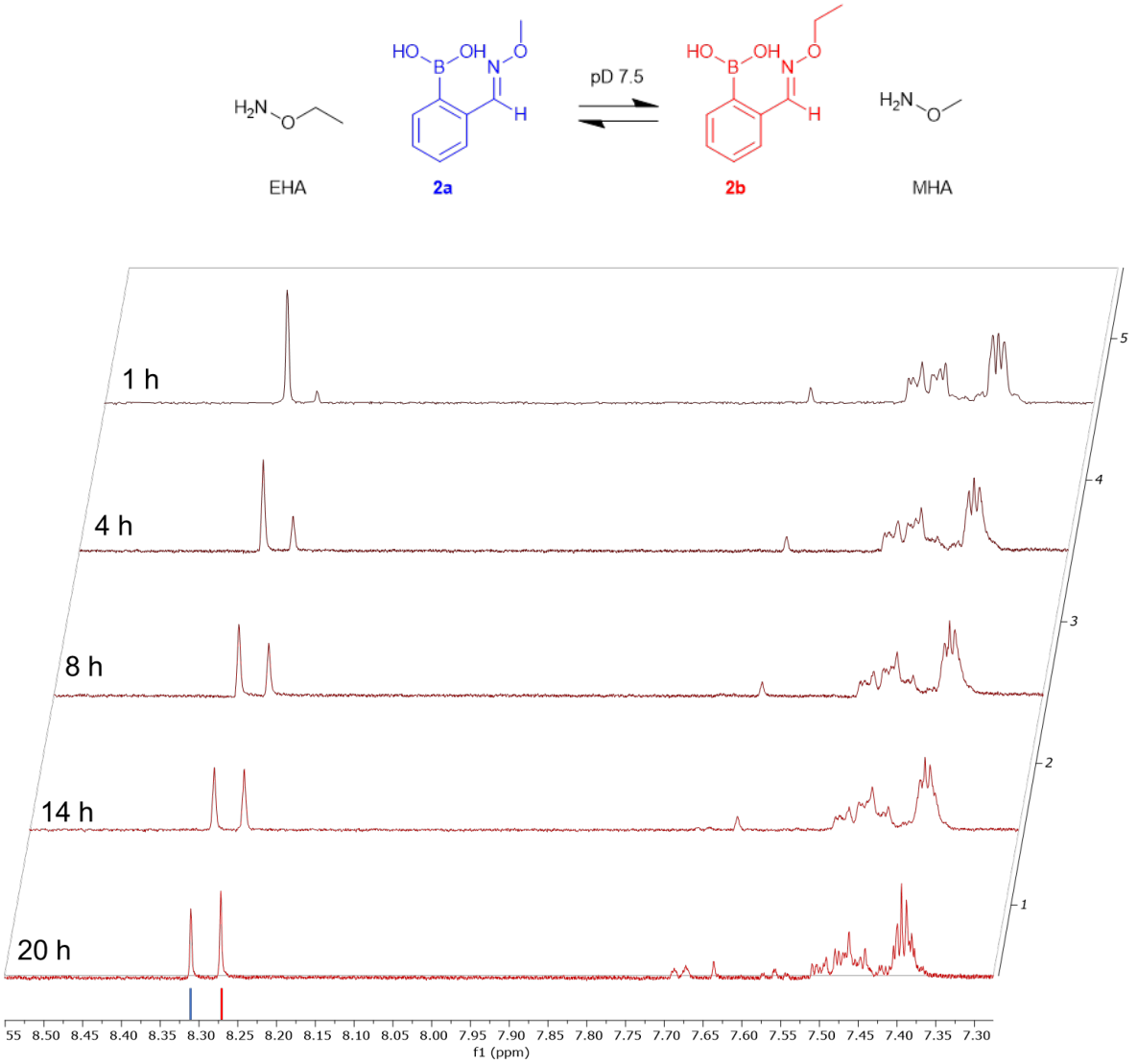

Figure S13a. Aromatic region of the time-course ^{1}H NMR spectra of the degenerate exchange between **2a** and EHA at pD 7.5 (200 mM PB). The ratios between **2a** and **2b** were measured by integrating imine-type CH proton peaks and were confirmed by terminal methyl proton integrations. Dimethyl sulfone (20 μL, 50 mM) was used as an internal standard (δ 3.02).

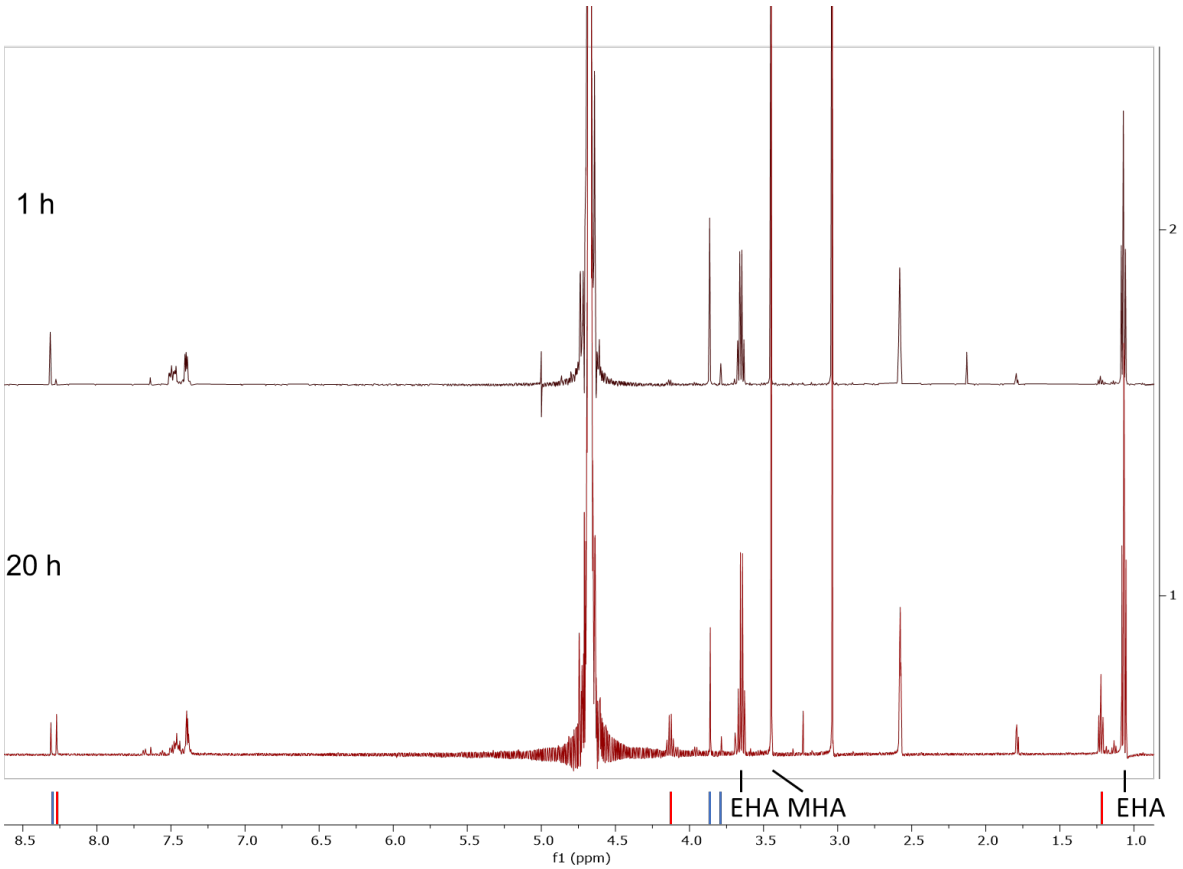

Figure S13b. Time course ^{1}H NMR spectra of the degenerate exchange between **2a** and EHA at pD 7.5 (200 mM PB). The ratios between **2a** and **2b** were measured by integrating imine-type CH proton peaks and were confirmed by terminal methyl proton integrations. Dimethyl sulfone (20 μL, 50 mM) was used as an internal standard (δ 3.02).

*M2. Oxime exchange between **2a** and iPHA at pD 7.5 at room temperature*

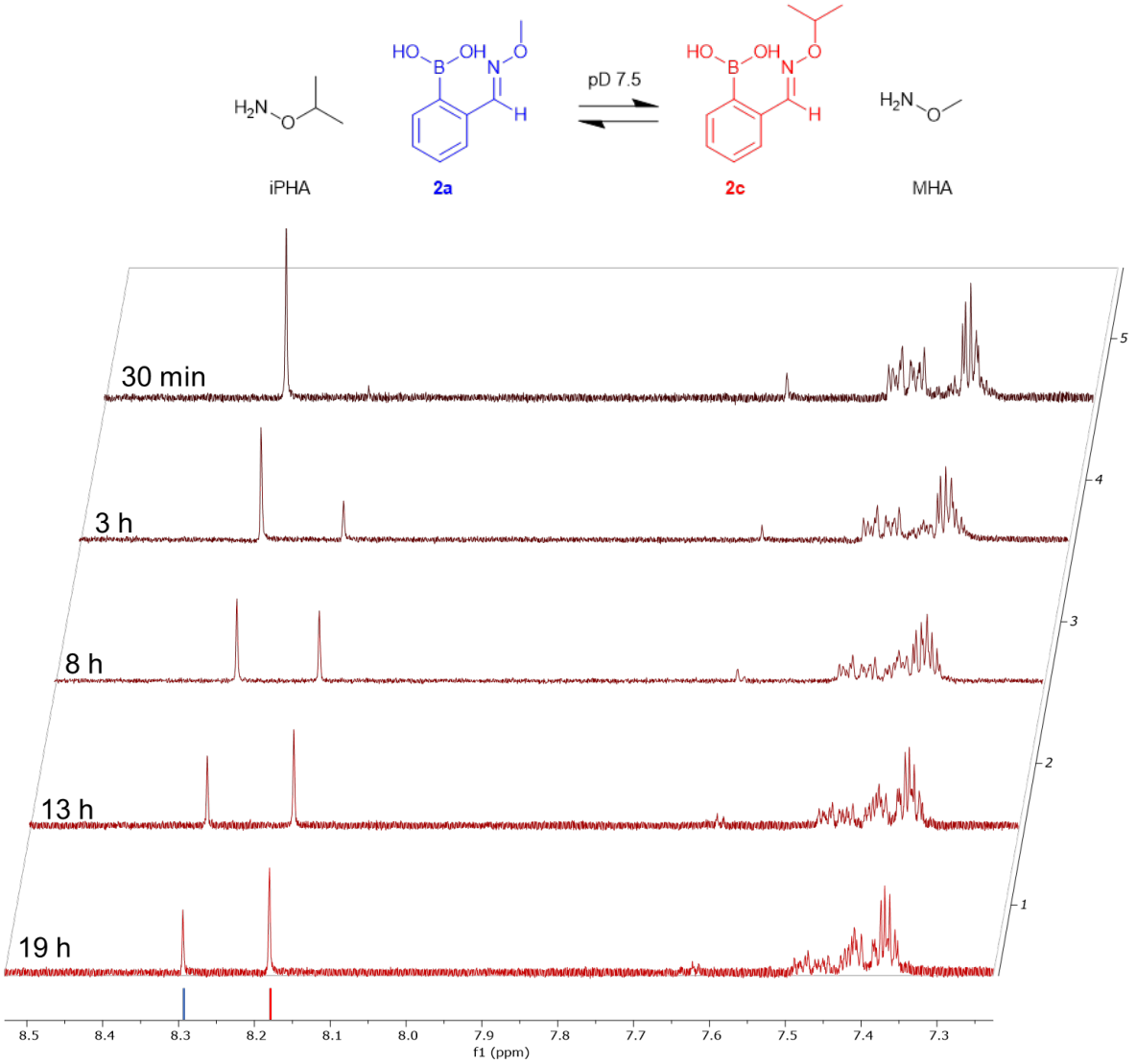

Figure S14a. Aromatic region of the time-course ^{1}H NMR spectra of the degenerate exchange between **2a** and iPHA at pD 7.5 (200 mM PB). The ratios between **2a** and **2c** were measured by integrating imine-type CH proton peaks and were confirmed by terminal methyl proton integrations.

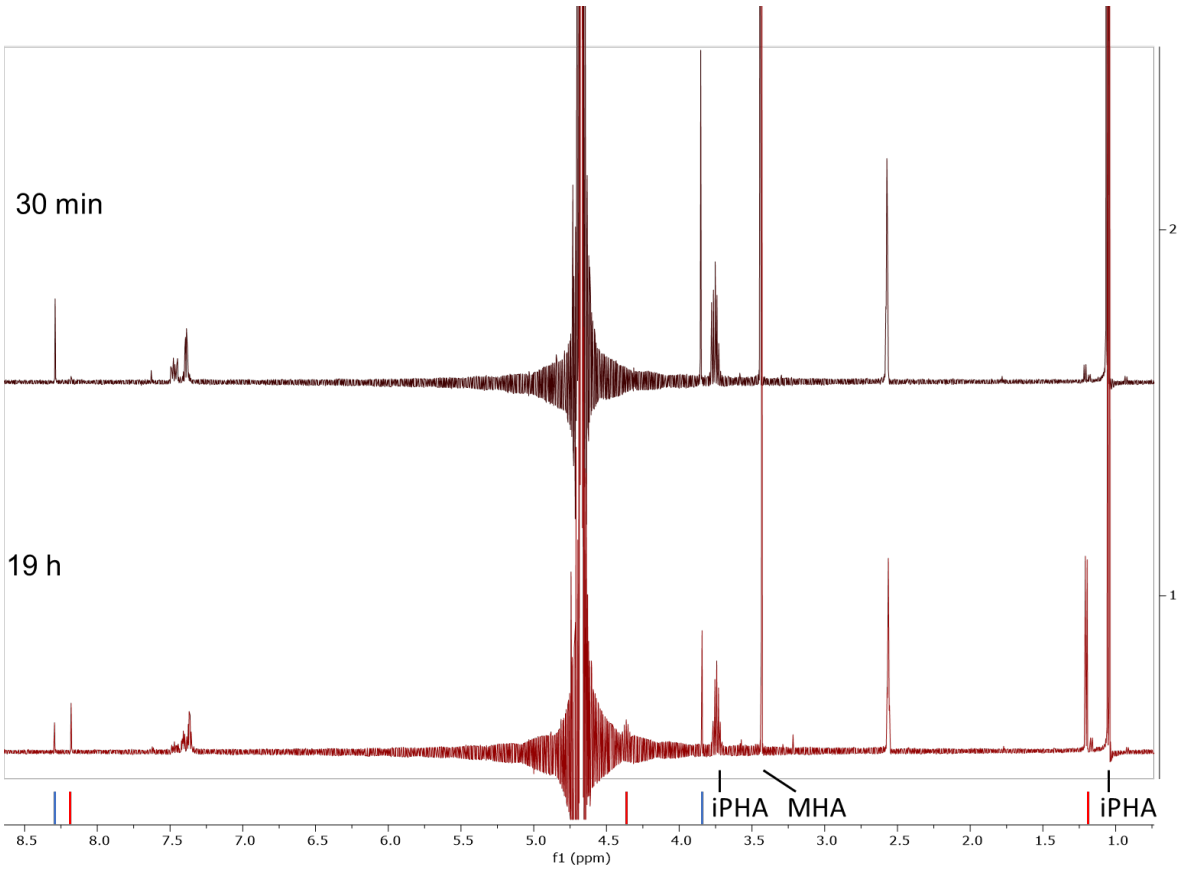

Figure S14b. Time-course ^{1}H NMR spectra of the degenerate exchange between **2a** and iPHA at pD 7.5 (200 mM PB). The ratios between **2a** and **2c** were measured by integrating imine-type CH proton peaks and were confirmed by terminal methyl proton integrations.

*M3. Oxime exchange between **2a** and tBHA at pD 7.5 at room temperature*

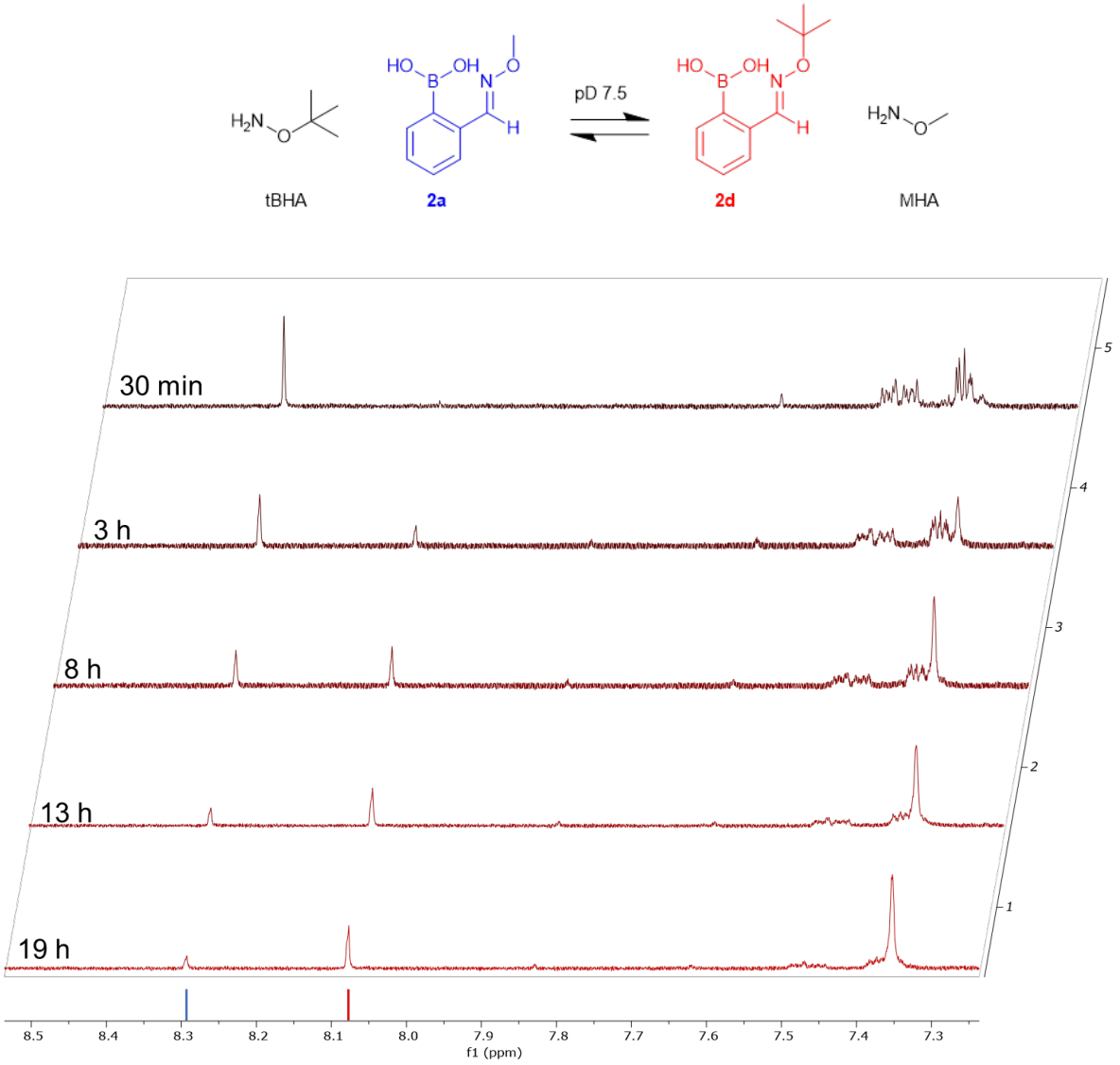

Figure S15a. Aromatic region of the time-course ^{1}H NMR spectra of the degenerate exchange between **2a** and tBHA at pD 7.5 (200 mM PB). The ratios between **2a** and **2d** were measured by integrating imine-type CH proton peaks and were confirmed by terminal methyl proton integrations.

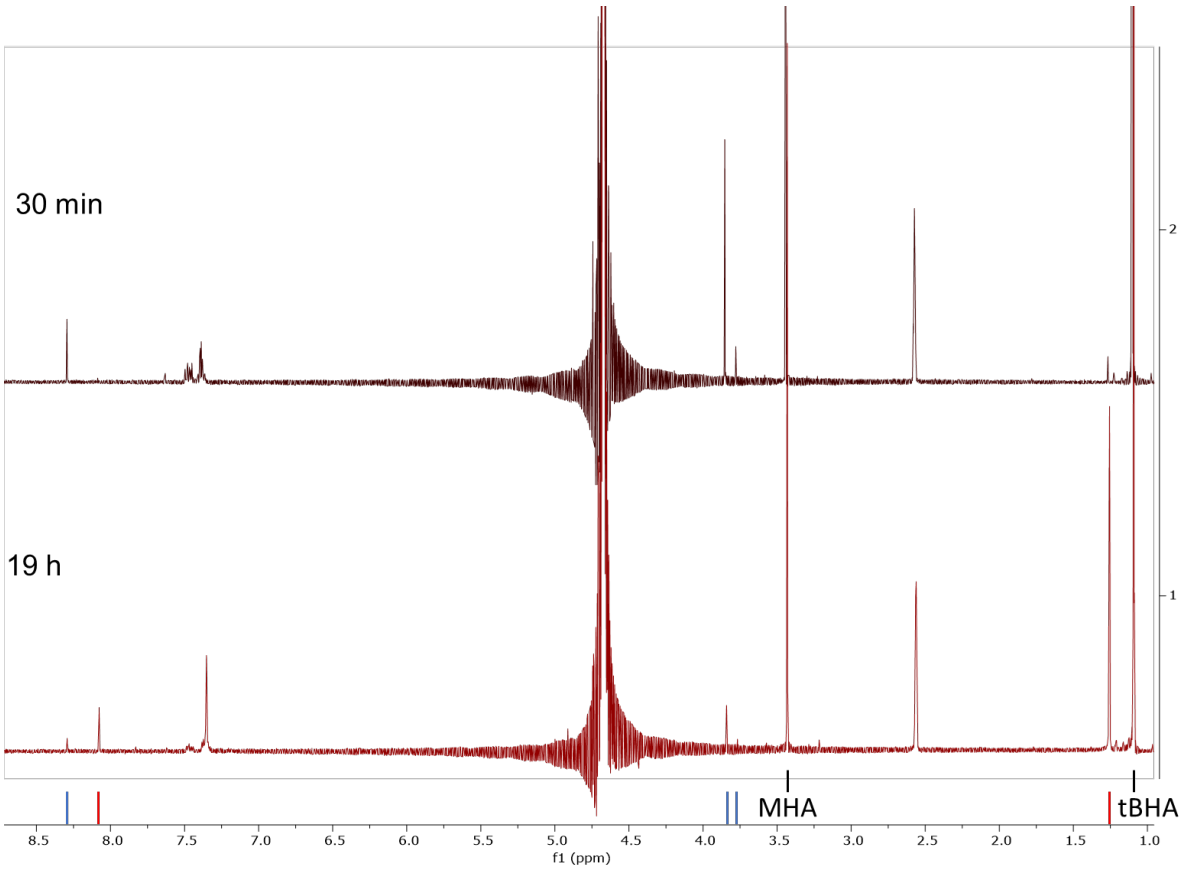

Figure S15b. Time-course ^{1}H NMR spectra of the degenerate exchange between **2a** and tBHA at pD 7.5 (200 mM PB). The ratios between **2a** and **2d** were measured by integrating imine-type CH proton peaks and were confirmed by terminal methyl proton integrations.

*M4. Oxime exchange between **2a** and EHA at pD 12.0 at room temperature*

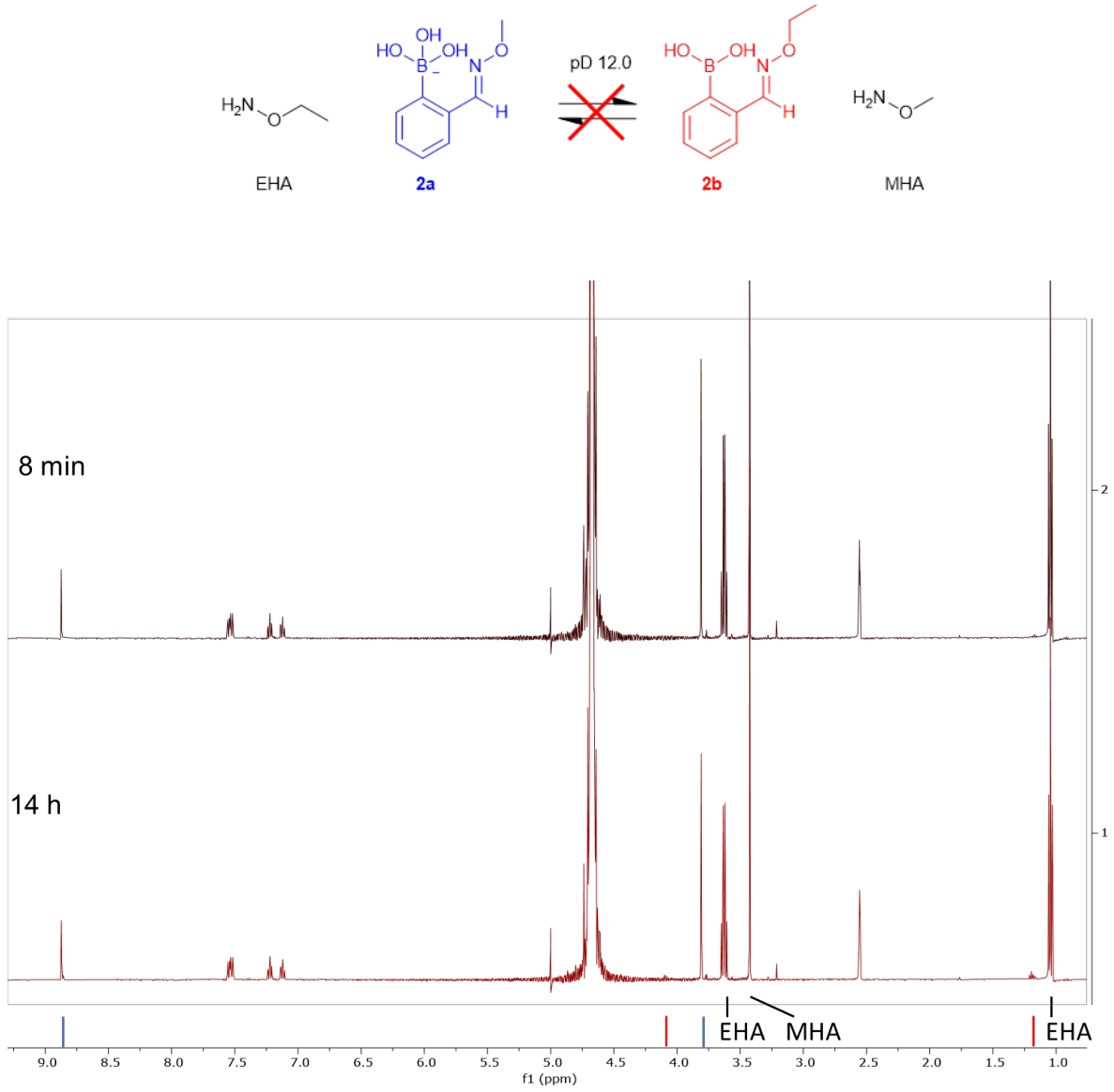

Figure S16. Aromatic region of the time-course ^{1}H NMR spectra of the degenerate exchange between **2a** and EHA at pD 12.0 (200 mM PB). The ratios between **2a** and **2b** were measured by integrating terminal methyl protons.

*M5. Oxime exchange between **2a** and iPHA at pD 12.0 at room temperature*

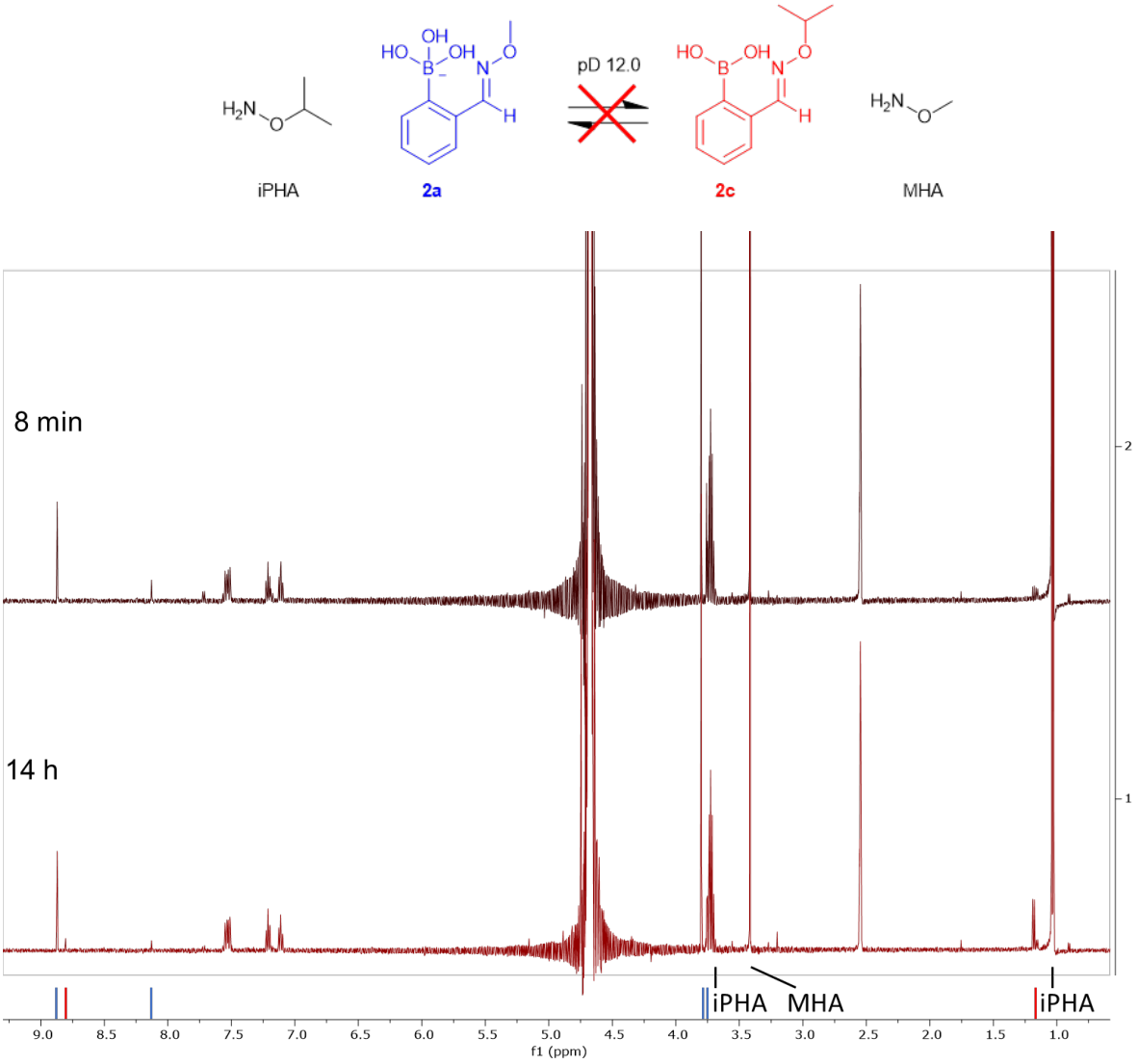

Figure S17. Aromatic region of the time-course ^{1}H NMR spectra of the degenerate exchange between **2a** and iPHA at pD 12.0 (200 mM PB). The ratios between **2a** and **2c** were measured by integrating terminal methyl protons.

*M6. Oxime exchange between **2a** and tBHA at pD 12.0 at room temperature*

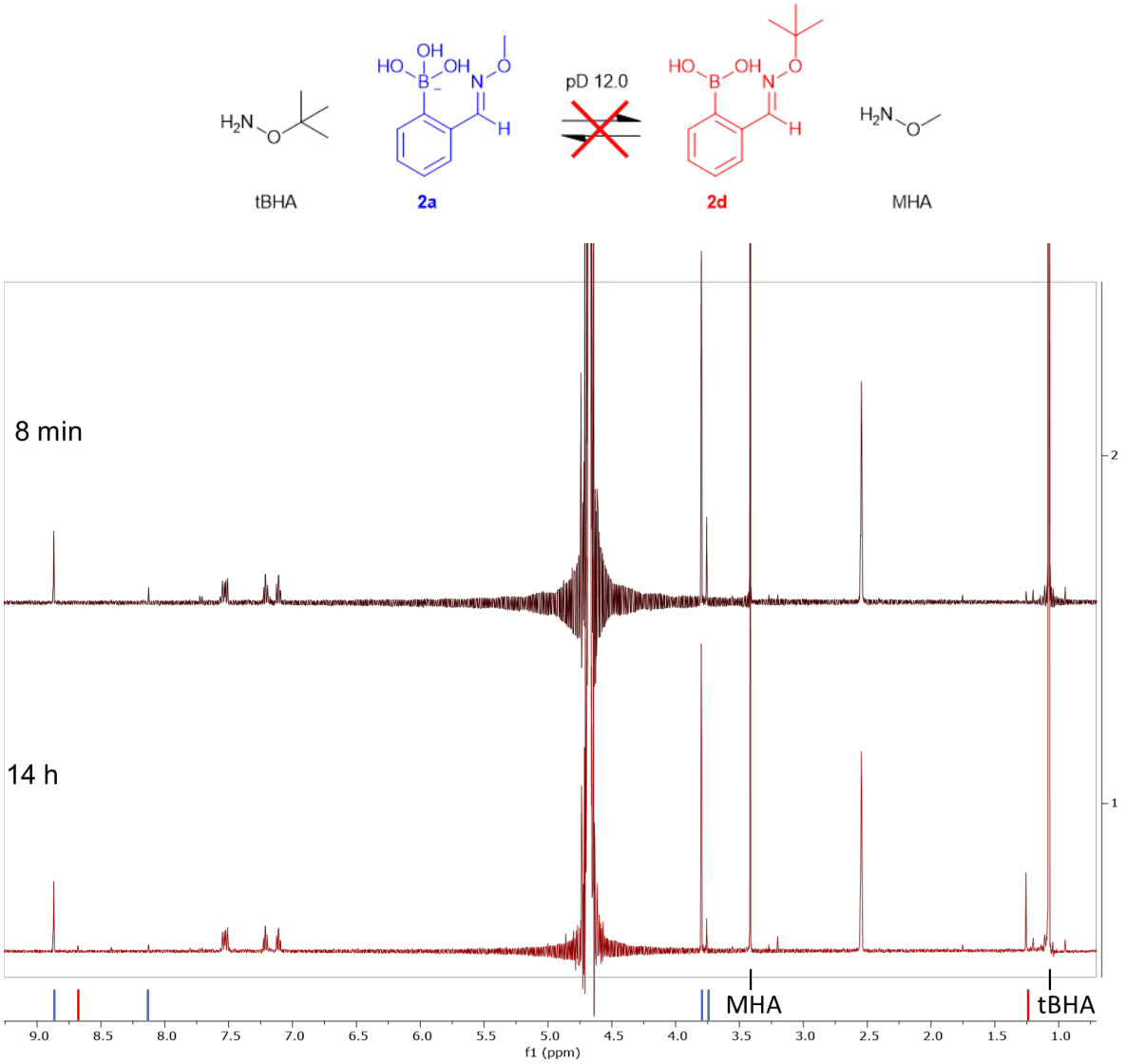

Figure S18. Aromatic region of the time-course ^{1}H NMR spectra of the degenerate exchange between **2a** and iPHA at pD 12.0 (200 mM PB). The ratios between **2a** and **2d** were measured by integrating terminal methyl protons.

N. Formation of hydrazone 3

The formation kinetics of **3** was measured, following the general procedure (section D). Data were fitted into the second-order reversible kinetic model (section F).

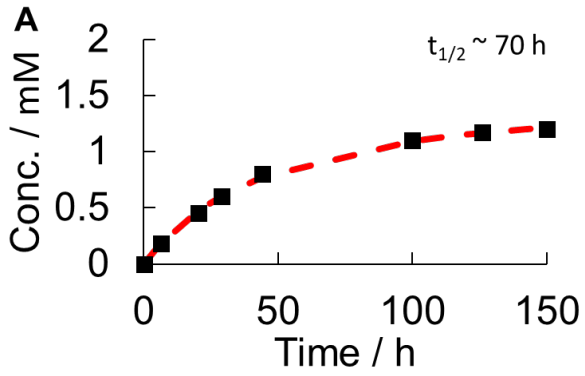

Figure S19. Reaction kinetics for formation of **3**. Fitting to the reversible kinetic model yields $k_1 = 2.6 \times 10^{-3}$ M^{-1} s^{-1} and $k_{-1} = 4.8 \times 10^{-7}$ s^{-1}.

O. Oxidation of 2a at pD 7.5

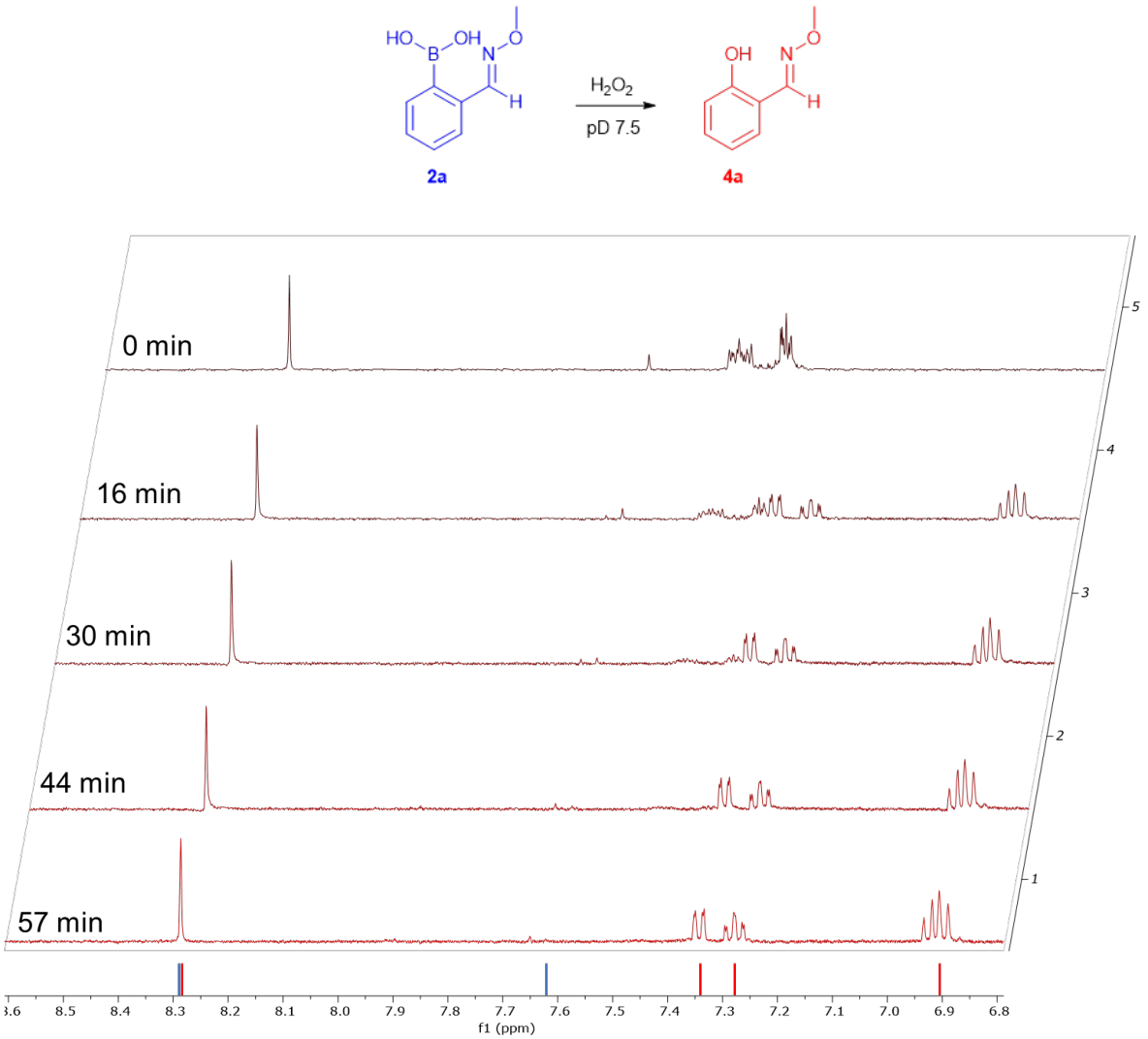

Figure S20a. Aromatic region of the time-course ^{1}H NMR spectra of oxidation of **2a** at pD 7.5. Dimethyl sulfone (20 µL, 50 mM) was used as an internal standard (δ 3.02). Imine-type CH proton peaks of **2a** and **4a** overlap at pD 7.5. The two protons are distinguishable when the oxidation is carried out at pD 6.5 (Fig. S21a-b). The ratio between **2** and **5** was determined by the ratio of the terminal methyl protons (δ 3.85 – 3.76 for **2**; δ 3.87 for **5**).

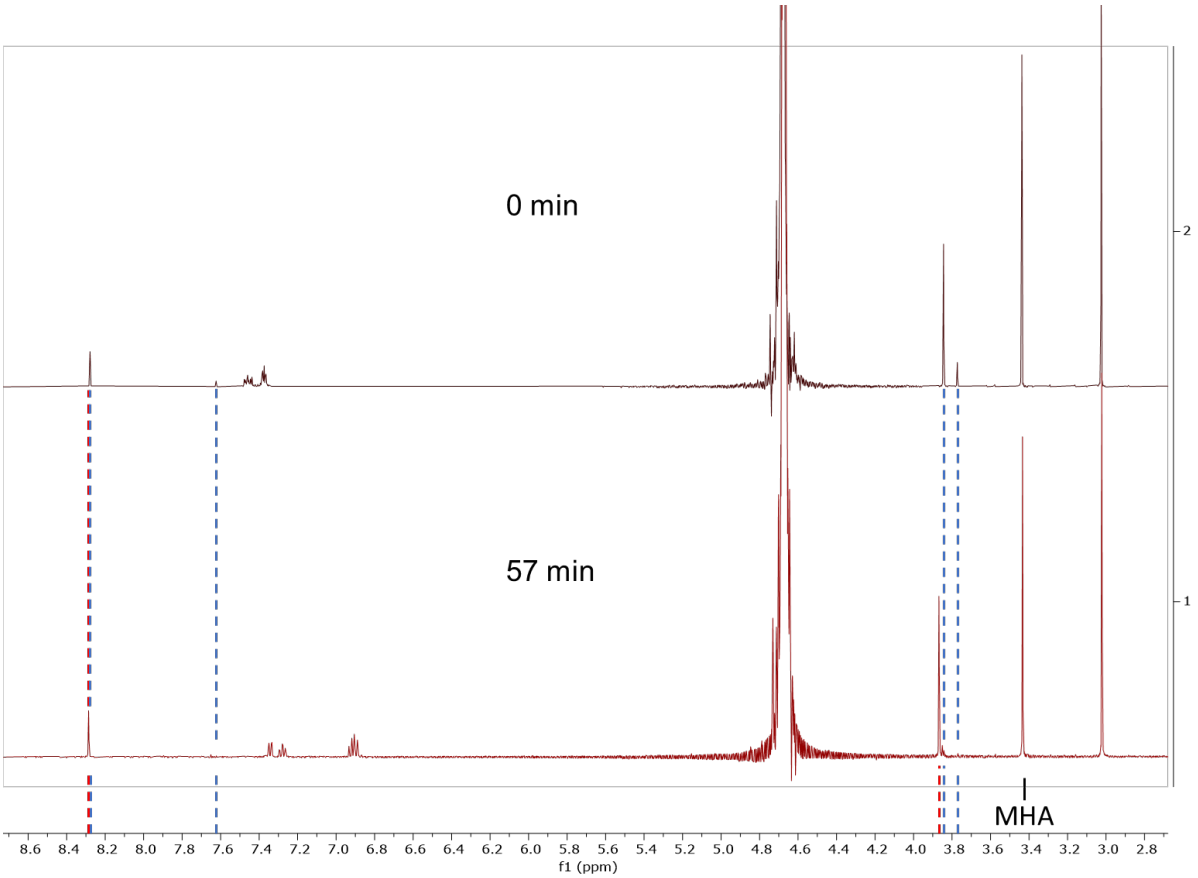

Figure S20b. Time-course ^{1}H NMR spectra of oxidation of **2a** at pD 7.5. Dimethyl sulfone (20 μL, 50 mM) was used as an internal standard (δ 3.02). Imine-type CH proton peaks of **2a** and **4a** were found to overlap at pD 7.5. The two protons are distinguishable when the oxidation is carried out at pD 6.5 (Fig. S21a-b). The ratio between **2** and **5** was determined by the ratio of the terminal methyl protons (δ 3.85 – 3.76 for **2**; δ 3.87 for **5**).

P. Oxidation of 2a at pD 6.5

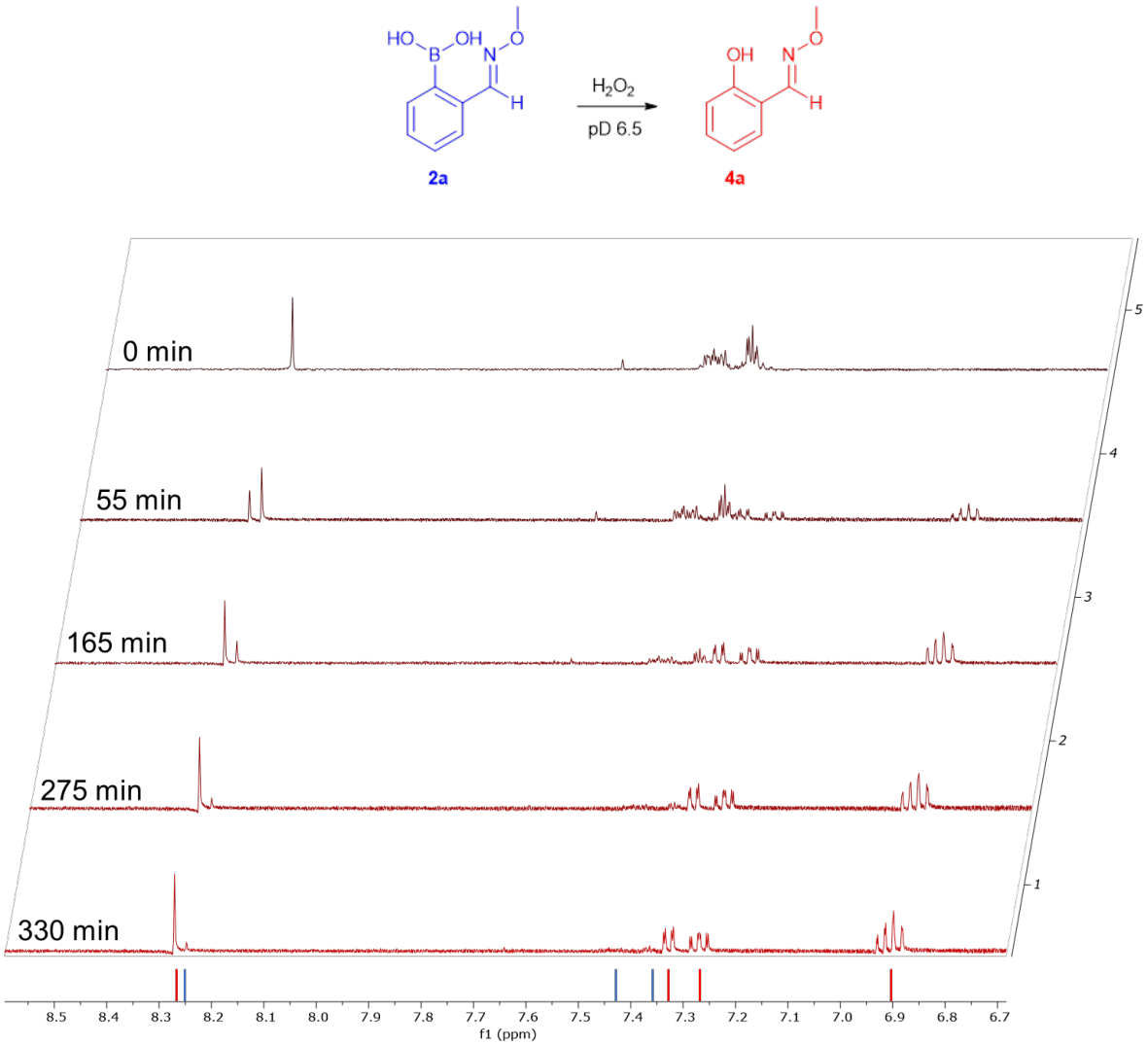

Figure S21a. Aromatic region of the time-course ^{1}H NMR spectra of oxidation of **2a** at pD 6.5. Imine-type CH proton peaks of **2a** and **4a** are distinguishable at pD 6.5.

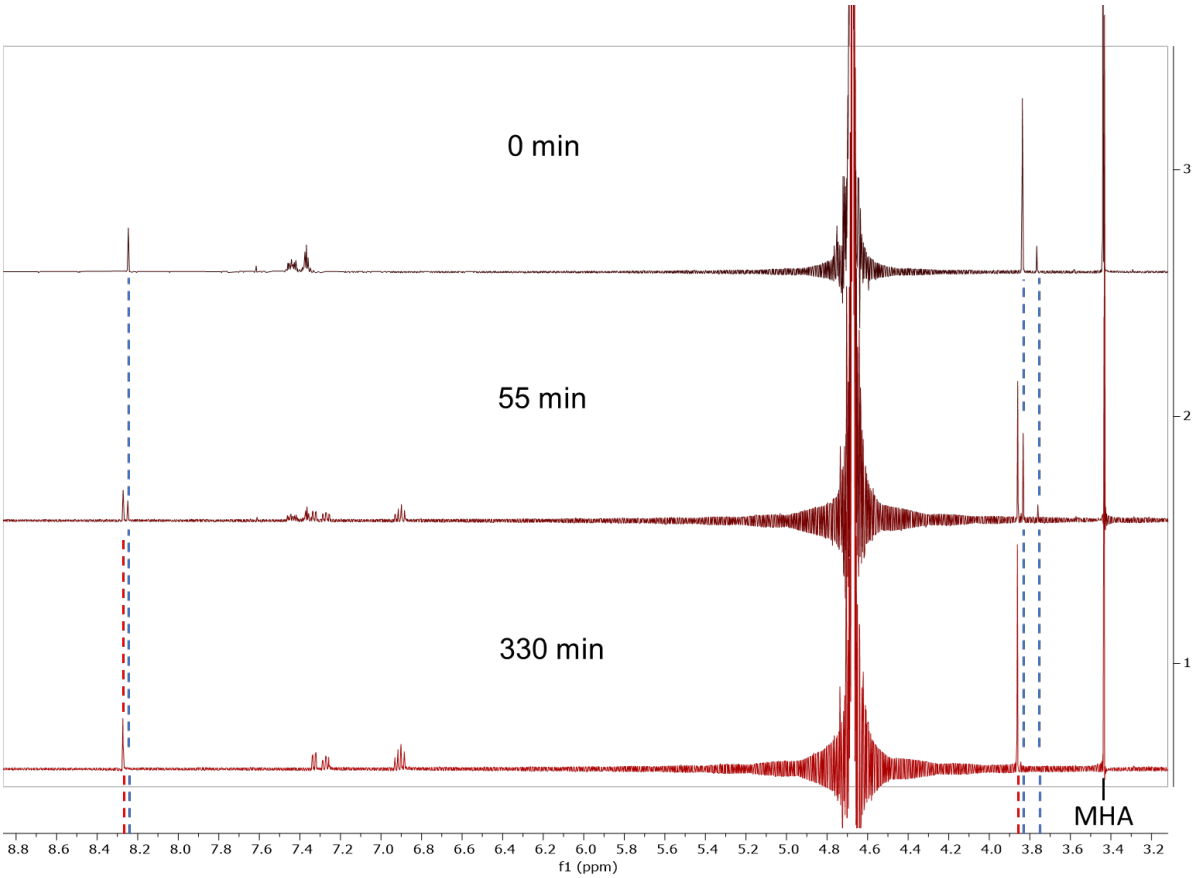

Figure S21b. Aromatic region of the time-course ^{1}H NMR spectra of oxidation of **2a** at pD 6.5. Imine-type CH proton peaks of **2a** and **4a** are distinguishable at pD 6.5.

Q. Oxidation of 1a at pD 7.5

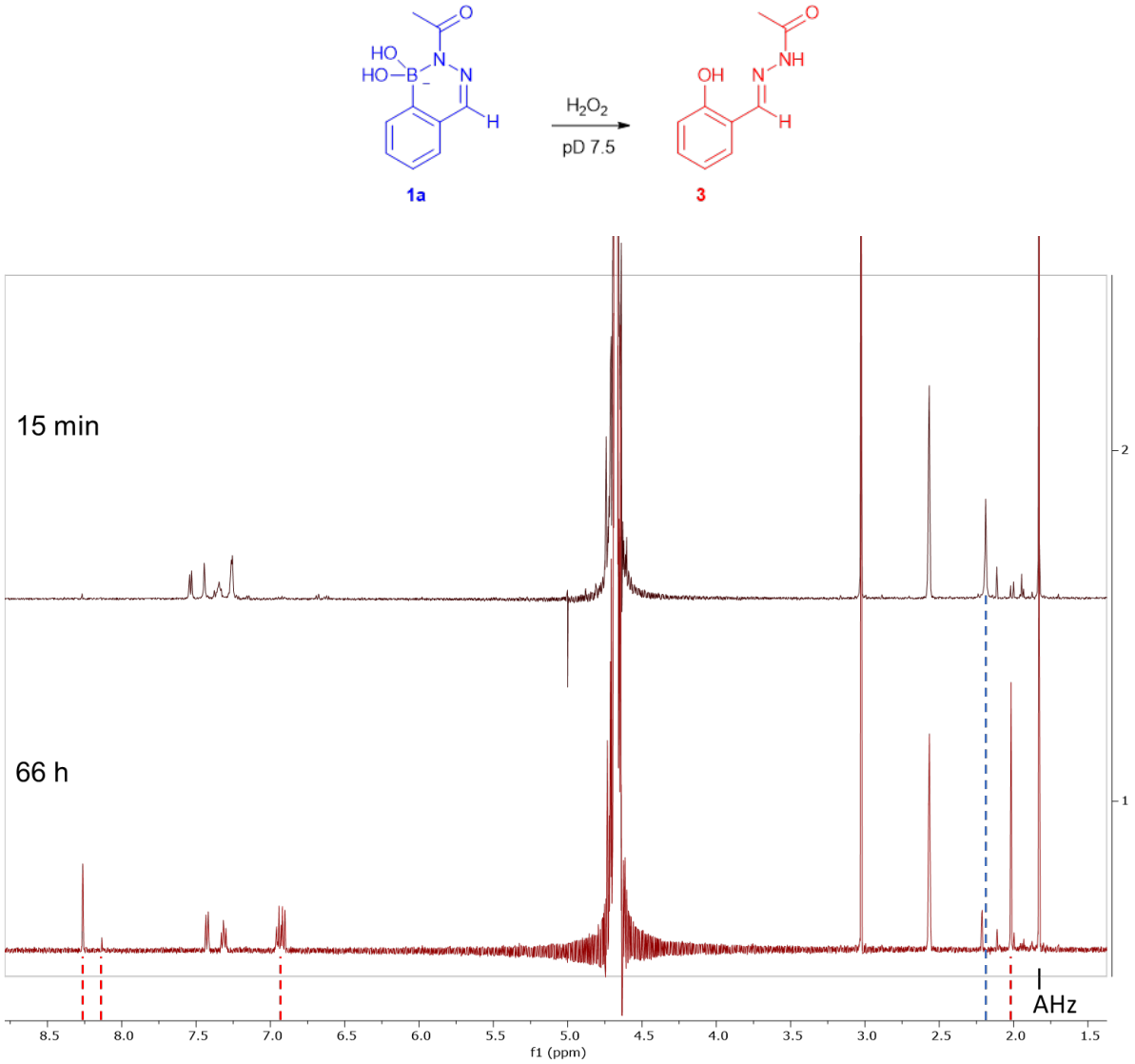

Figure S22. Initial and final ^{1}H NMR spectra of oxidation of **1a** at pD 7.5.

R. Hydrazone Exchanges with 3

*R1. Hydrazone exchange between **3** and iBHz at pD 7.5 at room temperature*

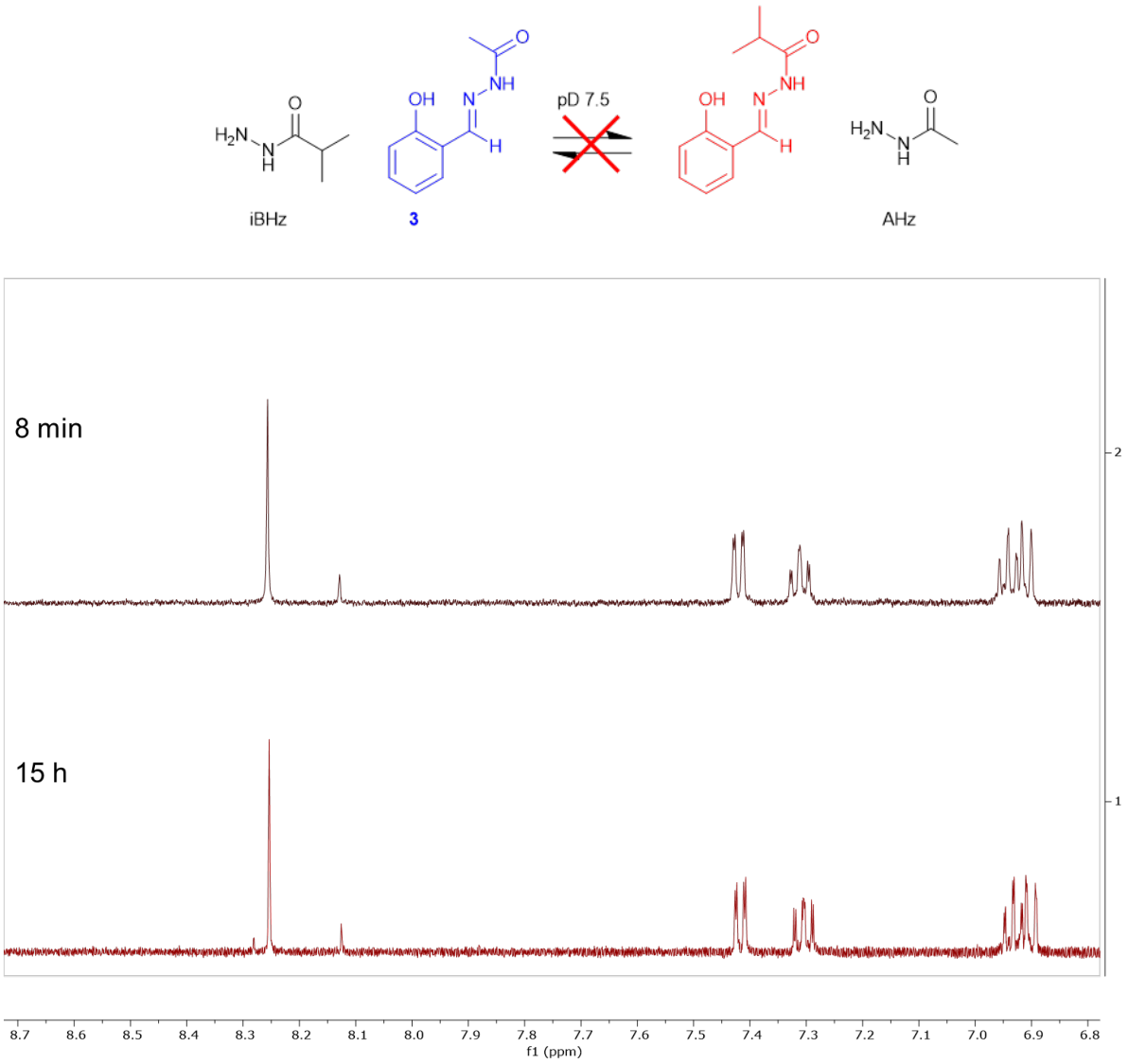

Figure S23. Aromatic region of the time-course ^{1}H NMR spectra of the degenerate exchange between **3** and iBHz at pD 7.5 (200 mM PB). No exchange was observed over 15 hours.

*R2. Hydrazone exchange between **3** and PivHz at pD 7.5 at room temperature*

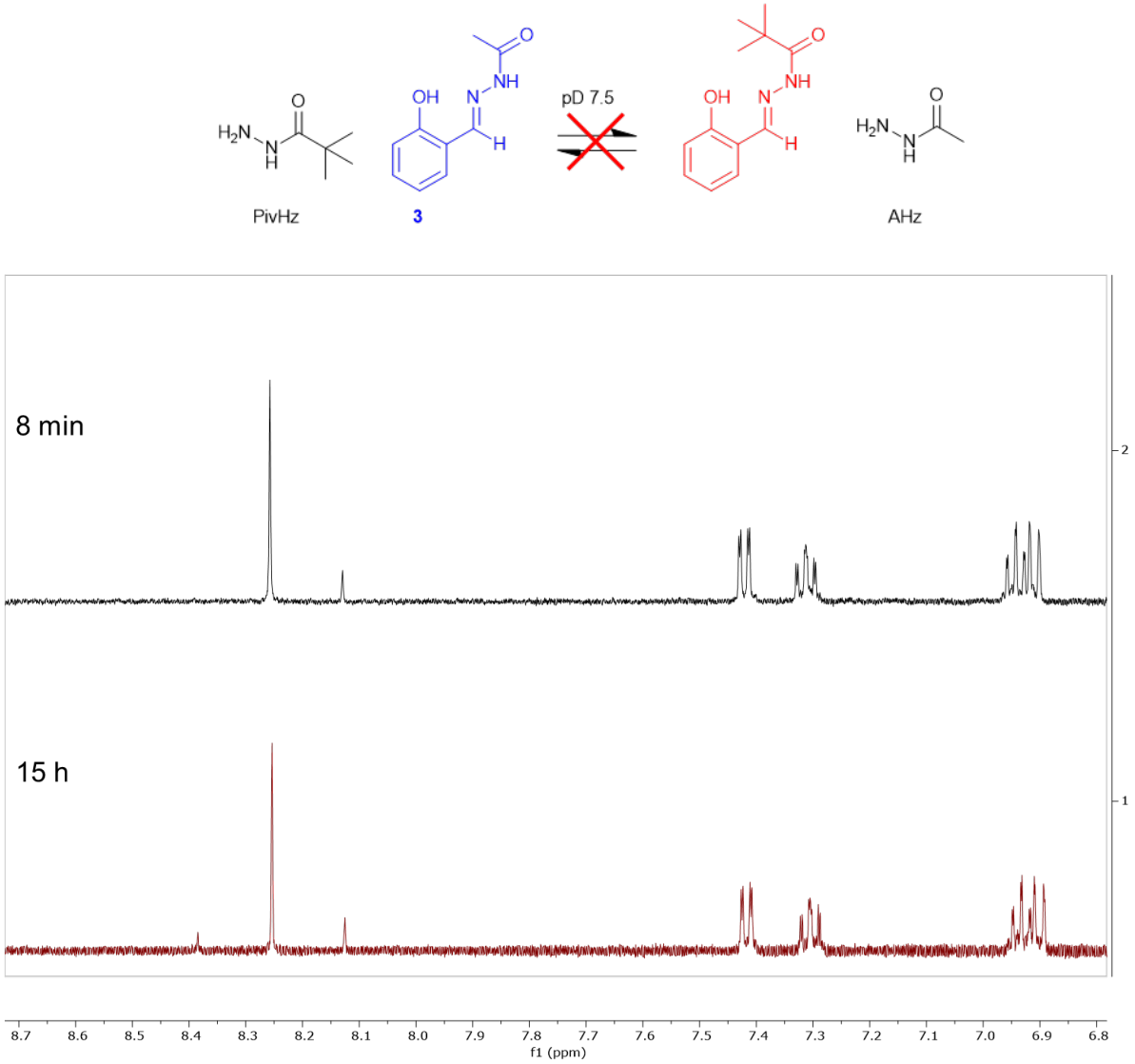

Figure S24. Aromatic region of the time-course ^{1}H NMR spectra of the degenerate exchange between **3** and PivHz at pD 7.5 (200 mM PB). No noticeable exchange was observed over 15 hours.

*R3. Hydrazone exchange between **3** and CAHz at pD 7.5 at room temperature*

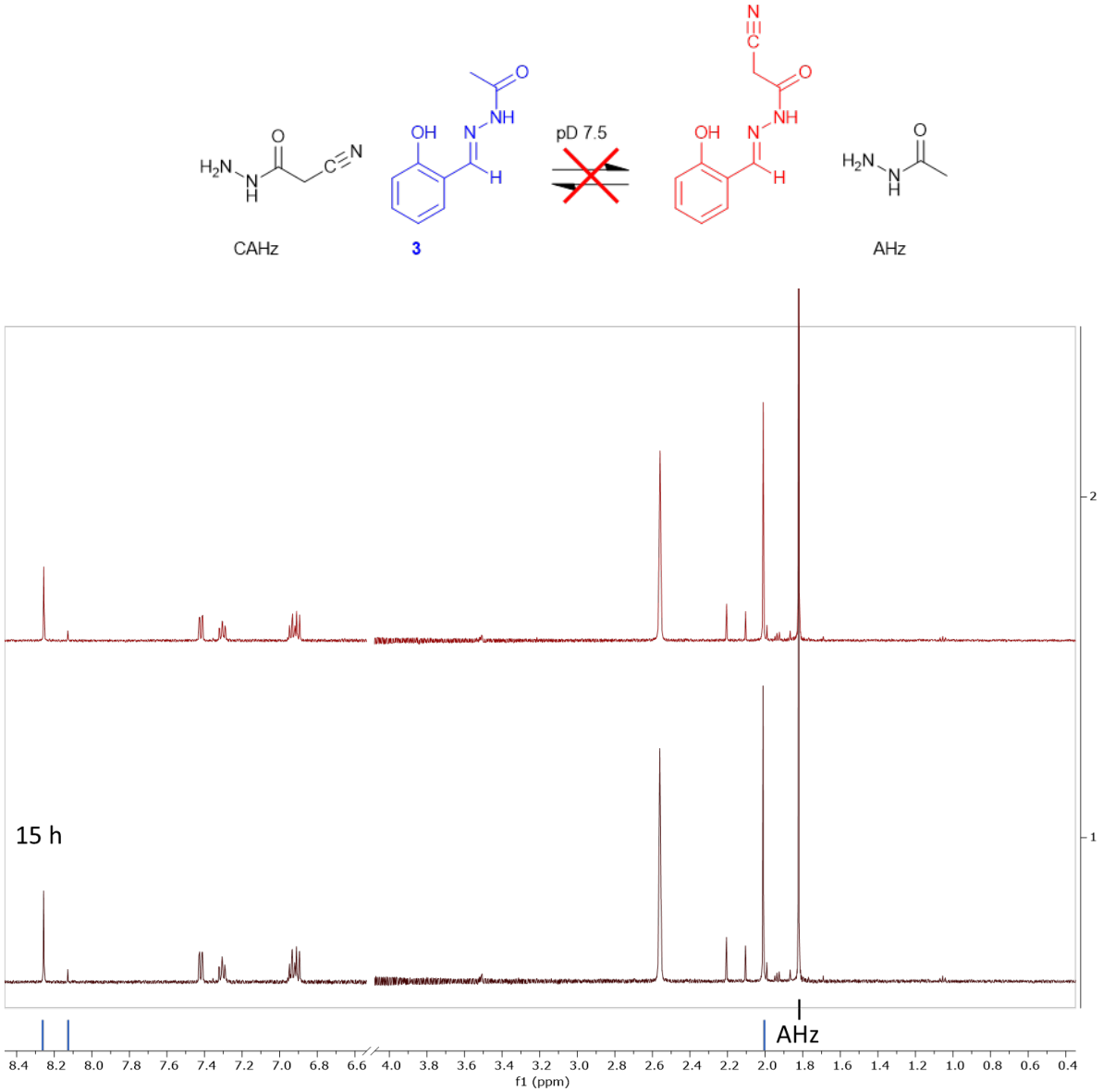

Figure S25a. Aromatic region of the time-course ^{1}H NMR spectra of the degenerate exchange between **3** and CAHz at pD 7.5 (200 mM PB). No exchange was observed over 15 hours.

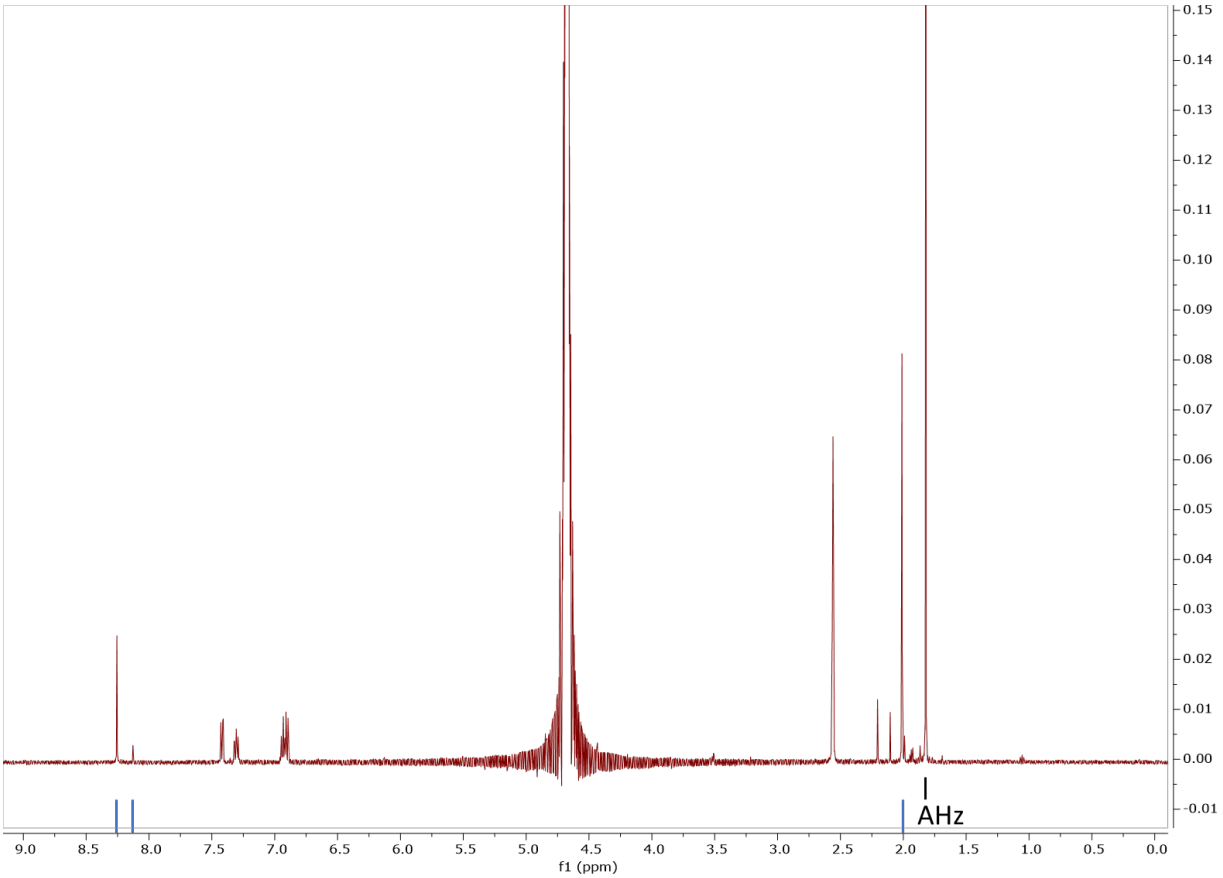

Figure S25b. Full ^{1}H NMR spectrum of the degenerate exchange between **3** and CAHz at pD 7.5 (200 mM PB) after 15 h.

*R4. Hydrazone exchange between **3** and tBCz at pD 7.5 at room temperature*

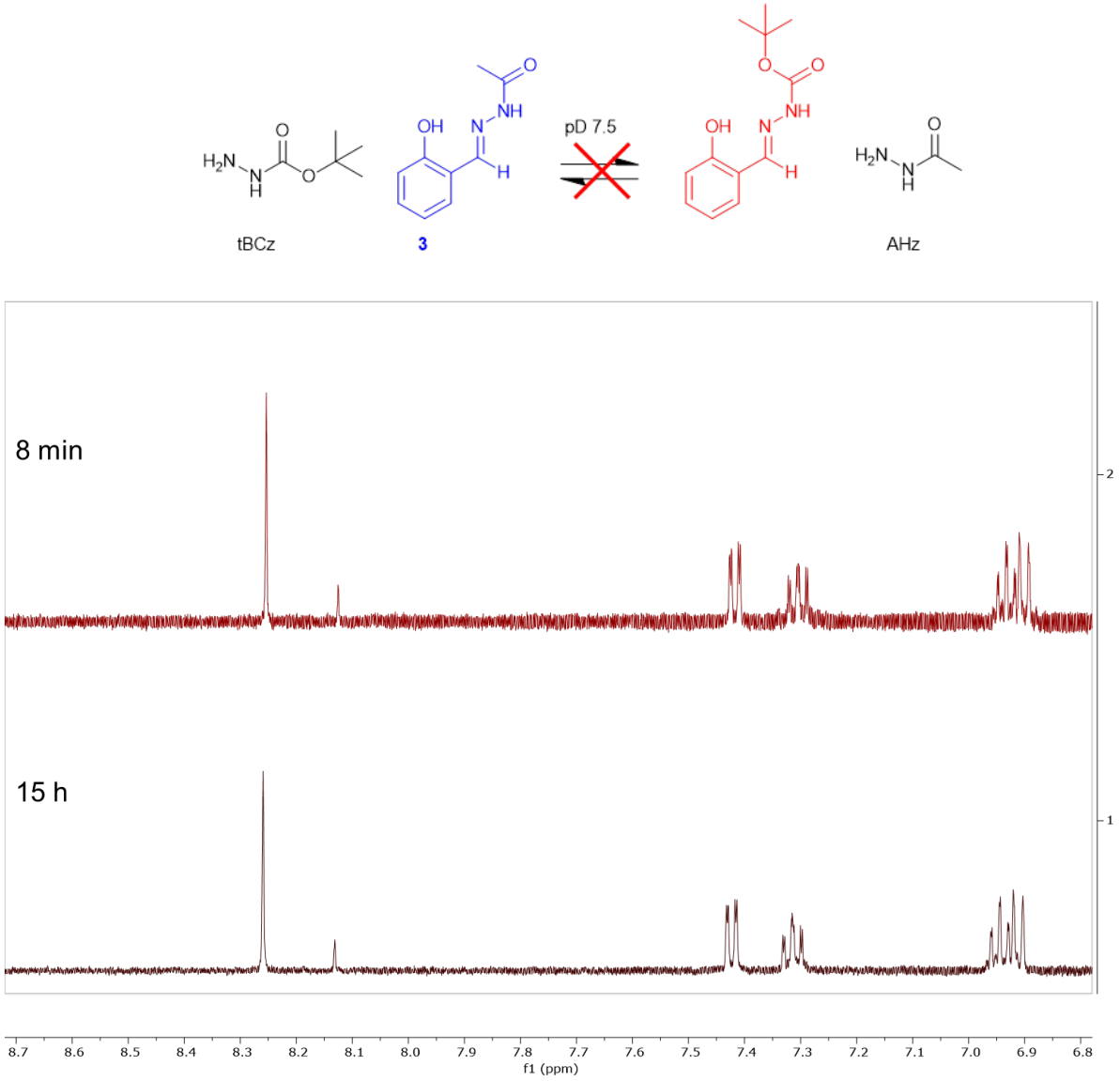

Figure S26a. Aromatic region of the time-course ^{1}H NMR spectra of the degenerate exchange between **3** and tBCz at pD 7.5 (200 mM PB). No exchange was observed over 15 hours.

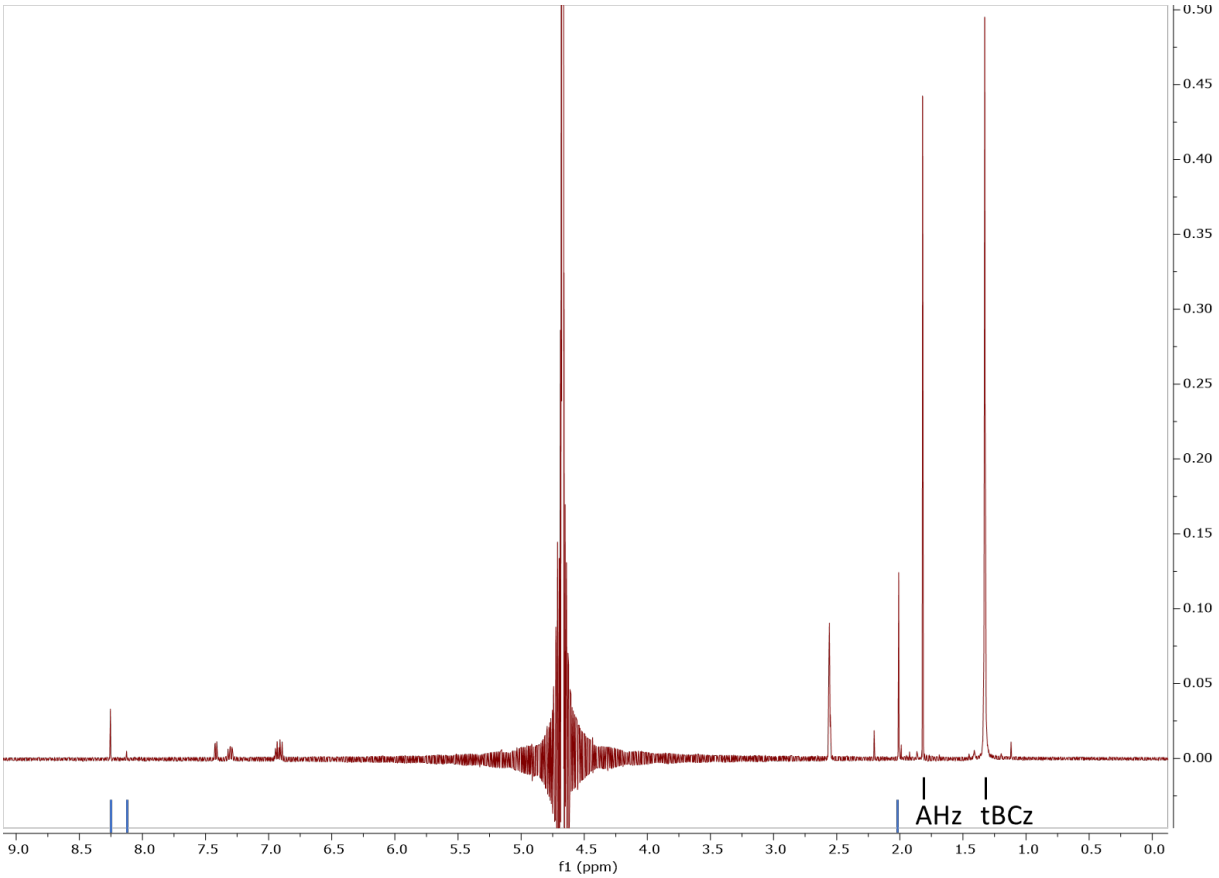

Figure S26b. Full ^{1}H NMR of the degenerate exchange between **3** and tBCz at pD 7.5 (200 mM PB) after 15 h.

S. Oxime Exchanges with 4a

*S1. Oxime exchange between **4a** and EHA at pD 7.5 at room temperature*

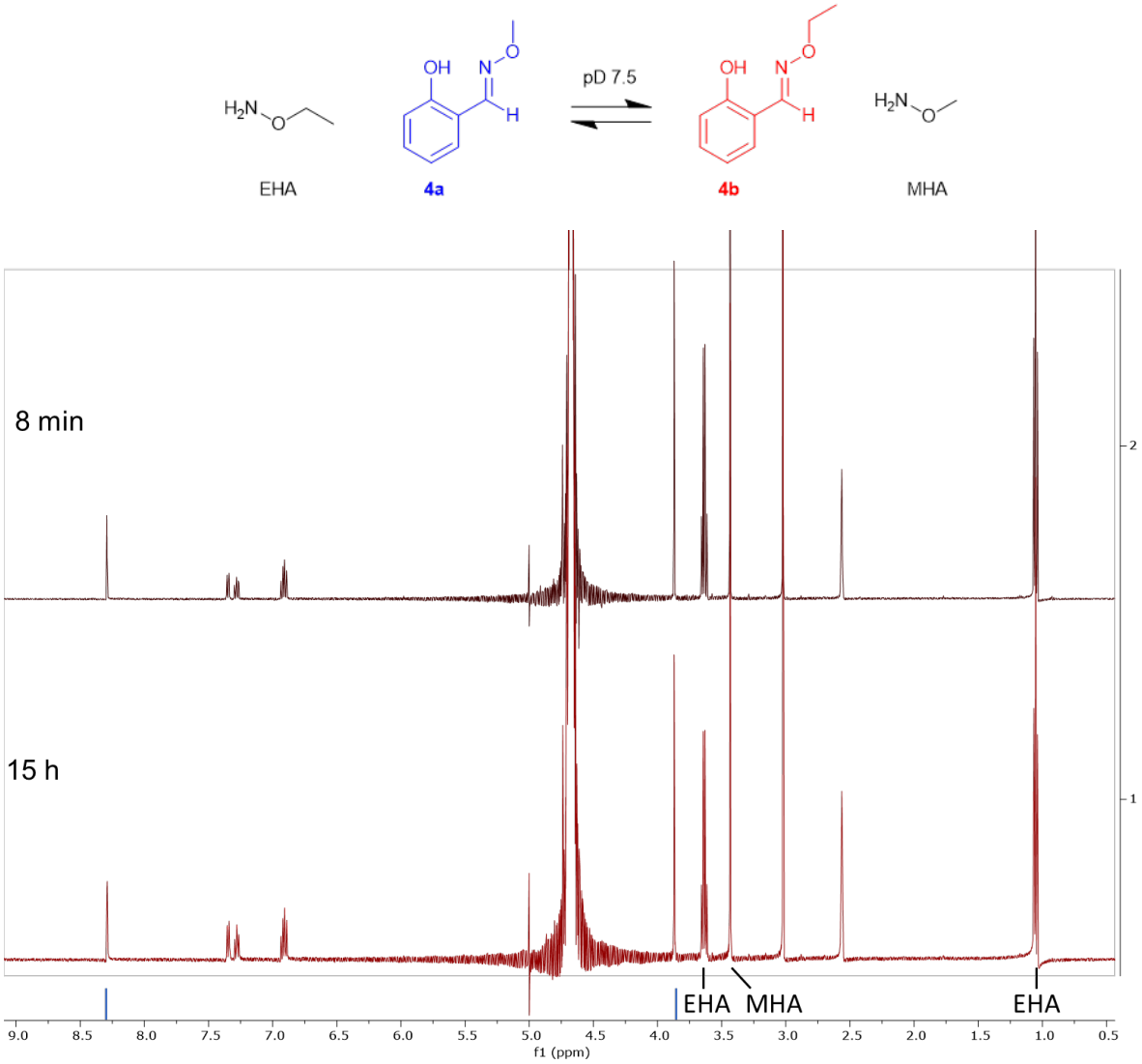

Figure S27. Time course ^{1}H NMR spectra of degenerate exchange between **4a** and EHA (200 mM, pD 7.5 PB, D_2O). Dimethyl sulfone (20 µL, 50 mM) was used as an internal standard (δ 3.02). No change was observed.

*S2. Oxime exchange between **4a** and iPHA at pD 7.5 at room temperature*

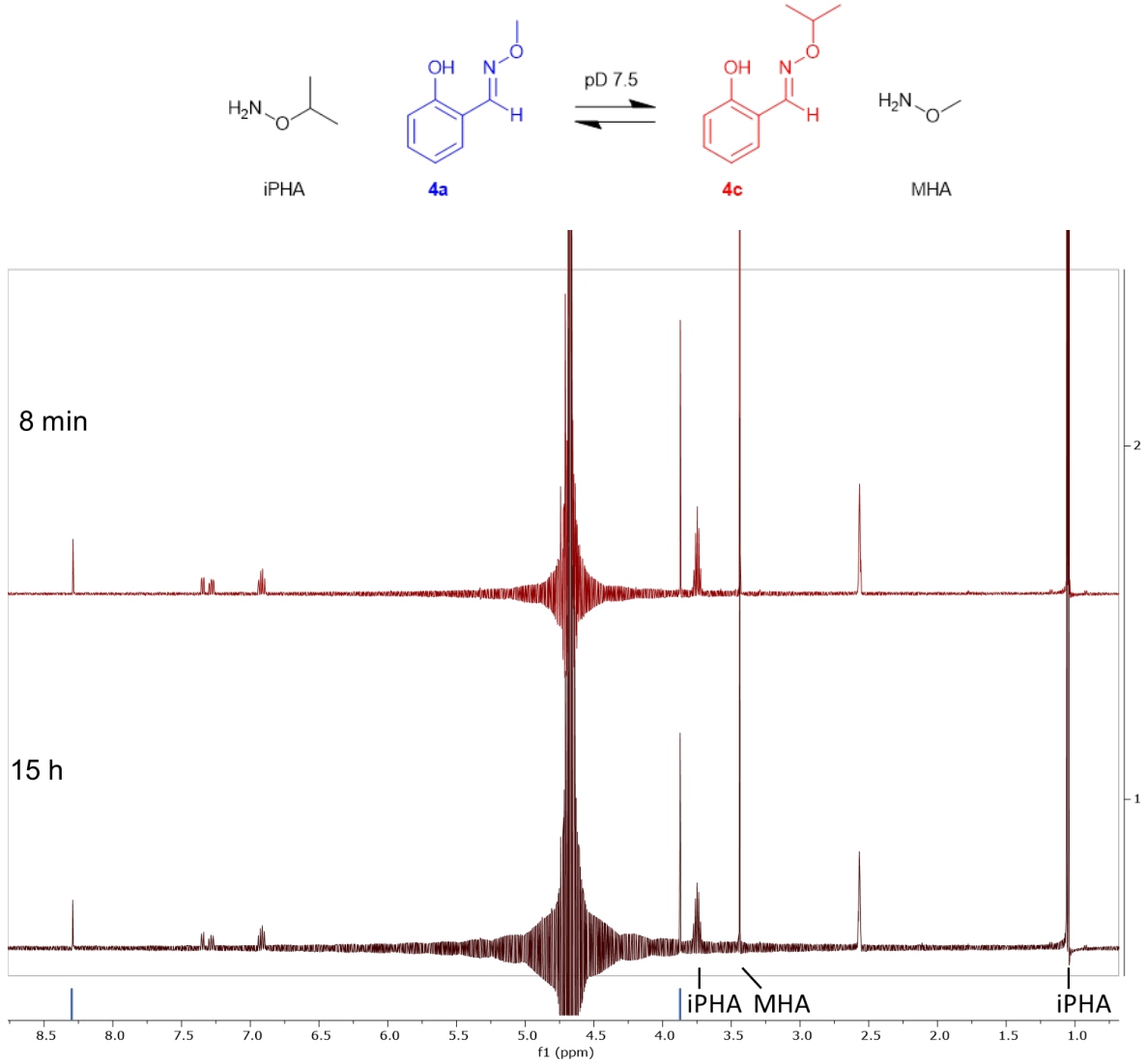

Figure S28. Time course ^{1}H NMR spectra of degenerate exchange between **4a** and iPHA (200 mM, pD 7.5 PB, D_2O). Dimethyl sulfone (20 µL, 50 mM) was used as an internal standard (δ 3.02). No change was observed.

*S3. Oxime exchange between **4a** and tBHA at pD 7.5 at room temperature*

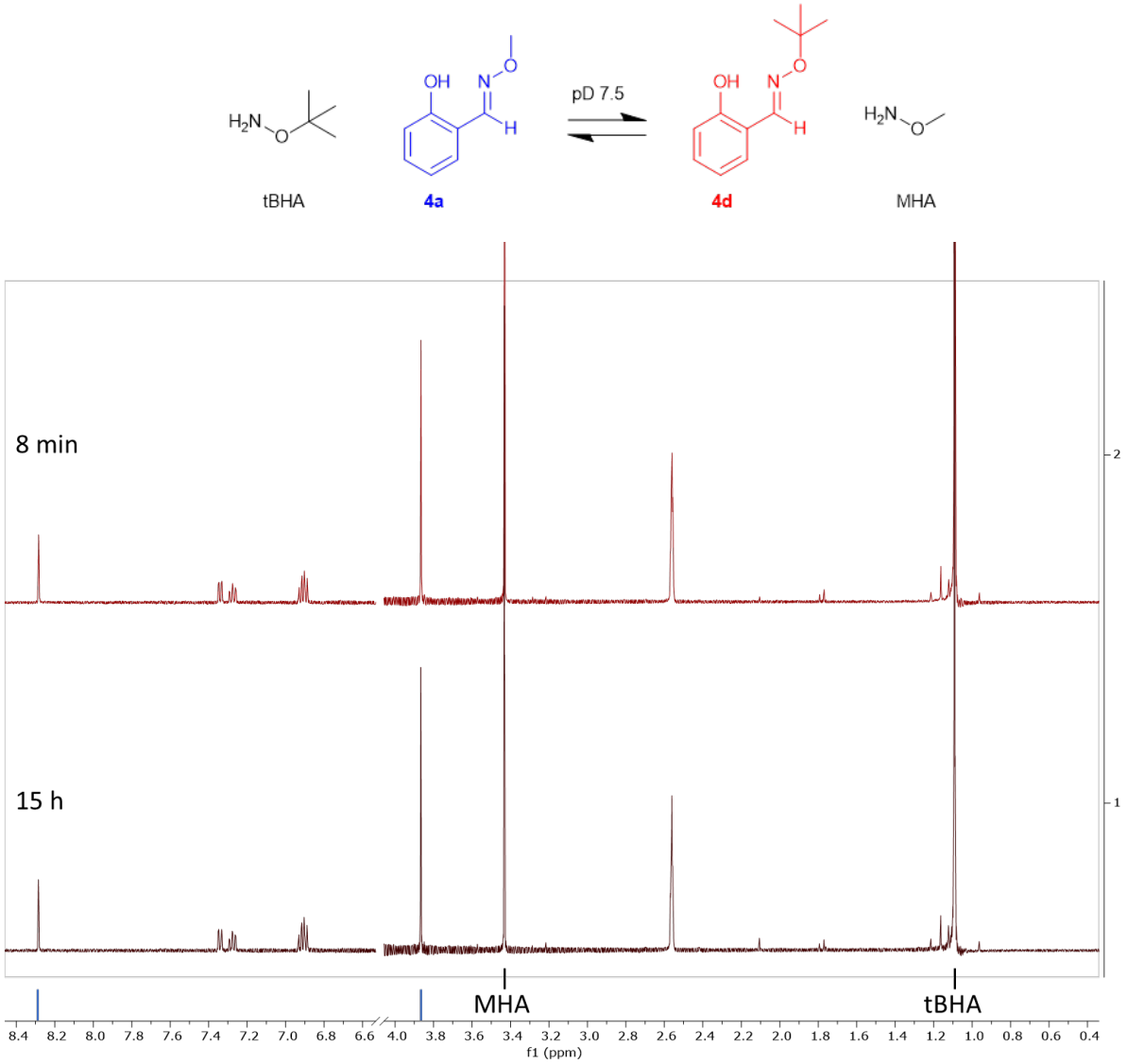

Figure S29. Time course ^{1}H NMR spectra of degenerate exchange between **4a** and tBHA (200 mM, pD 7.5 PB, D_2O). Dimethyl sulfone (20 µL, 50 mM) was used as an internal standard (δ 3.02). No change was observed.

T. Synthetic Procedures

Experimental note: When collecting ESI mass spectra of the boronic acid-containing compounds, it is important to use a low cone voltage (5V) to ensure detection of the monomeric species. High cone voltages (30V) lead to exclusive observation of the dimeric boronic acid anhydride. This phenomenon has been previously observed.[4]

2-Acetyl-1-hydroxy-2,3,1-benzodiazaborine (anhydro dimer) (1a dimer)

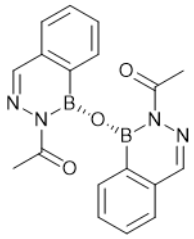

Acethydrazide (148 mg, 2.0 mmol) was dissolved in dd-H_2O (4 mL) in a 15 mL round-bottom flask. Separately, 2-FPBA (150 mg, 1.0 mmol) was added to DMSO (1 mL) and added to the acethydrazide solution. Immediately upon the addition of 2-FPBA, white precipitate started to form. After stirring the reaction mixture at room temperature for 1 hour, the precipitate was filtered, washed with dd-H_2O, dried *in vacuo*, and obtained as white powder (165 mg, 92%). In line with a report from the Bane group,[3] DAB dimer was observed in DMSO-d_6. Hydrated monomer [M-H] mass was detected when prepared in 2:1 H_2O:MeCN.

^{1}H NMR (500 MHz, DMSO-d_6) δ 8.11 (s, 1H), 7.62 – 6.58 (m, 1H), 7.58 – 7.53 (m, 1H), 7.51-7.44 (m, 2H), 2.36 (s, 3H). ^{13}C NMR (126 MHz, DMSO-d_6) δ 177.88, 151.86, 131.87, 130.90, 130.87, 129.11, 129.02, 19.32. HRMS (ESI-TOF) m/z [M-H] Calculated: 205.0786; Found: 205.0790

2-Isobutanoyl-1-hydroxy-2,3,1-benzodiazaborine (anhydro dimer) (1b dimer)

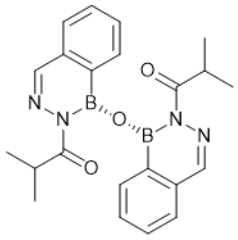

2-FPBA (300 mg, 2.0 mmol) was added to dd-H_2O (4 mL) in a 15 mL round-bottom flask. Separately, isobutyric acid hydrazide (102 mg, 1.0 mmol) was dissolved in DMSO (1 mL) and added to the 2-FPBA solution. Immediately upon the addition of isobutyric acid hydrazide, a white precipitate formed. After stirring the reaction mixture at room temperature overnight, the precipitate was filtered, washed with dd-H_2O, dried *in vacuo*, and obtained as white powder (196 mg, 95%). In line with a report from the Bane group,[3] DAB dimer was observed in DMSO-d_6.

^{1}H NMR (500 MHz, DMSO-d_6) δ 8.13 (S, 1H), 7.60 – 7.53 (m, 2H), 7.50 – 7.43 (m, 2H), 3.84-3.73 (sept, J = 7.0 Hz, 1H), 1.02 – 0.95 (d, J = 7.0 Hz, 3H), 0.95 – 0.87 (d, J = 7.0 Hz, 3H). ^{13}C NMR (126 MHz, DMSO-d_6) δ 182.76, 152.03, 131.95, 130.78, 130.73, 129.12, 128.99, 28.76, 18.76, 18.69. HRMS (ESI-TOF) m/z [M-H] Calculated: 233.1100; Found: 233.1101

2-Pivaloyl-1-hydroxy-2,3,1-benzodiazaborine (1c)

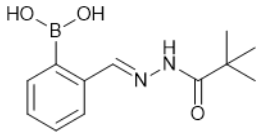

2-FPBA (300 mg, 2.0 mmol) was added to dd-H_2O (4 mL) in a 15 mL round-bottom flask. Separately, pivalic acid hydrazide (116 mg, 1.0 mmol) was dissolved in DMSO (2 mL) and added to the 2-FPBA solution. Upon the addition of pivalic acid hydrazide, hard white precipitate formed. After stirring the reaction mixture at room temperature overnight, flaky white precipitate was formed. The precipitate was filtered, washed with dd-H_2O, dried *in vacuo*, and obtained as white powder (203 mg, 88%). The hydrazone monomer was observed in DMSO-*d*$_6$. Hydrated monomer [M-H] mass was detected when prepared in 2:1 H_2O:MeCN.

^{1}H NMR (500 MHz, DMSO-*d*$_6$) δ 10.98 (s, 1H), 8.60 (s, 1H), 8.49 (s, 2H), 7.82 – 7.77 (d, J = 7.5 Hz,1H), 7.60 – 7.56 (d, J = 7.3 Hz, 1H), 7.41 – 7.35 (td, J1 = 7.5 Hz, J2 = 1.4 Hz, 1H), 7.34 – 7.29 (td, J1 = 7.3 Hz, J2 = 1.1 Hz, 1H), 1.16 (s, 9H). ^{13}C NMR (126 MHz, DMSO-*d*$_6$) δ 174.34, 148.79, 138.10, 134.63, 129.59, 129.08, 126.49, 38.29, 27.68, 27.49. HRMS (ESI-TOF) m/z [M-H] Calculated: 247.1256; Found: 247.1263

2-Cyanoacetyl-1-hydroxy-2,3,1-benzodiazaborine (1d)

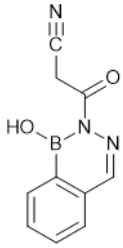

Cyanoacetohydrazide (198 mg, 2.0 mmol) was dissolved in dd-H_2O (4.5 mL) in a 15 mL round-bottom flask. Separately, 2-FPBA (150 mg, 1.0 mmol) was dissolved in DMSO (0.5 mL) and added to the cyanoacetohydrazide solution. Immediately upon the addition of 2-FPBA, pale brown precipitate started to form. After stirring the reaction mixture at room temperature for 1 hour, the precipitate was filtered, washed with dd-H_2O, dried *in vacuo*, and obtained as white powder (154 mg, 72%). DAB monomer was observed in $CDCl_3$. **1d** was unstable in DMSO-*d*$_6$. Hydrated monomer [M-H] mass was detected when prepared in 2:1 H_2O:MeCN.

^{1}H NMR (500 MHz, $CDCl_3$) δ 8.61 (s, 1H), 8.26 – 8.20 (d, J = 7.5 Hz,1H), 8.02 (s, 1H), 7.81 – 7.75 (td, J1 = 7.5 Hz, J2 = 1.3, 1H), 7.72 – 7.67 (td, J1 = 7.5 Hz, J2 = 0.9 Hz, 1H), 7.67 – 7.63 (d, J = 7.8 Hz, 1H), 4.25 (s, 2H). ^{13}C NMR (126 MHz, $CDCl_3$) δ 175.61, 144.39, 134.10, 133.40, 132.65, 131.33, 128.12, 113.80, 27.00. HRMS (ESI-TOF) m/z [M-H] Calculated: 230.0739; Found: 230.0744

2-*tert*-butoxycarbonyl-1-hydroxy-2,3,1-benzodiazaborine (1e)

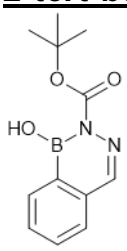

2-FPBA (300 mg, 2.0 mmol) was added to dd-H_2O (4 mL) in a 15 mL round-bottom flask. Separately, *tert*-butyl carbazate (132 mg, 1.0 mmol) was dissolved in DMSO (1 mL) and added to the 2-FPBA solution. Immediately upon the addition of *tert*-butyl carbazate, white precipitate started to form. After stirring the reaction mixture at room temperature for 1 hour, the precipitate was filtered, washed with dd-H_2O, dried *in vacuo*, and obtained as white powder (230 mg, 93%). DAB monomer was observed in $CDCl_3$. Hydrated monomer [M-H] mass was detected when prepared in 2:1 H_2O:MeCN.

^{1}H NMR (500 MHz, $CDCl_3$) δ 8.58 (s, 1H), 8.23 – 8.18 (d, J = 7.4 Hz,1H), 8.07 (s, 1H), 7.75 – 7.69 (tt, J1 = 7.5 Hz, J2 = 1.2 Hz, 1H), 7.66 – 7.59 (m, 2H), 1.67 (s, 9H). ^{13}C NMR (126 MHz, $CDCl_3$) δ 143.09, 134.63, 132.62, 132.13, 130.45, 127.45, 84.88, 28.23. HRMS (ESI-TOF) m/z [M-H] Calculated: 263.1205; Found: 263.1205

2-(((Methoxy)imino)methyl)phenylboronic acid (2a)

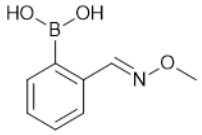

O-methylhydroxylamine hydrochloride (167 mg, 2.0 mmol) was dissolved in dd-H_2O (4.5 mL) in a 15 mL round-bottom flask. Separately, 2-FPBA (150 mg, 1.0 mmol) was dissolved in DMSO (0.5 mL) and added to the *O*-methylhydroxoylamine solution. Immediately upon the addition of 2-FPBA, white precipitate started to form. After stirring the reaction mixture at room temperature for 1 hour, the precipitate was filtered, washed with dd-H_2O, air-dried, and obtained as white powder (137 mg, 77%). [M-H] was detected at 5V cone voltage when prepared in 2:1 H_2O:MeCN.

^{1}H NMR (500 MHz, DMSO-d_6) δ 8.5.0 (s, 1H), 8.22 (s, 2H), 7.70 – 7.65 (m, 1H), 7.57 – 7.51 (m, 1H), 7.39 – 7.29 (m, 2H), 3.83 (s, 1H). ^{13}C NMR (126 MHz, DMSO-d_6) δ 150.42, 135.50, 134.42, 129.62, 129.21, 125.76, 61.95. HRMS (ESI-TOF) m/z [M-H] Calculated: 178.0677; Found: 178.0687

2-(((Ethoxy)imino)methyl)phenylboronic acid (2b)

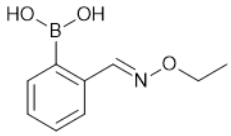

O-ethylhydroxylamine hydrochloride (195 mg, 2.0 mmol) was dissolved in dd-H_2O (4.5 mL) in a 15 mL round-bottom flask. Separately, 2-FPBA (150 mg, 1.0 mmol) was dissolved in DMSO (0.5 mL) and added to the *O*-ethylhydroxoylamine solution. Immediately upon the addition of *O*-ethylhydroxylamine, white precipitate started to form. After stirring the reaction mixture at room temperature for 1 hour, the precipitate was filtered, washed with dd-H_2O, air-dried, and obtained as white powder (135 mg, 70%). [M-H] was detected at 5V cone voltage when prepared in 2:1 H_2O:MeCN.

^{1}H NMR (500 MHz, DMSO-d_6) δ 8.47 (s, 1H), 8.19 (s, 1H), 7.68 – 7.64 (m, 1H), 7.54 – 7.49 (m, 1H), 7.37 – 7.29 (m, 2H), 4.12 – 4.06 (q, J = 7.0 Hz, 2H), 1.24 – 1.19 (t, J = 7.0 Hz, 3H). ^{13}C NMR (126 MHz, DMSO-d_6) δ 150.07, 135.68, 134.26, 129.51, 129.10, 125.94, 69.40, 15.12. HRMS (ESI-TOF) m/z [M-H] Calculated: 192.0834; Found: 192.0833

2-(((Isopropoxy)imino)methyl)phenylboronic acid (2c)

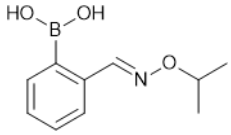

2-FPBA (300 mg, 2.0 mmol) was dissolved in a mixture of dd-H_2O (4.5 mL) and DMSO (0.5 mL) in a 15 mL round-bottom flask. *O*-isopropylhydroxylamine hydrochloride (112 mg, 1.0 mmol) was added to the 2-FPBA solution. Immediately upon the addition of *O*-isopropylhydroxylamine, white precipitate started to form. After stirring the reaction mixture at room temperature for 1 hour, the precipitate was filtered,

washed with dd-H_2O, air-dried, and obtained as white powder (168 mg, 81%). [M-H] was detected at 5V cone voltage when prepared in 2:1 H_2O:MeCN.

^{1}H NMR (500 MHz, DMSO-d_6) δ 8.41 (s, 1H), 8.14 (s, 1H), 7.66 – 7.62 (m, 1H), 7.52 – 7.48 (m, 1H), 7.36 – 7.28 (m, 2H), 4.36 – 4. 27 (sept, J = 6.3 Hz, 1H), 1.24 – 1.19 (d, 6.3 Hz, 6H). ^{13}C NMR (126 MHz, DMSO-d_6) δ 149.55, 135.82, 134.08, 129.39, 128.99, 126.15, 75.35, 22.08. HRMS (ESI-TOF) m/z [M-H] Calculated: 206.0990; Found: 206.0991

2-(((*tert*-butoxy)imino)methyl)phenylboronic acid (2d)

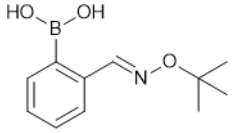

2-FPBA (300 mg, 2.0 mmol) was dissolved in a mixture of dd-H_2O (4.5 mL) and DMSO (0.5 mL) in a 15 mL round-bottom flask. *O-tert*-butylhydroxylamine hydrochloride (126 mg, 1.0 mmol) was added to the 2-FPBA solution. Immediately upon the addition of *O-tert*-butylhydroxylamine, white precipitate started to form. After stirring the reaction mixture at room temperature for 1 hour, the precipitate was filtered, washed with dd-H_2O, air-dried, and obtained as white powder (183 mg, 83%). [M-H] was detected at 5V cone voltage when prepared in 2:1 H_2O:MeCN.

^{1}H NMR (500 MHz, DMSO-d_6) δ 8.32 (s, 1H), 8.04 (s, 2H), 7.60 – 7.56 (m, 1H), 7.46 – 7.42 (m, 1H), 7.35 – 7.26 (m, 2H), 1.27 (s, 9H). ^{13}C NMR (126 MHz, DMSO-d_6) δ 148.80, 135.94, 133.58, 129.10, 128.83, 126.77, 79.14, 28.03. HRMS (ESI-TOF) m/z [M-H] Calculated: 220.1147; Found: 220.1152

2-(((Acetamido)imino)methyl)phenol (3)

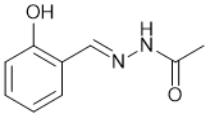

Acethydrazide (148 mg, 2.0 mmol) was dissolved in dd-H_2O (4 mL) in a 15 mL round-bottom flask. Separately, salicylaldehyde (122 mg, 1.0 mmol) was added to DMSO (1 mL) and added to the acethydrazide solution. After stirring the reaction mixture at room temperature overnight, white precipitate formed. The precipitate was filtered, washed with dd-H_2O, dried *in vacuo*, and obtained as white powder (163 mg, 91%). Both E/Z isomers are observed by ^{1}H NMR and ^{13}C NMR in DMSO-d_6.

^{1}H NMR (500 MHz, DMSO-d_6) δ 11.65 – 11.18 (s, 1H), 11.18 – 10.00 (s, 1H), 8.31 – 8.21 (s, 1H), 7.60 – 7.42 (d, *J* = 8.0 Hz, 1H), 7.27 – 7.16 (t, *J* = 7.0 Hz, 1H), 6.90 – 6.79 (t, *J* = 7.5 Hz, 2H), 2.16 – 1.90 (s, 3H). ^{13}C NMR (126 MHz, DMSO-d_6) δ 172.14, 165.94, 157.82, 156.87, 146.76, 141.30, 131.70, 131.42, 129.98, 127.24, 120.55, 119.95, 119.82, 119.13, 116.86, 116.64, 21.90, 21.01. HRMS (ESI-TOF) m/z [M-H] Calculated: 177.0664; Found: 177.0666

Alternatively, acethydrazide (148 mg, 2.0 mmol) was dissolved in dd-H_2O (4 mL) in a 15 mL round-bottom flask. Separately, 2-FPBA (150 mg, 1.0 mmol) was added to DMSO (1 mL) and added to the acethydrazide solution. After stirring the reaction mixture at room temperature for 1 hour, hydrogen peroxide (9.8 M, 3.0 mmol) was added to the reaction mixture. The resulting mixture was stirred at room temperature overnight, which resulted in the formation of a slightly off-white

precipitate. The precipitate was filtered, washed with dd-H_2O, dried *in vacuo*, and obtained as white powder (148 mg, 83%). Both E/Z isomers are observed by ^{1}H NMR and ^{13}C NMR in DMSO-d_6.

^{1}H NMR (500 MHz, DMSO-d_6) δ 11.65 – 11.18 (s, 1H), 11.18 – 10.00 (s, 1H), 8.31 – 8.21 (s, 1H), 7.60 – 7.42 (d, *J* = 8.0 Hz, 1H), 7.27 – 7.16 (t, *J* = 7.0 Hz, 1H), 6.90 – 6.79 (t, *J* = 7.5 Hz, 2H), 2.16 – 1.90 (s, 3H). ^{13}C NMR (126 MHz, DMSO-d_6) 172.06, 165.95, 157.83, 156.89, 146.79, 141.75, 131.69, 131.42, 129.99, 127.27, 120..53, 119.94, 119.80, 119.12, 116.86, 116.64, 21.89, 20.87. HRMS (ESI-TOF) m/z [M-H] Calculated: 177.0664; Found: 177.0674

2-(((Methoxy)imino)methyl)phenol (4a)

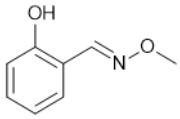

O-methylhydroxylamine hydrochloride (167 mg, 2.0 mmol) was dissolved in dd-H_2O (4 mL) in 15 mL round-bottom flask. Separately, salicylaldehyde (122 mg, 1.0 mmol) was added to DMSO (1 mL) and added to the *O*-methylhydroxoylamine solution. After stirring the reaction mixture at room temperature overnight, white precipitate formed. The precipitate was filtered, washed with dd-H_2O, air-dried, and obtained as white powder (107 mg, 71%).

^{1}H NMR (500 MHz, DMSO-d_6) δ 9.91 (s, 1H), 8.34 (s, 1H), 7.52 – 7.47 (d, *J* = 7.7 Hz, 1H), 7.24 – 7.19 (t, *J* = 8.0 Hz, 1H), 6.88 – 6.84 (d, *J* = 8.2 Hz, 1H), 6.83 – 6.78 (t, *J* = 7.6 Hz, 1H), 3.85 (s, 3H). ^{13}C NMR (126 MHz, DMSO-d_6) δ 156.57, 146.84, 131.82, 127.65, 119.95, 118.12, 116.71, 62.16. GC-MS m/z [M-H] Calculated: 151.06; Found: 151.1

Alternatively, *O*-methylhydroxylamine hydrochloride (167 mg, 2.0 mmol) was dissolved in dd-H_2O (4 mL) in a 15 mL round-bottom flask. Separately, 2-FPBA (150 mg, 1.0 mmol) was added to DMSO (1 mL) and added to the *O*-methylhydroxoylamine solution. After stirring the reaction mixture at room temperature for 1 hour, hydrogen peroxide (9.8 M, 3.0 mmol) was added to the reaction mixture. The resulting mixture was stirred at room temperature overnight, which resulted in the formation of a slightly off-white precipitate. The precipitate was filtered, washed with dd-H_2O, air-dried, and obtained as white powder (115 mg, 76%).

^{1}H NMR (500 MHz, DMSO-d_6) δ 9.91 (s, 1H), 8.34 (s, 1H), 7.52 – 7.47 (d, *J* = 7.7 Hz, 1H), 7.24 – 7.19 (t, *J* = 8.0 Hz, 1H), 6.88 – 6.84 (d, *J* = 8.2 Hz, 1H), 6.83 – 6.78 (t, *J* = 7.6 Hz, 1H), 3.85 (s, 3H). ^{13}C NMR (126 MHz, DMSO-d_6) δ 156.57, 146.90, 131.82, 127.64, 119.95, 118.12, 116.71. GC-MS m/z [M-H] Calculated: 151.06; Found: 151.1

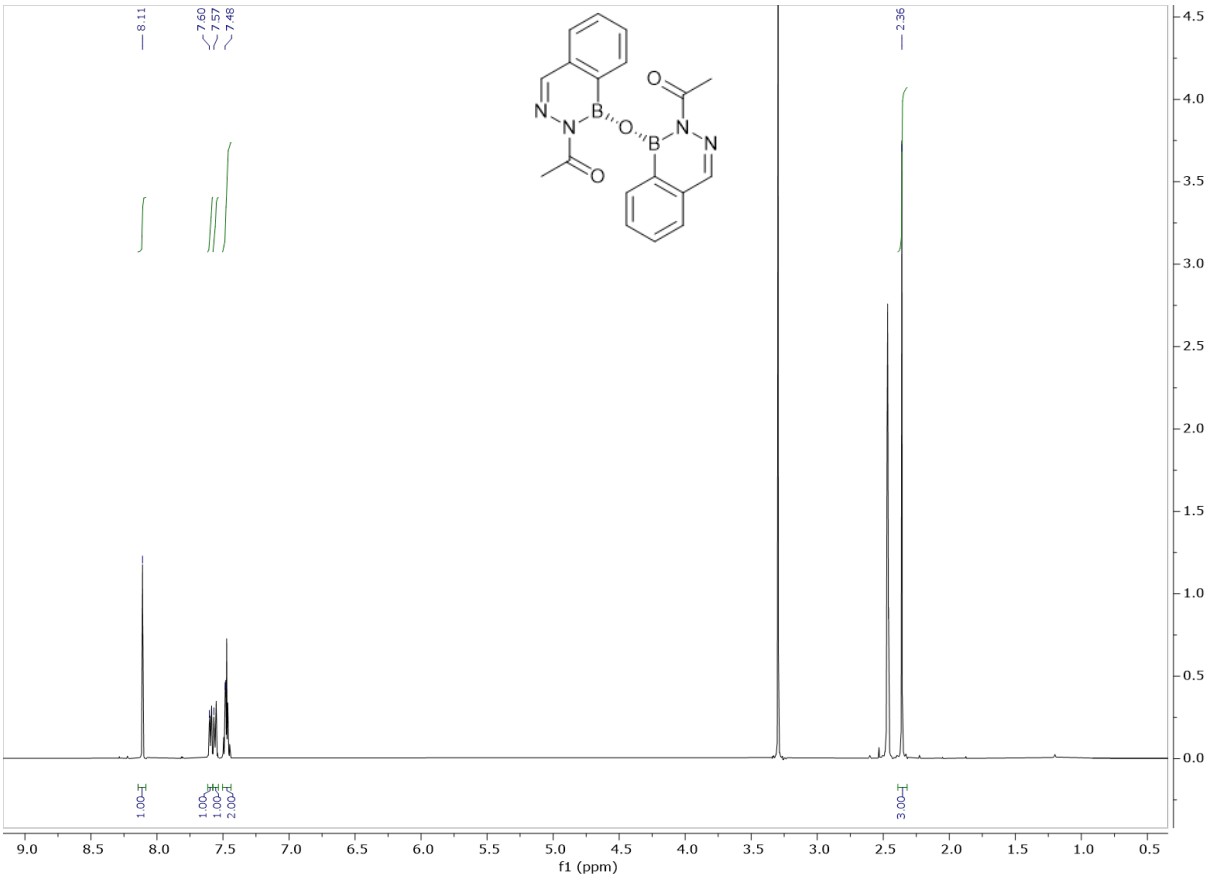

Fig. S30. ^{1}H NMR spectrum of **1a** in DMSO-d_6.

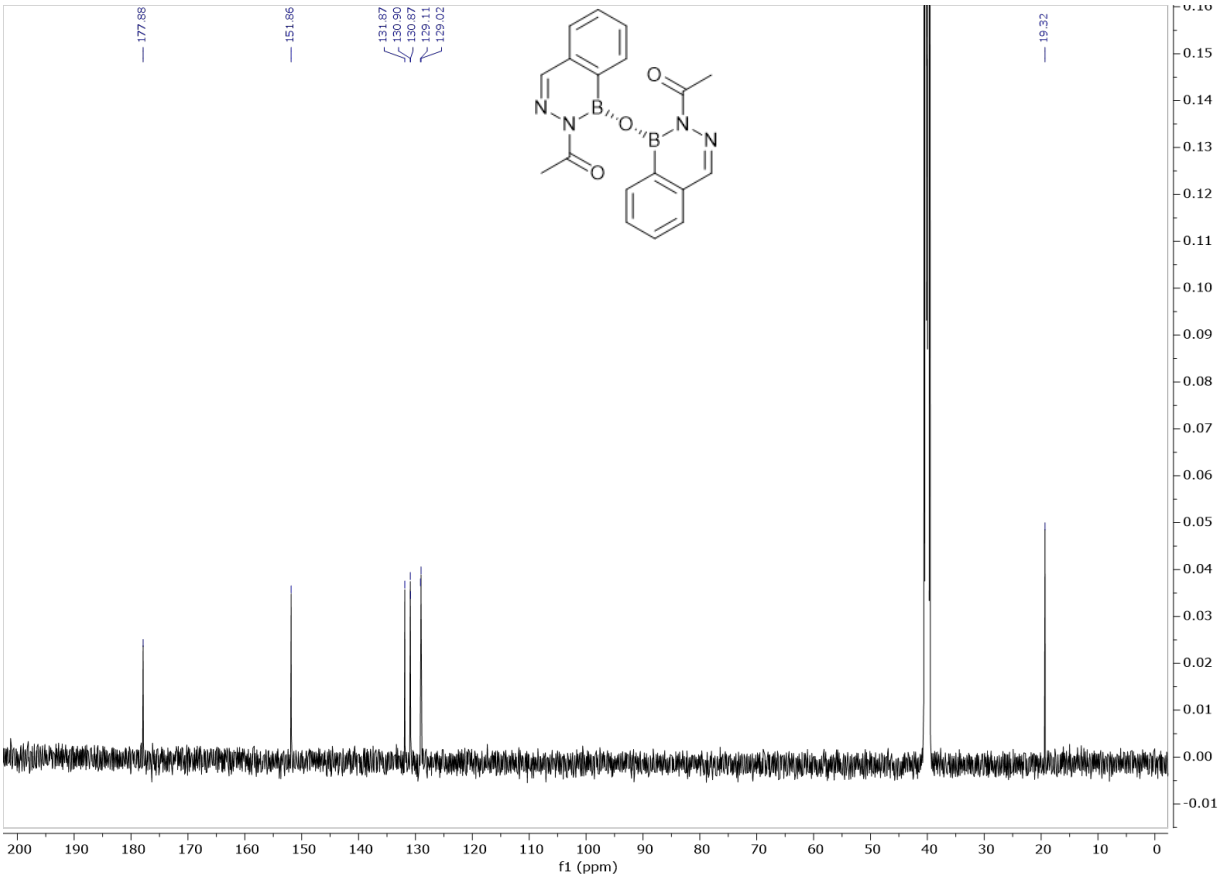

Fig. S31. ^{13}C NMR spectrum of **1a** in DMSO-d_6.

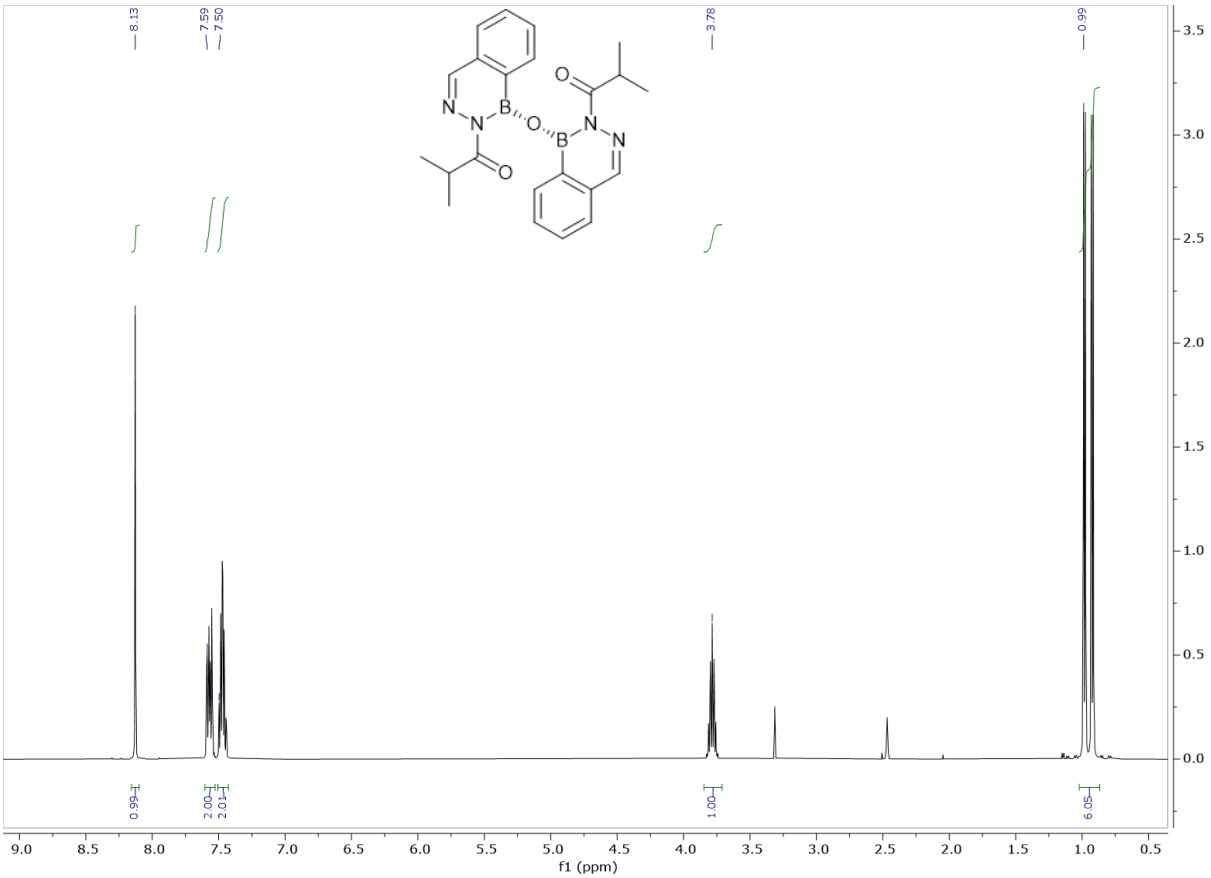

Fig. S32. ^{1}H NMR spectrum of **1b** in DMSO-d_6.

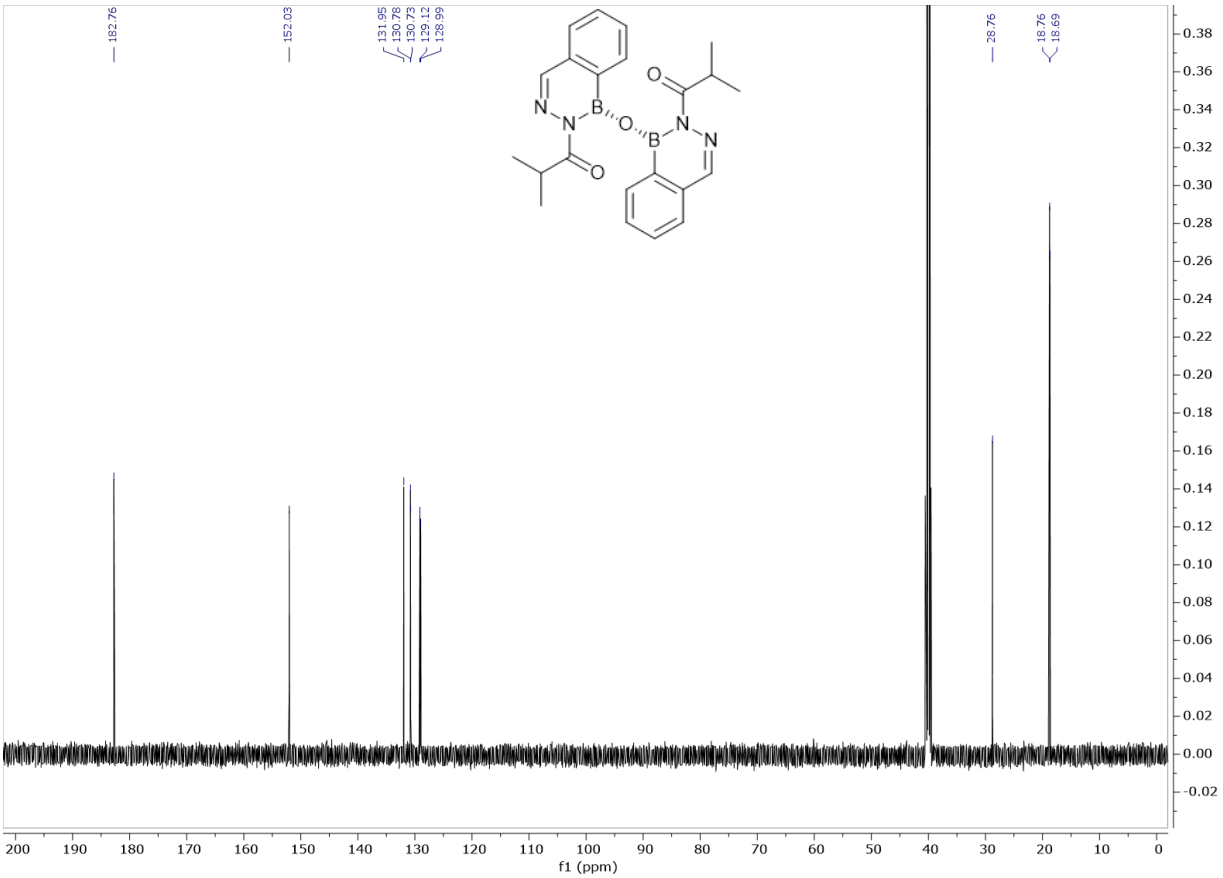

Fig. S33. ^{13}C NMR spectrum of **1b** in DMSO-*d*$_6$.

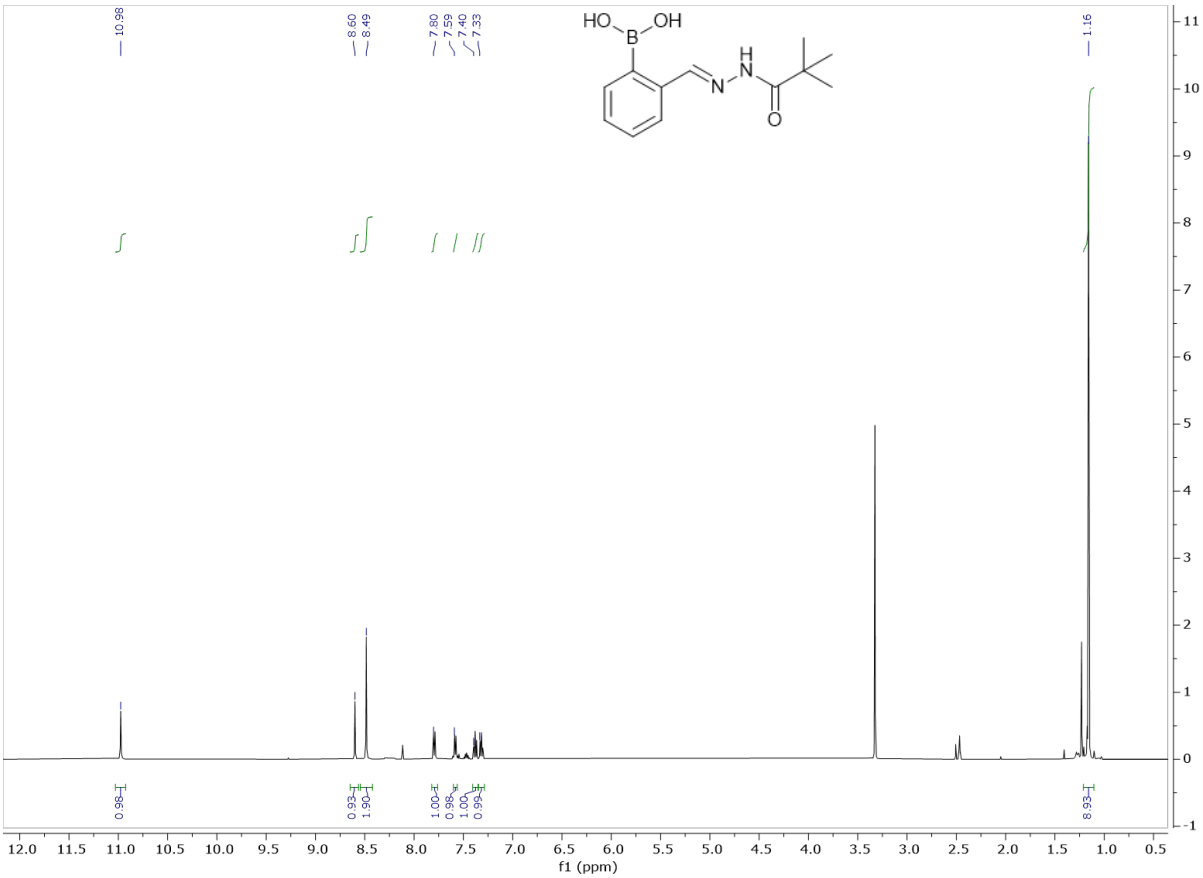

Fig. S34. ^{1}H NMR spectrum of **1c** in DMSO-d_6.

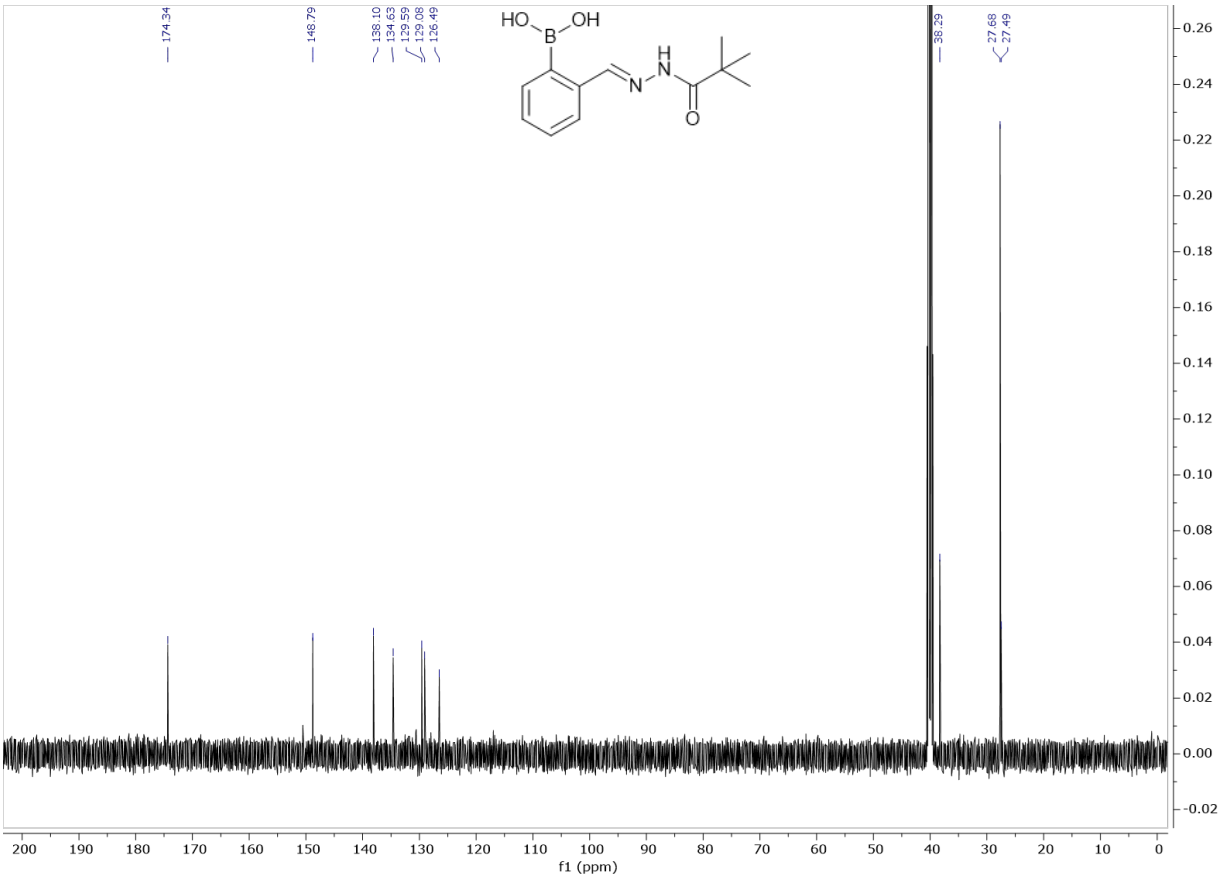

Fig. S35. ^{13}C NMR spectrum of **1c** in DMSO-d_6.

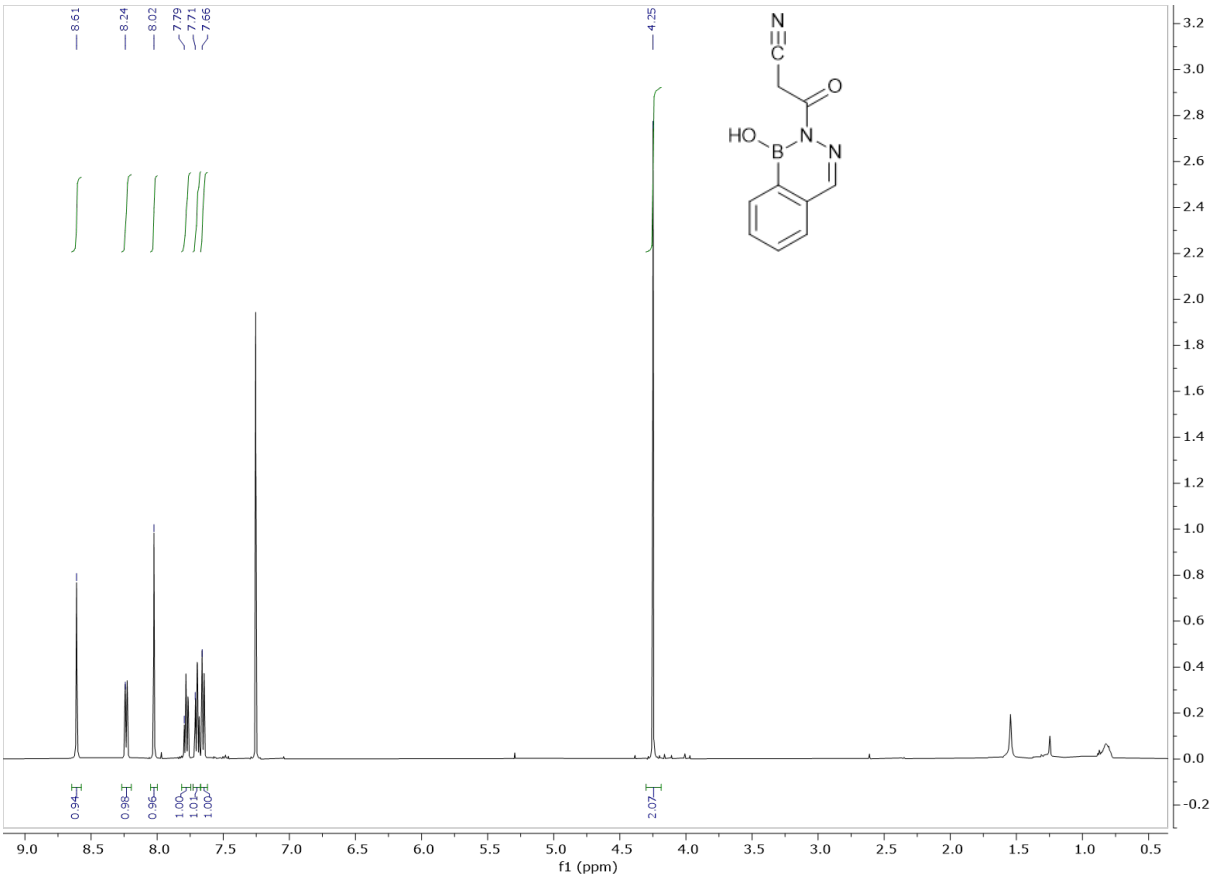

Fig. S36. ^{1}H NMR spectrum of **1d** in $CDCl_3$.

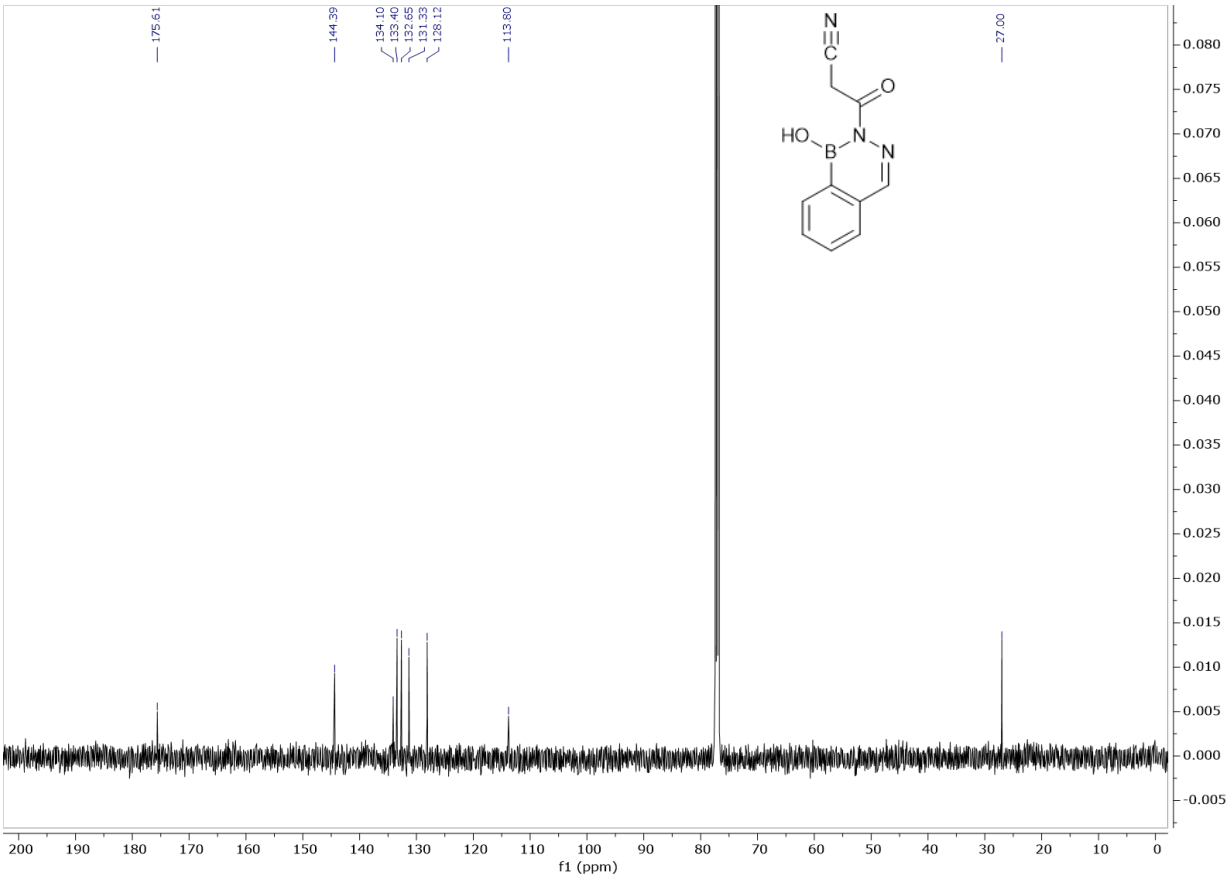

Fig. S37. ^{13}C NMR spectrum of **1d** in $CDCl_3$.

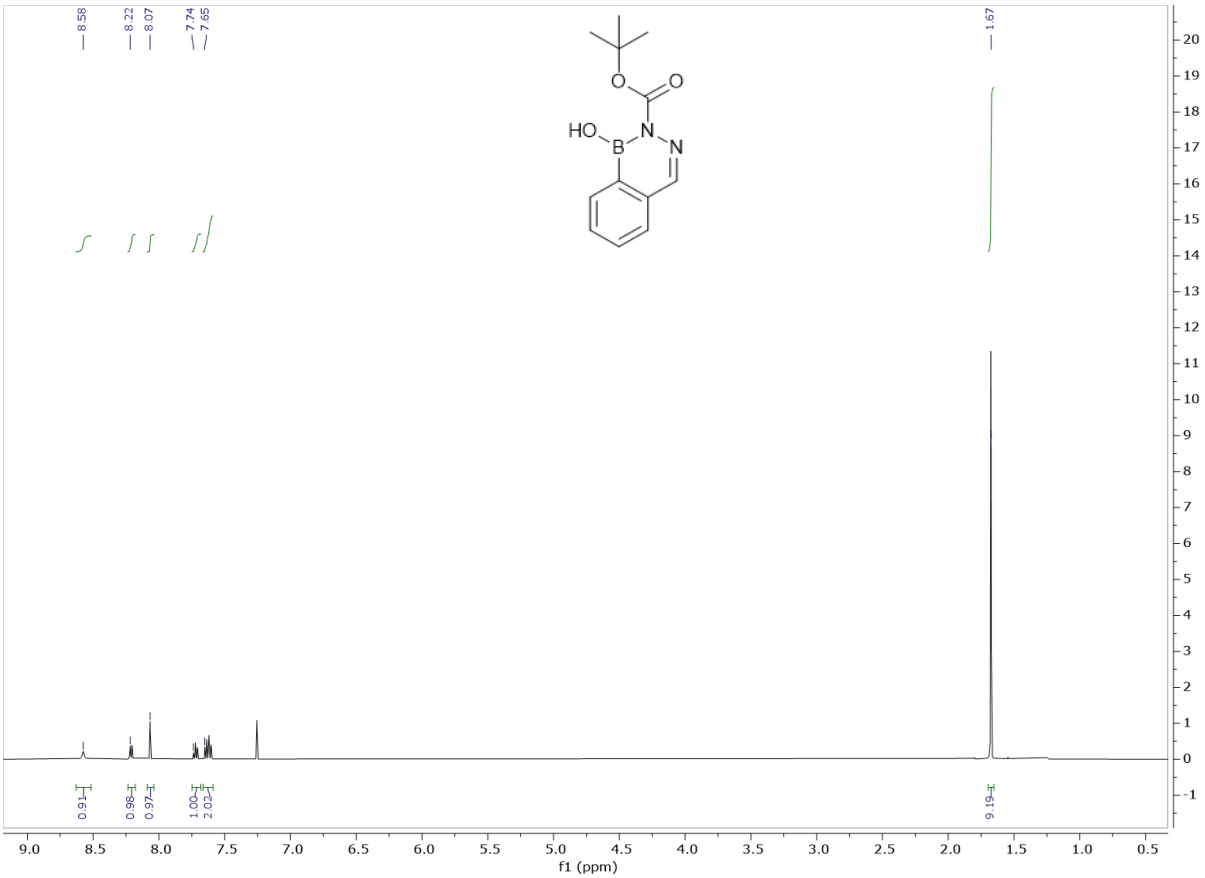

Fig. S38. ^{1}H NMR spectrum of **1e** in $CDCl_3$.

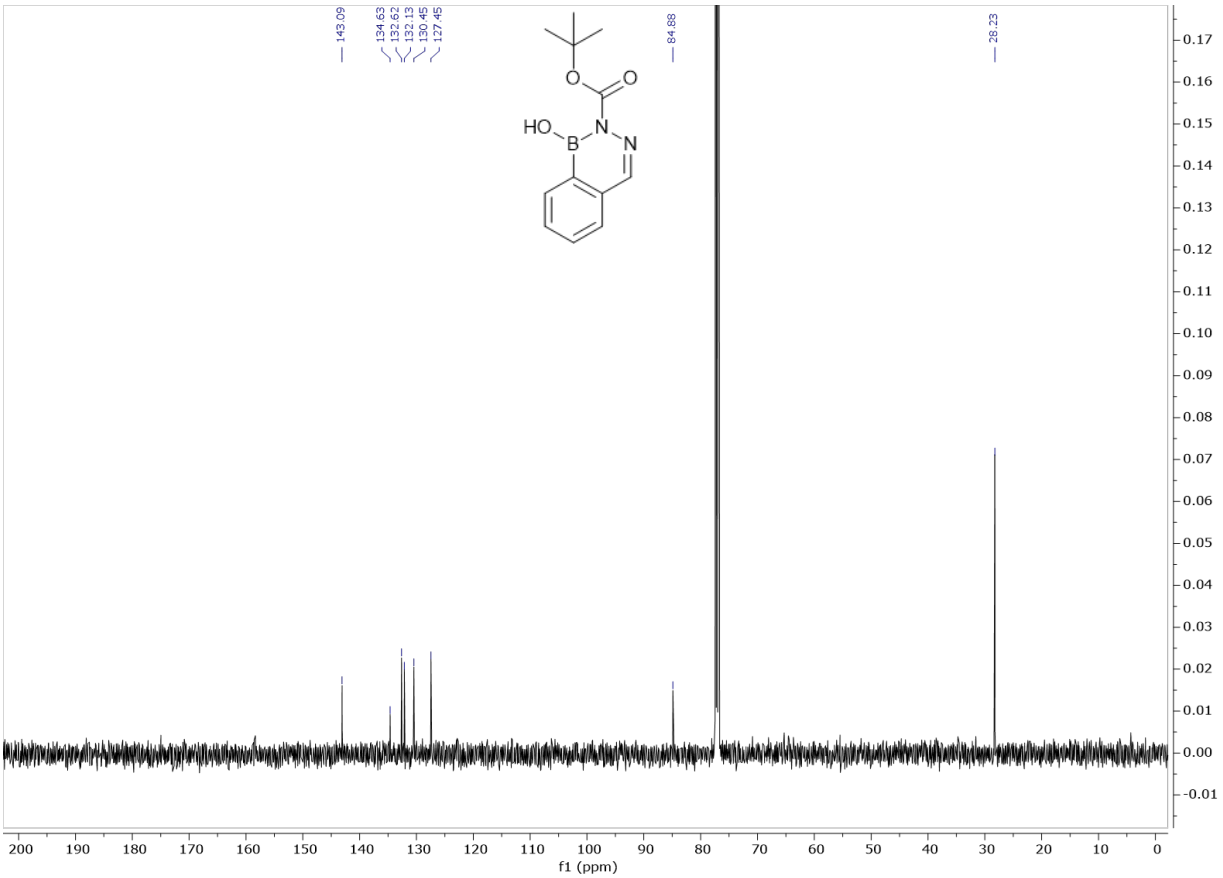

Fig. S39. ^{13}C NMR spectrum of **1e** in $CDCl_3$.

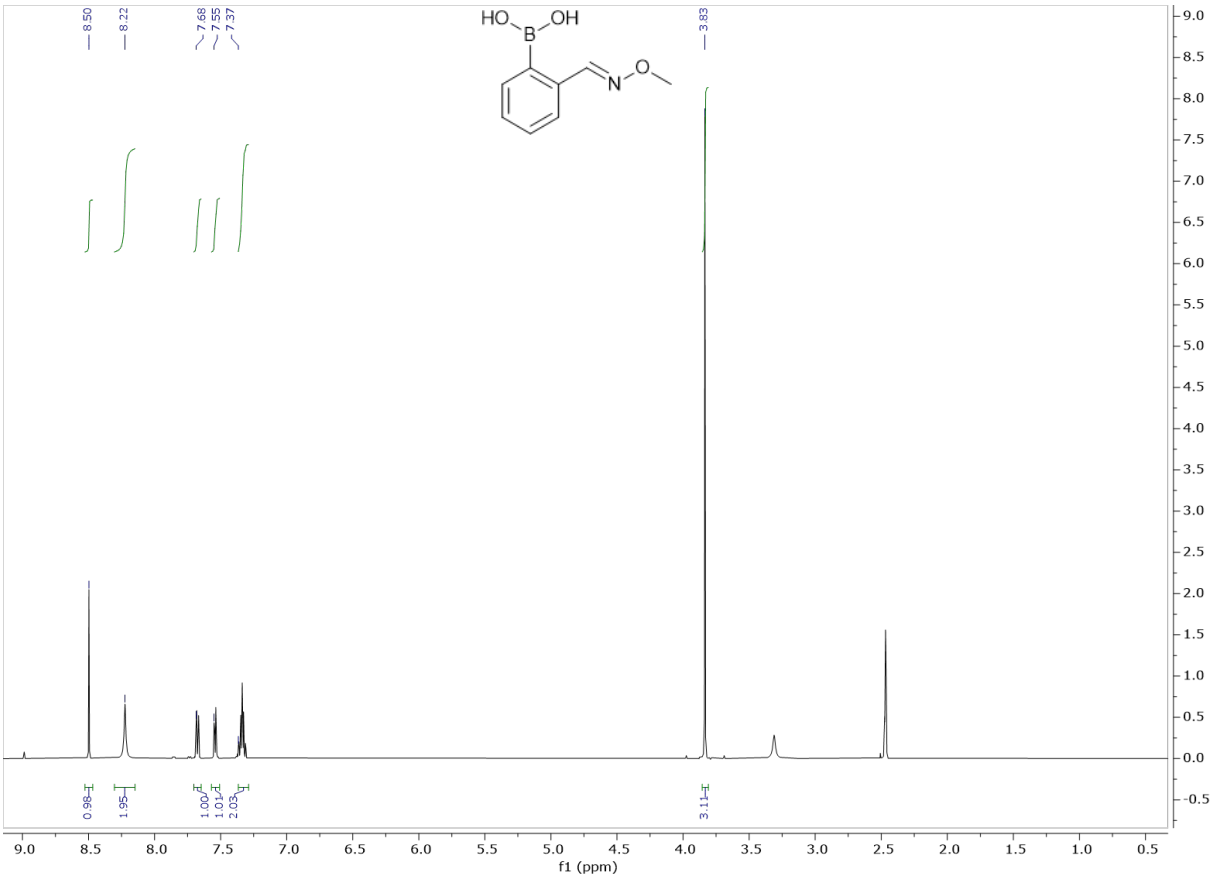

Fig. S40. ^{1}H NMR spectrum of **2a** in DMSO-d_6.

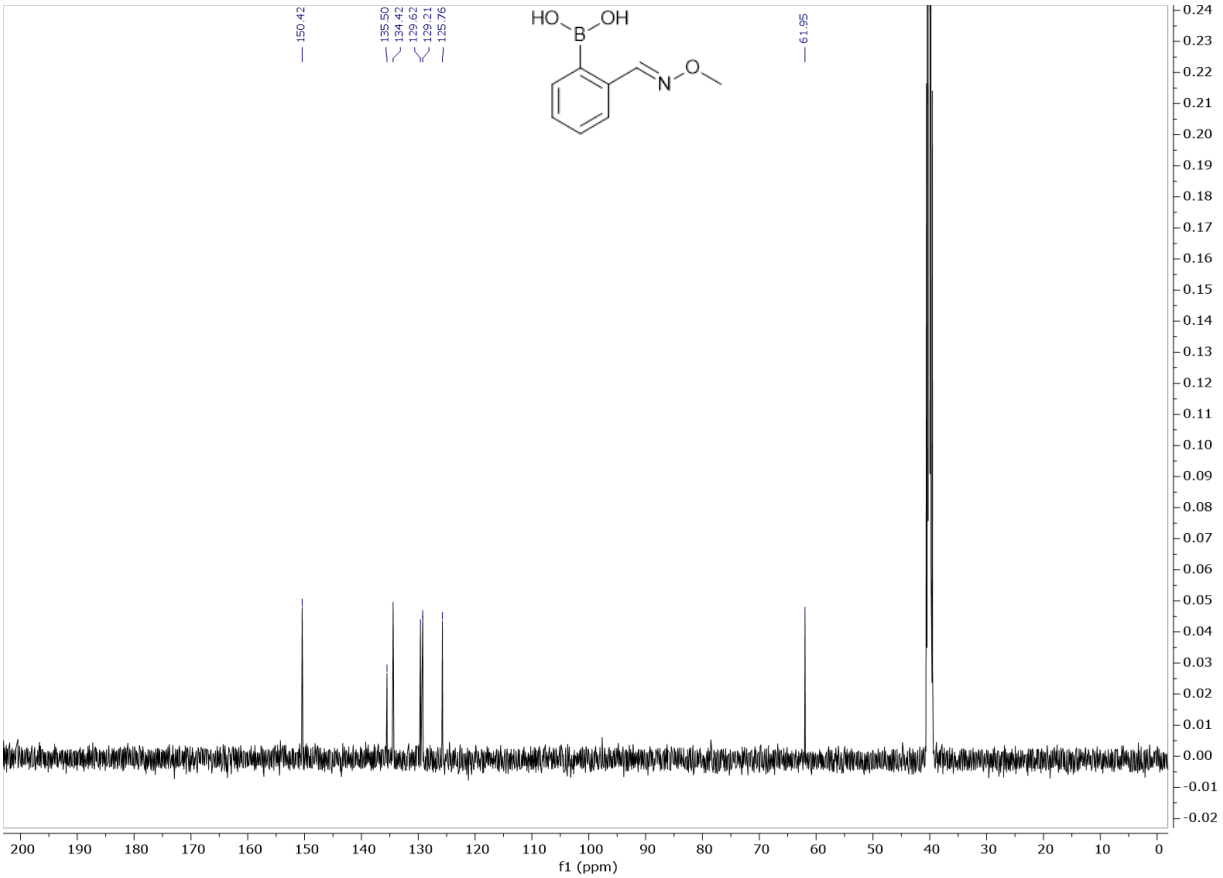

Fig. S41. ^{13}C NMR spectrum of **2a** in DMSO-d_6.

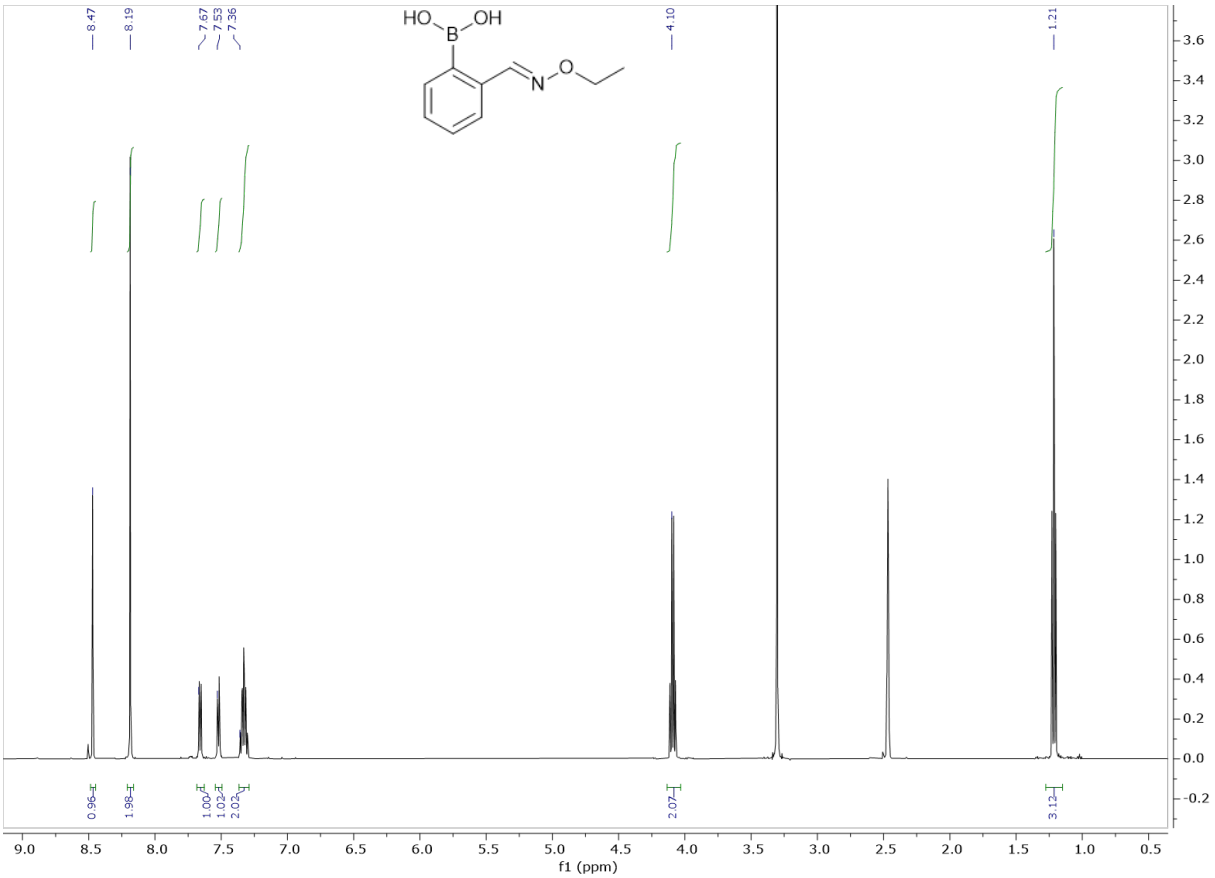

Fig. S42. ^{1}H NMR spectrum of **2b** in DMSO-d_6.

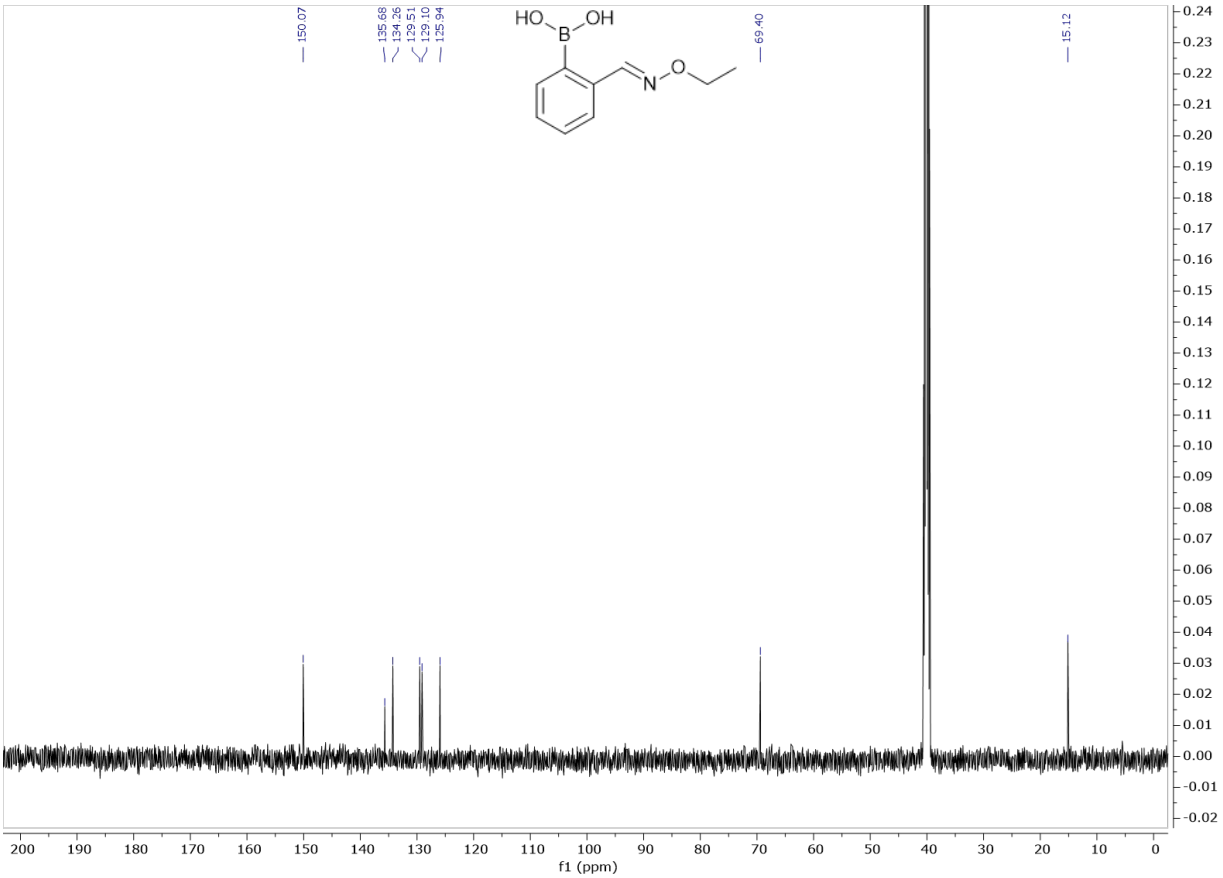

Fig. S43. ^{13}C NMR spectrum of **2b** in DMSO-*d*$_6$.

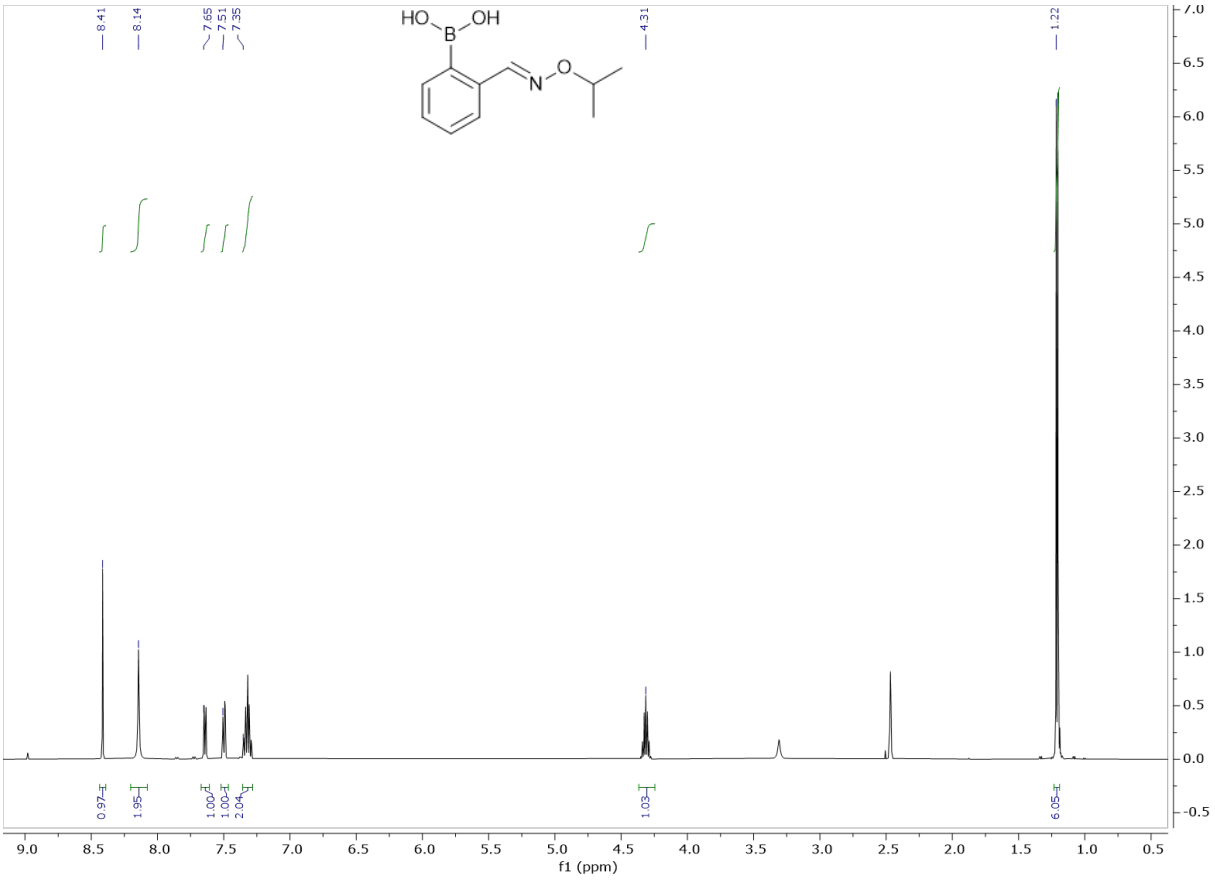

Fig. S44. ^{1}H NMR spectrum of **2c** in DMSO-d_6.

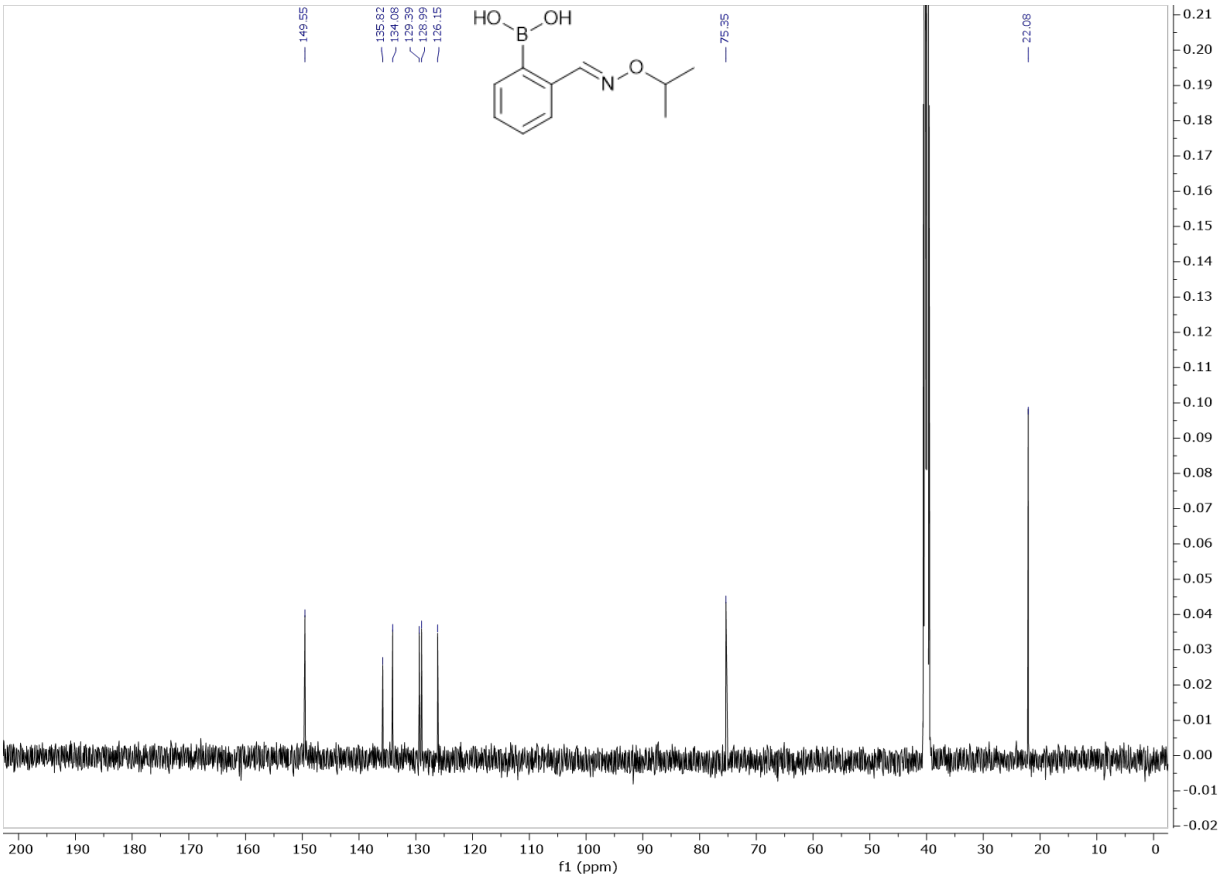

Fig. S45. ^{13}C NMR spectrum of **2c** in DMSO-d_6.

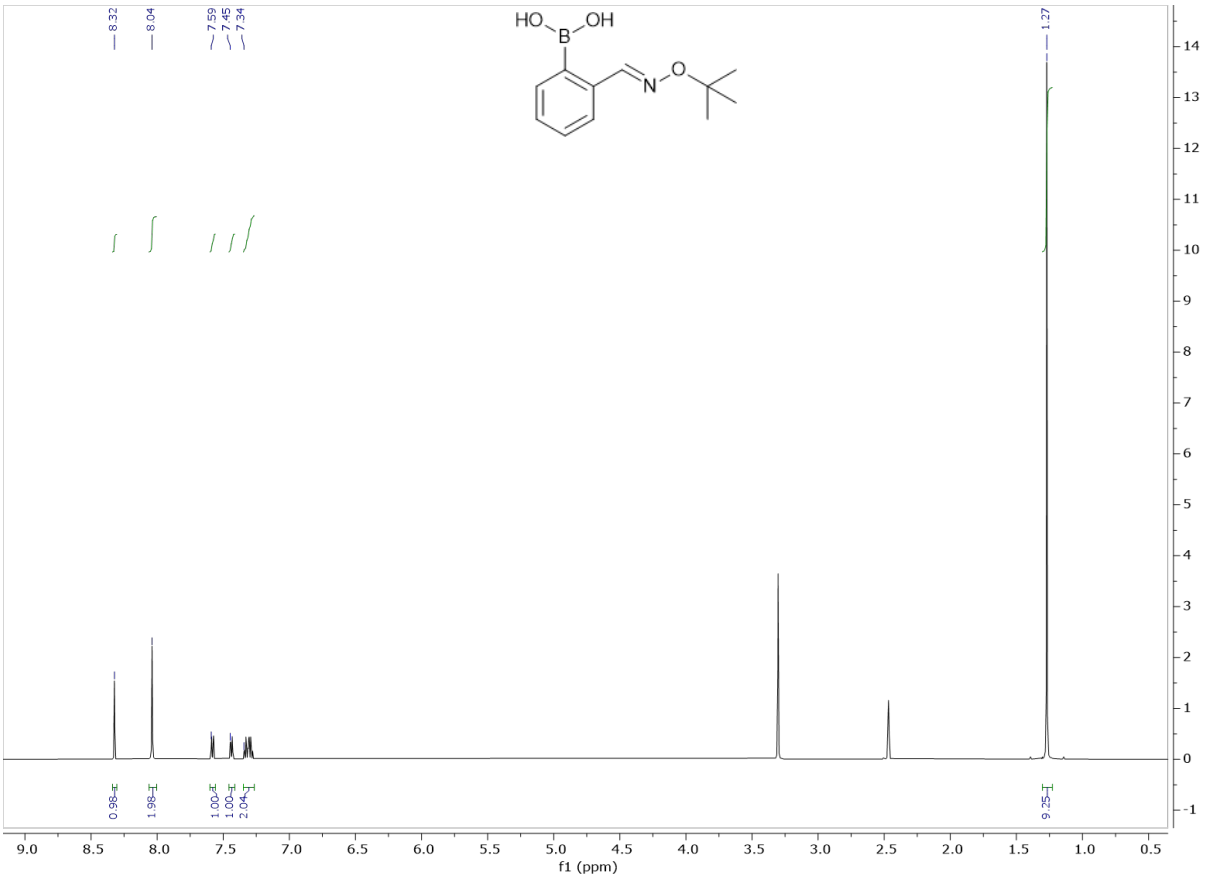

Fig. S46. ^{1}H NMR spectrum of **2d** in DMSO-d_6.

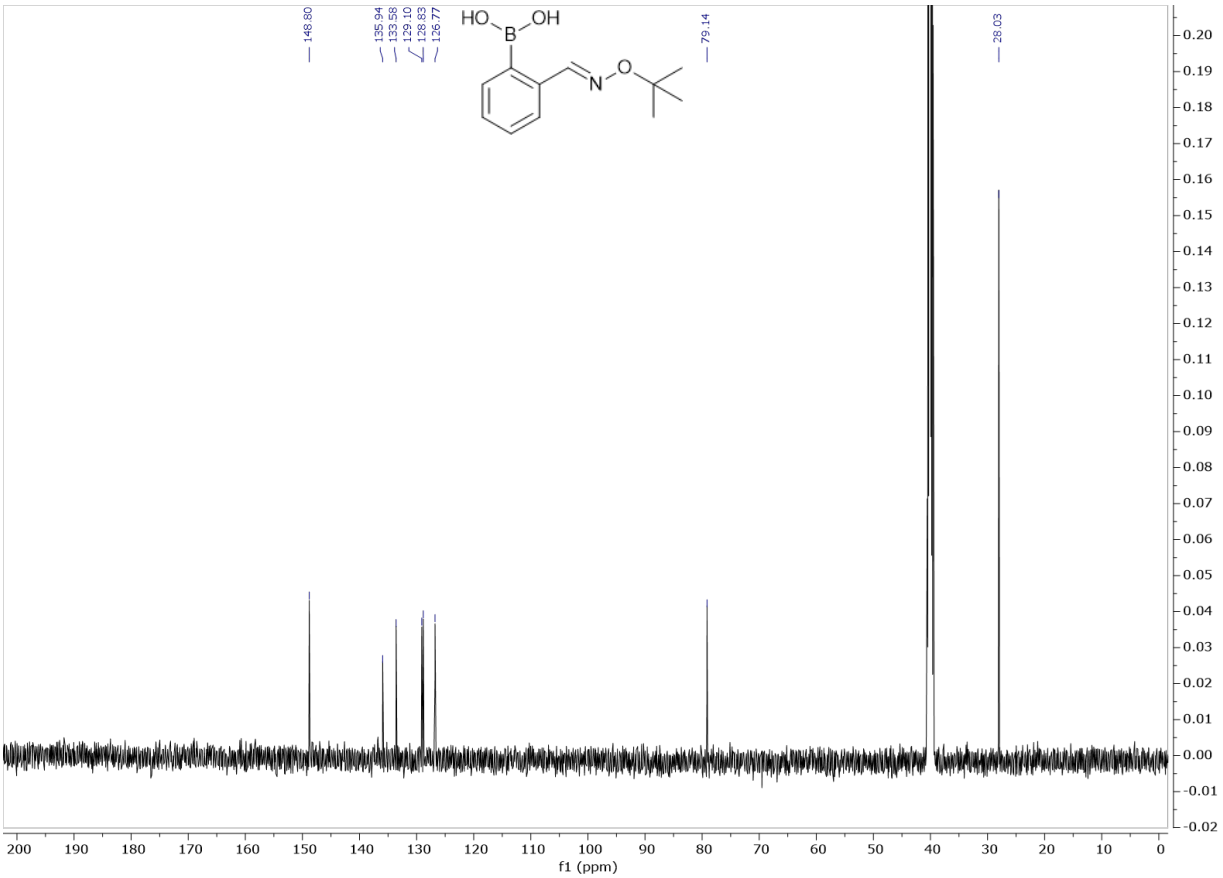

Fig. S47. ^{13}C NMR spectrum of **2d** in DMSO-*d*$_6$.

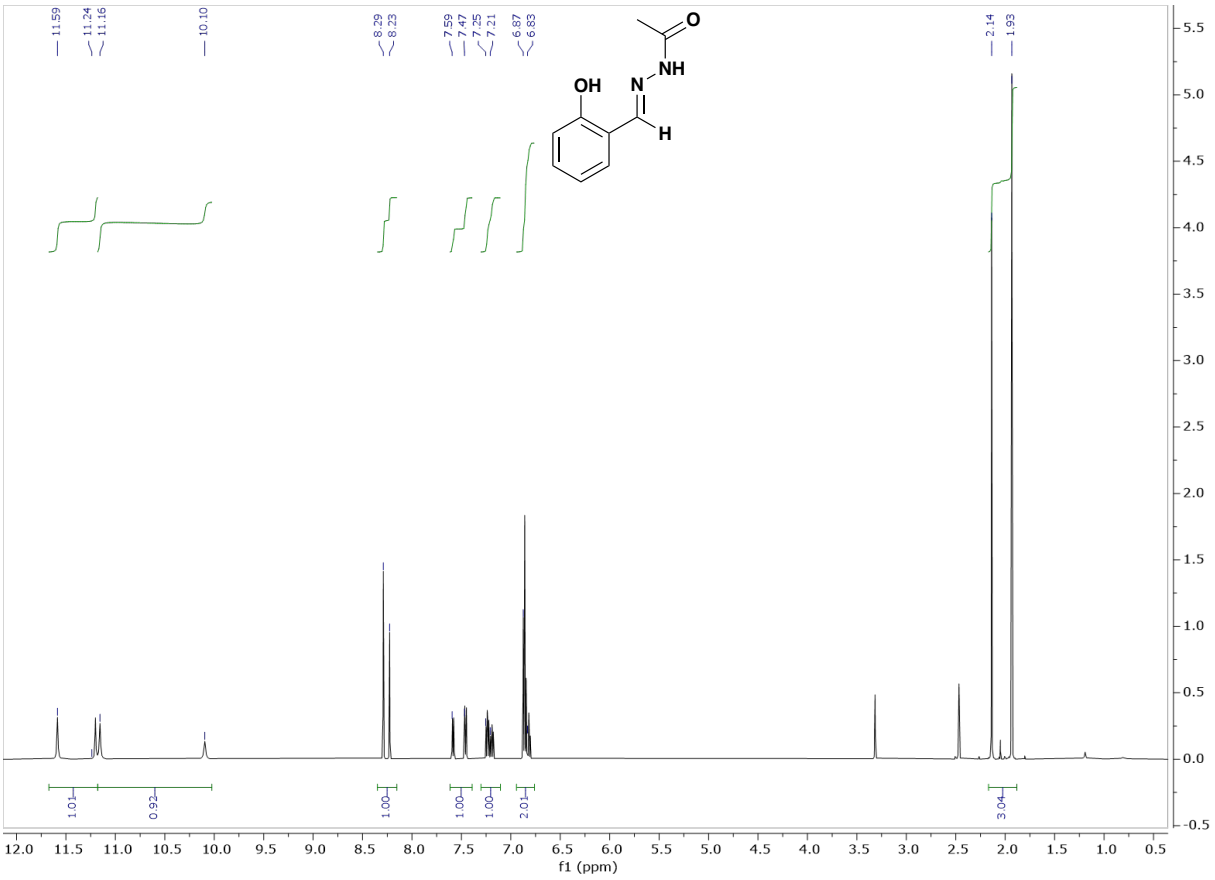

Fig. S48. ^{1}H NMR spectrum of **3** in DMSO-d_6. Here, **3** was prepared via condensation between salicylaldehyde and AHz.

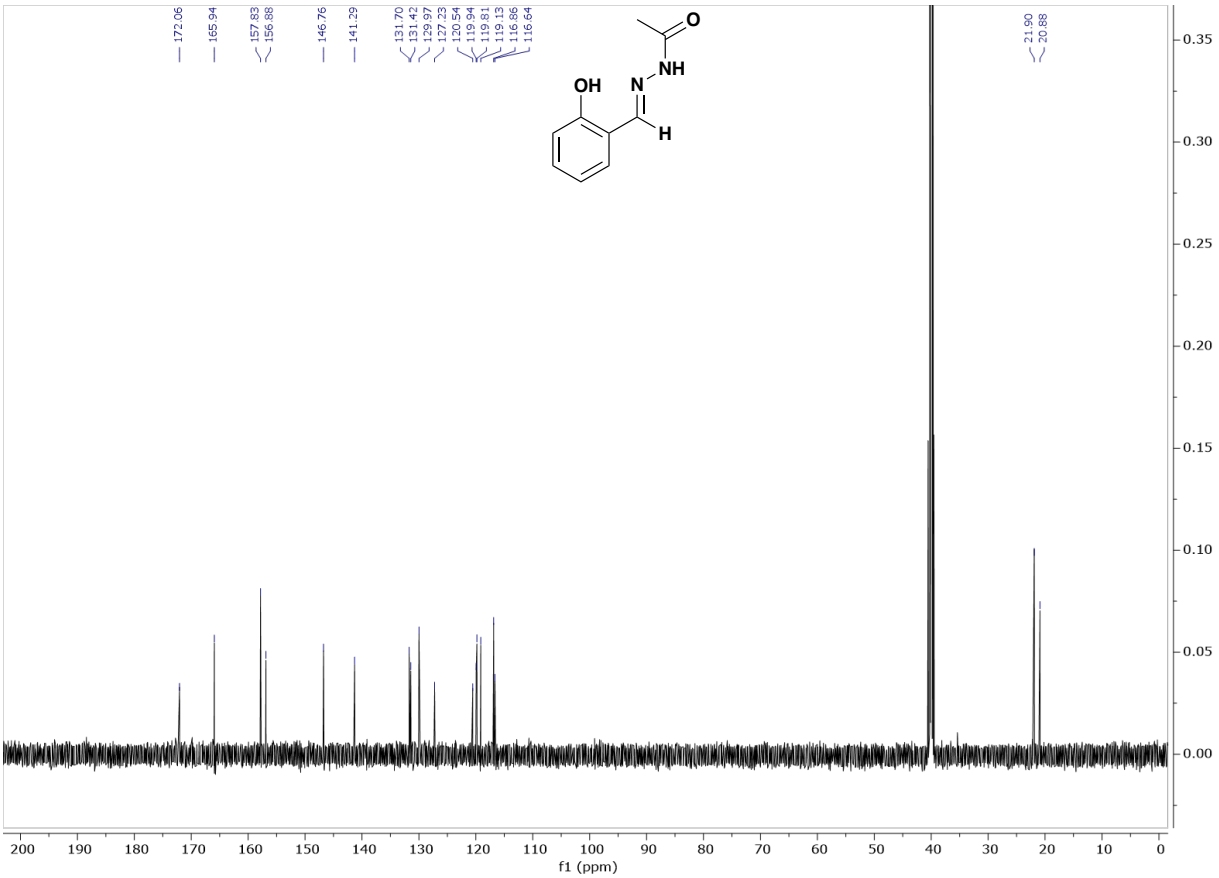

Fig. S49. ^{13}C NMR spectrum of **3** in DMSO-*d*$_6$. Here, **3** was prepared via condensation between salicylaldehyde and AHz.

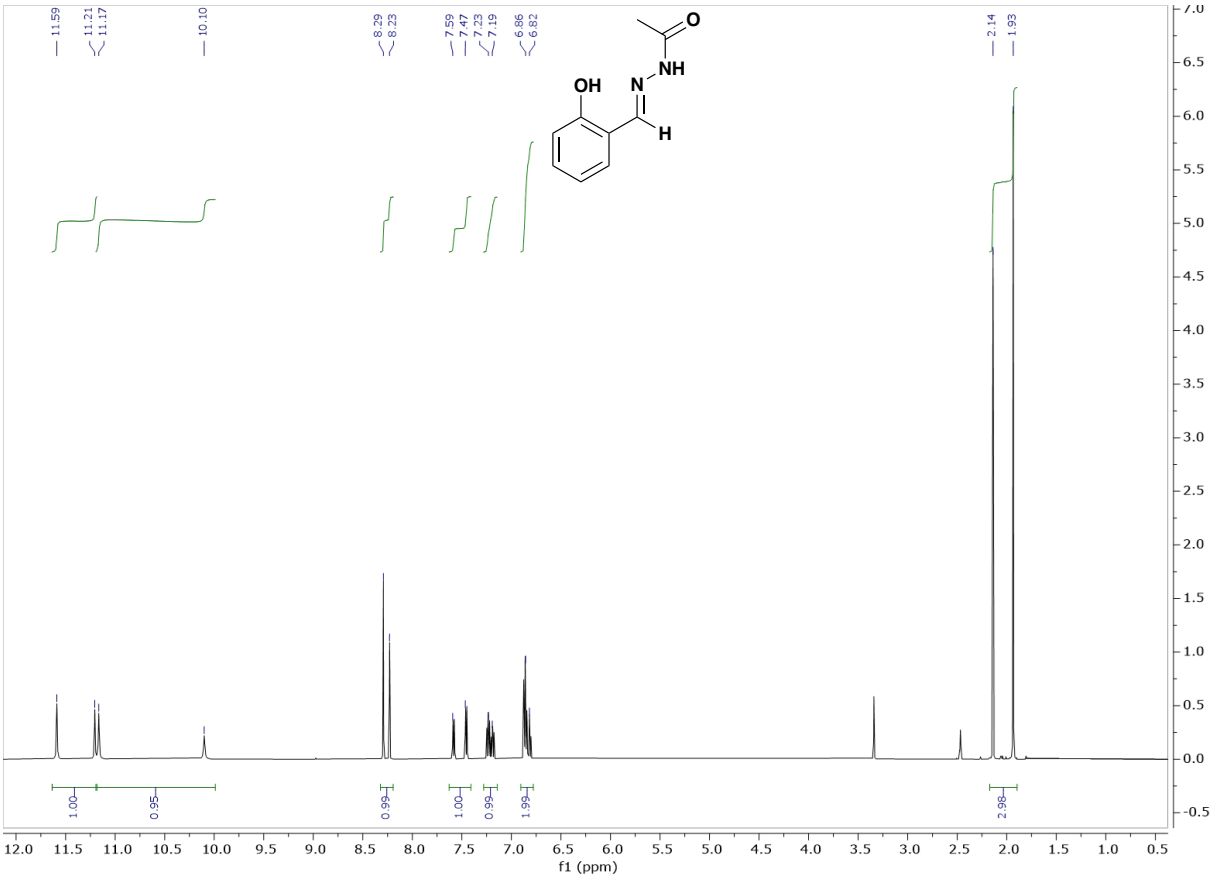

Fig. S50. ^{1}H NMR spectrum of **3** in DMSO-*d*$_6$. Here, **3** was prepared by oxidizing **1a**.

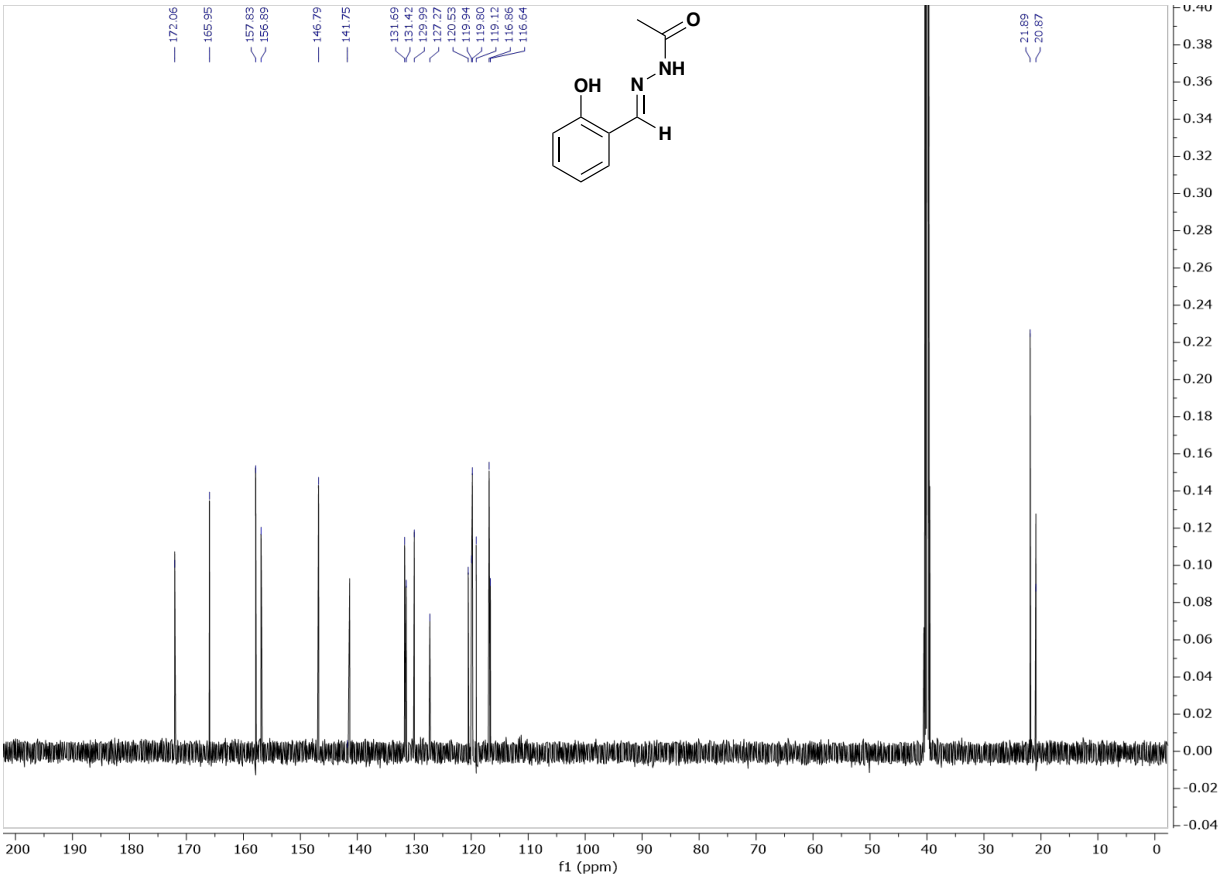

Fig. S51. ^{13}C NMR spectrum of **3** in DMSO-*d*$_6$. Here, **3** was prepared by oxidizing **1a**.

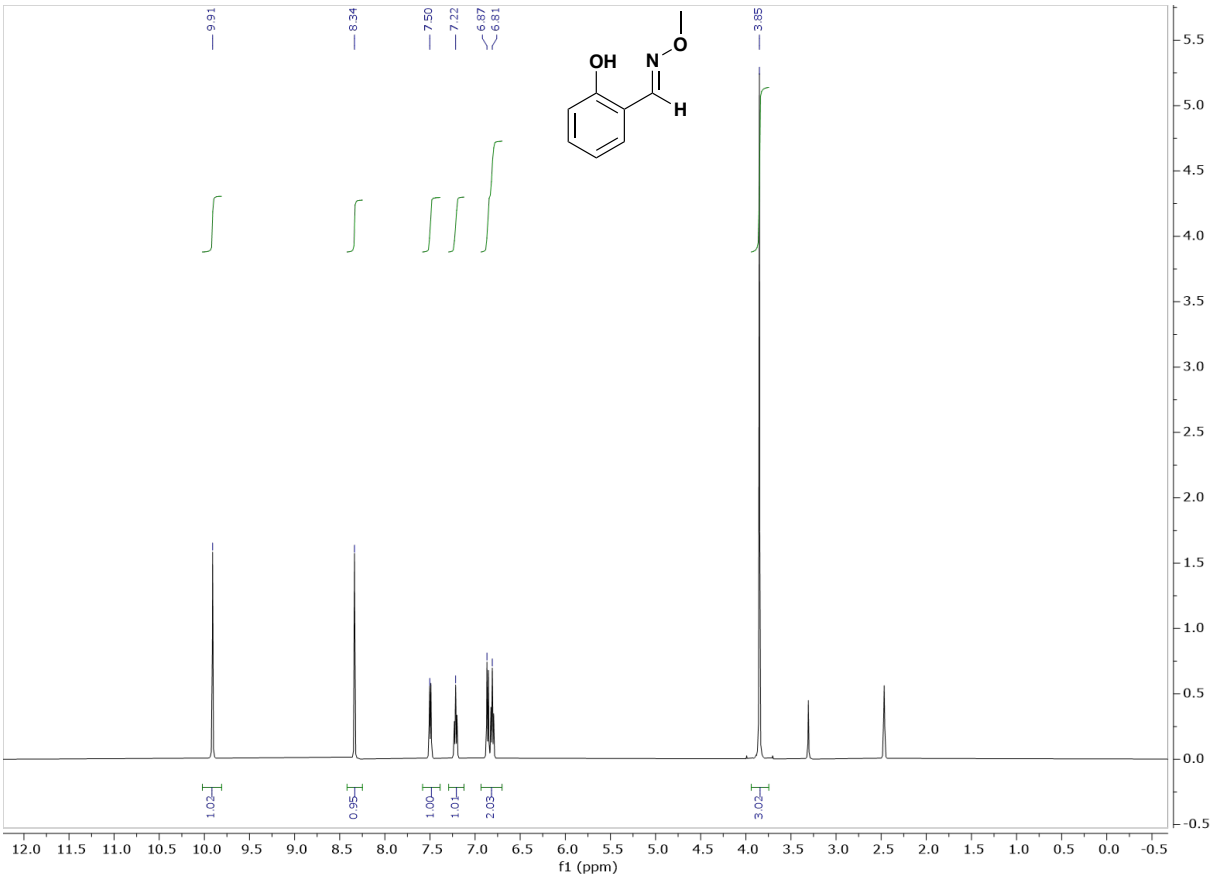

Fig. S52. ^{1}H NMR spectrum of **4a** in DMSO-d_6. Here, **4a** was prepared via condensation between salicylaldehyde and MHA.

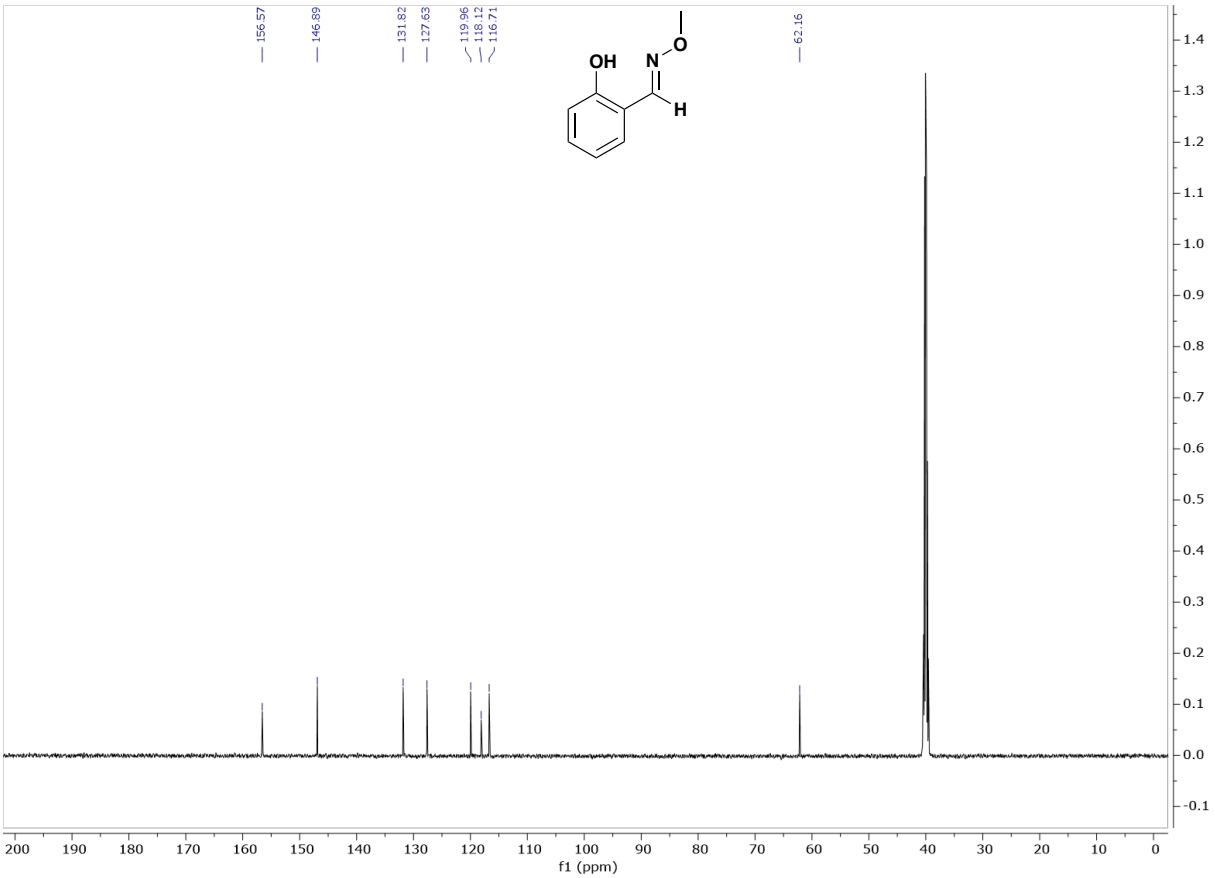

Fig. S53. ^{13}C NMR spectrum of **4a** in DMSO-d_6. Here, **4a** was prepared via condensation between salicylaldehyde and MHA.

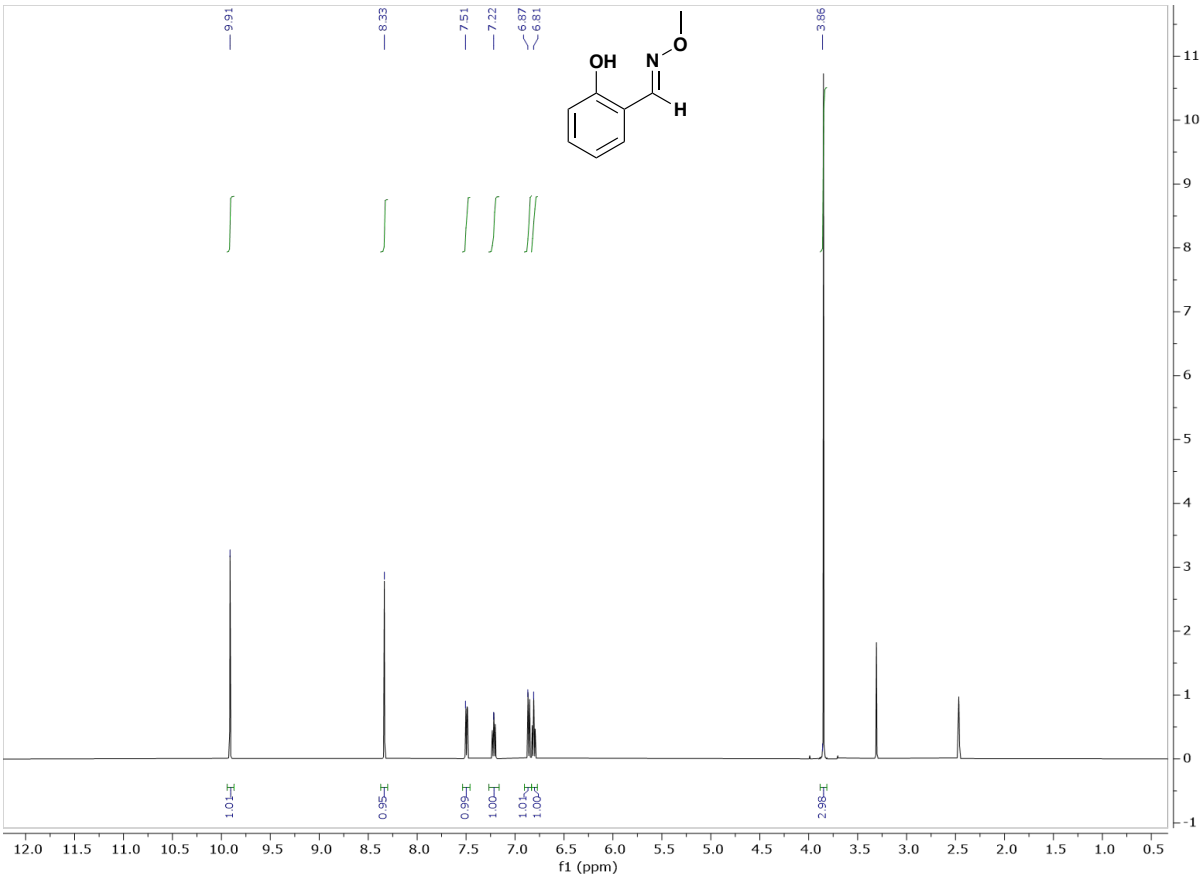

Fig. S54. ^{1}H NMR spectrum of **4a** in DMSO-d_6. Here, **4a** was prepared by oxidizing **2a**.

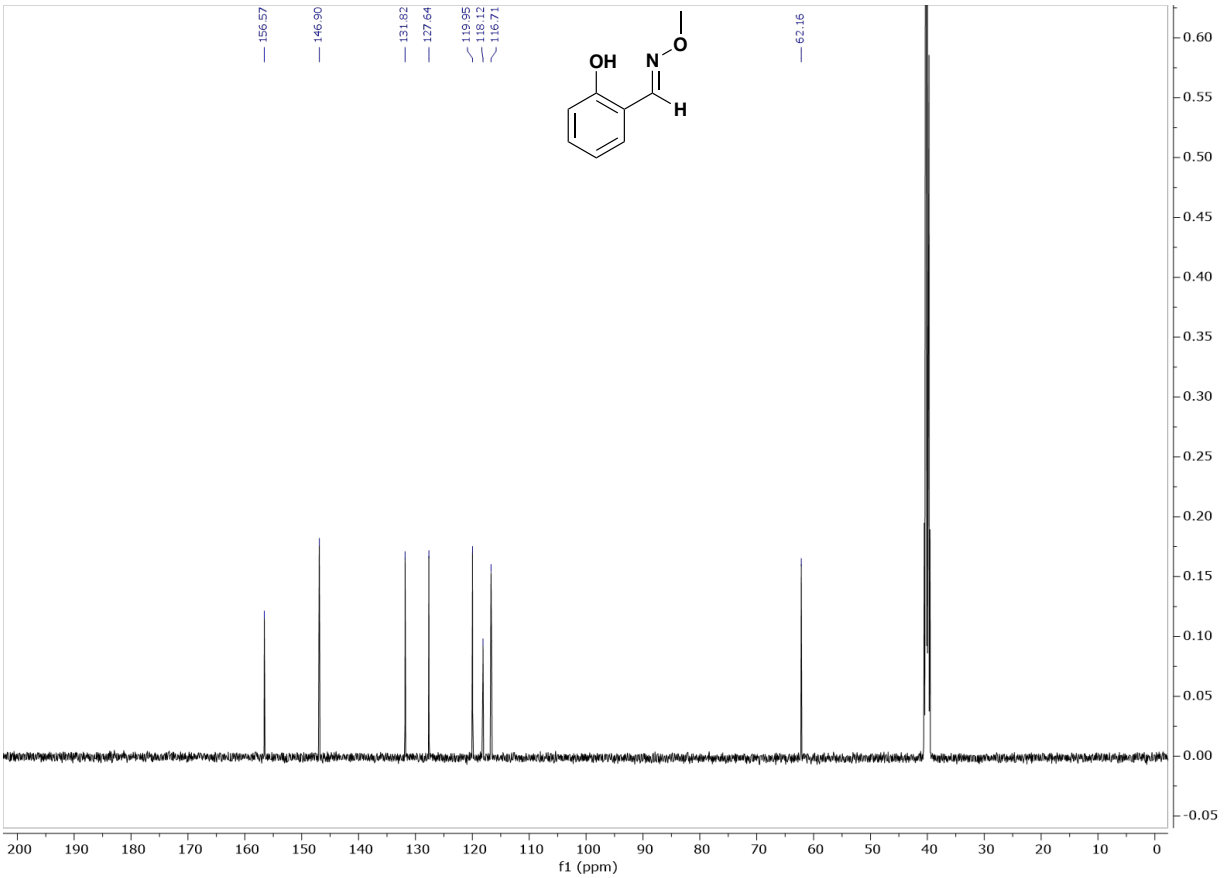

Fig. S55. ^{13}C NMR spectrum of **4a** in DMSO-d_6. Here, **4a** was prepared by oxidizing **2a.**

1. C. L. Perrin, *J. Chem. Educ.*, 2017, **94**, 669–672.
2. A. Dirksen, S. Dirksen, T. M. Hackeng and P. E. Dawson, *J. Am. Chem. Soc.*, 2006, **128**, 15602–15603.
3. H. Gu, T. I. Chio, Z. Lei, R. J. Staples, J. S. Hirschi and S. Bane, *Org. Biomol. Chem.*, 2017, **15**, 7543–7548.
4. Wang, L., Dai, C., Burroughs, S.K., Wang, S.L. and Wang, B. *Chem. Eur. J.*, 2013, **19**, 7587-7594.